WORK COPY — A.C.J.

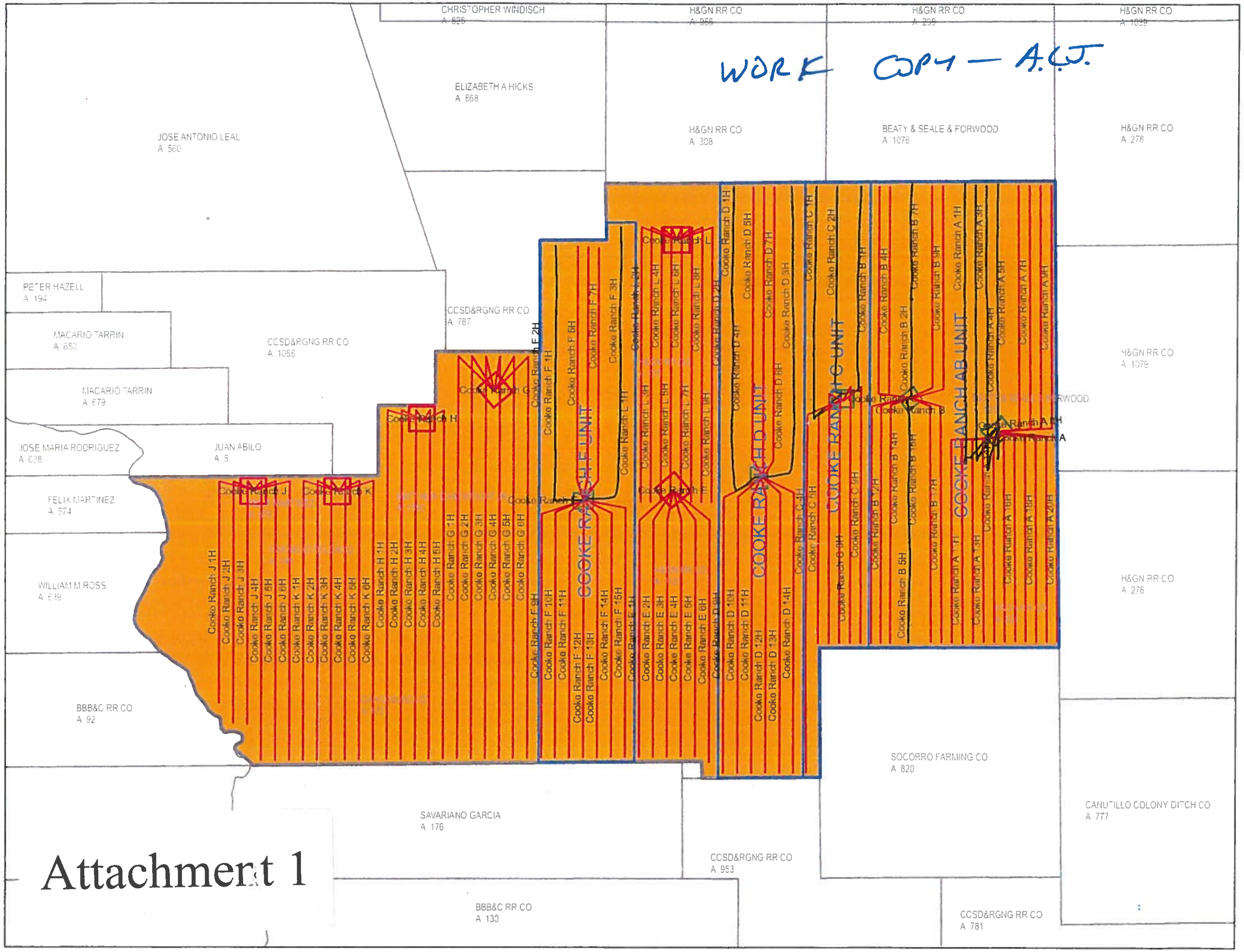

CHRISTOPHER WINDISCH A 826
H&GN RR CO A 956
H&GN RR CO A 295
H&GN RR CO A 1099
ELIZABETH A HICKS A 868
JOSE ANTONIO LEAL A 560
H&GN RR CO A 308
BEATY & SEALE & FORWOOD A 1076
H&GN RR CO A 278
PETER HAZELL A 194
MACARIO TARRIN A 650
CCSD&RGNG RR CO A 1058
CCSD&RGNG RR CO A 787
MACARIO TARRIN A 679
JOSE MARIA RODRIGUEZ A 628
JUAN ABILO A 5
FELIX MARTINEZ A 574
WILLIAM M ROSS A 639
BBB&C RR CO A 92
H&GN RR CO A 1079
H&GN RR CO A 276
SOCORRO FARMING CO A 820
SAVARIANO GARCIA A 176
CCSD&RGNG RR CO A 953
CANUTILLO COLONY DITCH CO A 777
BBB&C RR CO A 130
CCSD&RGNG RR CO A 781
COOKE RANCH F UNIT
COOKE RANCH D UNIT
COOKE RANCH C UNIT
COOKE RANCH AB UNIT
Cooke Ranch L
Cooke Ranch G
Cooke Ranch H
Cooke Ranch J
Cooke Ranch K
Cooke Ranch F
Cooke Ranch E
Cooke Ranch B
Cooke Ranch A

Attachment 1

Cooke Ranch Unit Boundaries

Wellbores

STATUS

Drilled Well

Planned Well

Wellpads

STATUS

🟥 Wellpad - Planned

🟦 Wellpad - Scouted

🟩 Wellpad - Built

☐ Wellpad - Reclaimed (Partial)

Exhibit No. 23

DOCKET NO. 01-0297078, et al.

Talisman Energy USA, Inc.

September 9, 2015

Notes:

TALISMAN ENERGY

Cooke Ranch Development Map

UNCONVENTIONAL RESOURCES TECHNOLOGY CONFERENCE
FUELED BY SPE • AAPG • SEG

URTeC: 2153935

New Findings in Expected Ultimate Field Recoveries: Implications of Staggered Lateral Downspacing in the Eagle Ford Shale

Paolo Grossi, Devery Neumann, and Farshad Lalehrokh, Talisman Energy USA Inc.

Copyright 2015, Unconventional Resources Technology Conference (URTeC) **DOI 10.15530/urtec-2015-2153935**

This paper was prepared for presentation at the Unconventional Resources Technology Conference held in San Antonio, Texas, USA, 20-22 July 2015.

The URTeC Technical Program Committee accepted this presentation on the basis of information contained in an abstract submitted by the author(s). The contents of this paper have not been reviewed by URTeC and URTeC does not warrant the accuracy, reliability, or timeliness of any information herein. All information is the responsibility of, and, is subject to corrections by the author(s). Any person or entity that relies on any information obtained from this paper does so at their own risk. The information herein does not necessarily reflect any position of URTeC. Any reproduction, distribution, or storage of any part of this paper without the written consent of URTeC is prohibited.

Abstract

The Eagle Ford Shale has emerged as one of the premier unconventional resources in North America. Explosive development has propelled the play to current volumes of 1700 Mbbls/day of oil and 7 bcf/day gas (EIA, March 2015). Despite this incredible achievement many operators are wanting more; utilizing innovative development strategies to enhance overall field recoveries. This strategy seems to be warranted given expected recoveries are typically low for an immense ultimate technically recoverable resource of 17 Tcf gas and 4.2 Bbbls oil (EIA, 2014). From these metrics it is clear to see that optimizing recovery can have dramatic and profound impacts; a conservative 5% recovery increase would yield an additional 1Tcf gas and 200 MMbbls oil.

A systematic approach and associated findings in implementing optimized recovery methods by the use of multi-zone (staggered; chevron well pattern configuration) downspacing within the Eagle Ford development area will be presented. The approach will be outlined through the use of numerous datasets including: the review of public production data, published analogue data, decline curve analysis, reservoir modeling, wireline log datasets, buried array microseismic, and geochemical datasets. Current well results, including raw production volumes and rate transient analysis outputs, will be shown to be supporting predicted and modeled results.

This study will bring forward new findings in the effectiveness of current hydraulic fracturing techniques in regards to reservoir drainage limits, expected ultimate field recoveries, and the implications to staggered downspacing. The success of current staggered tests is expected to have a significant impact on future drilling inventory and subsequent asset value, with potential field recoveries being increased by 4 to 7 times current field averages.

Introduction

Optimizing recovery implies an increase in the recovery factor; defined as the percentage of total hydrocarbons recovered (ultimate producible volume) from a given field (rock volume) (Shepard, 2009). Fundamentally this process is tied to the geological (inherent reservoir parameters), but also the technological capabilities of the recovery method (the interplay of physical and economic elements) (Shepard, 2009).

The recovery of hydrocarbons in ultra-low permeability unconventional reservoirs involves producing out of induced hydraulic fractures. As such, this recovery method is largely dependent on the technical limitations and economics of the process. This is assumed to hold true within different plays, and even more so within specific fields or development areas where reservoir properties become ever more similar. In other words, it suggests that ultimate recovery is limited more so by the recovery method (i.e. hydraulic fracture process) than the rock.

An industry review of operator published well recoveries (estimated ultimate recoveries, EUR) was compiled with internal values to create an Eagle Ford dataset. This data was then compared to hydrocarbon in-place (HCIP) mapping of the Eagle Ford and Austin Chalk. These two parameters were then used to compute a recovery factor assuming a fixed area for in-place volumetrics. Computed recovery factor (RF) was grouped by main phase (oil or gas assuming a gas-oil ratio (GOR) cutoff) and in-place volumetrics arranged in ascending order (Figure 1). As seen

TALISMAN ENERGY USA INC.
DOCKET NO.: 01-0297078, et al.
September 09, 2015

Exhibit 46

Attachment 2

in Figure 1, recovery factors decrease with increasing volumetrics, in both the oil and gas cases. Assuming a linear relationship between in-place volumetrics and reservoir height, it is interpreted that in low volumetric areas (limited reservoir height) hydraulic fractures reach or nearly reach their full effective extent which results in high calculated recovery factors. Conversely in high volumetric areas, if the same fracture extent is reached, a larger volume will be under stimulated resulting in a lower computed recovery factors (Figure 2). This suggests that the assumption of a dynamic recovery factor is fundamentally related to fracture geometry, stimulation effectiveness and reservoir (net pay) height.

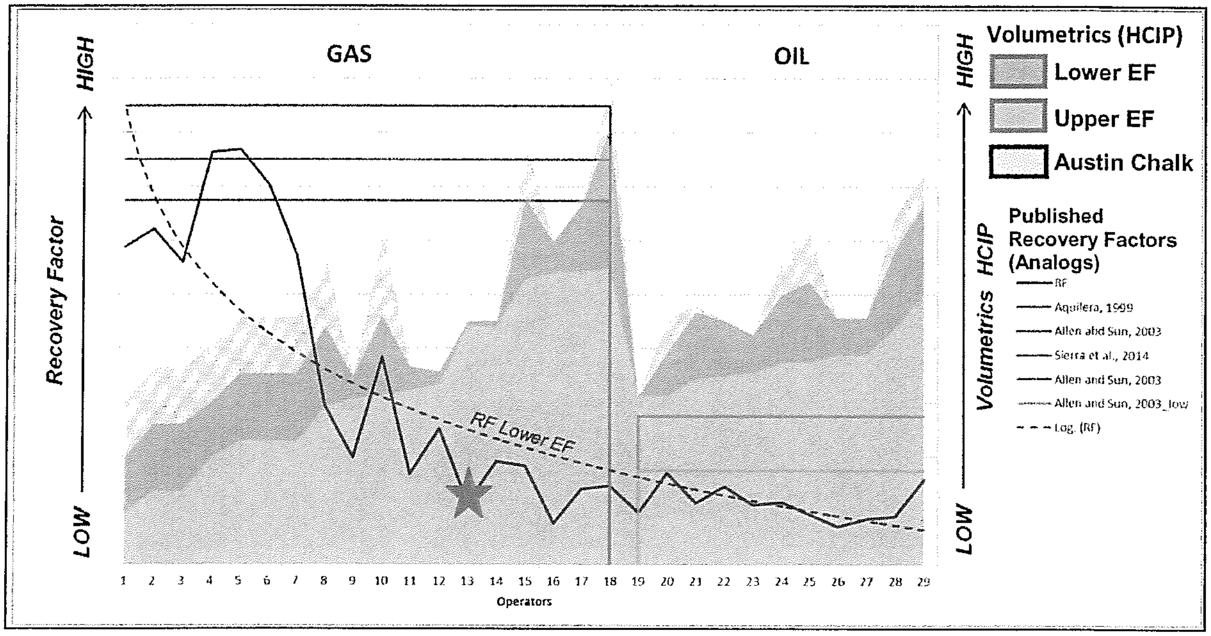

Figure 1: Relationship oberserved between estimated ultimate recoveries (EUR), volumetrics (hydrocarbon in-place - HCIP), and recovery factor (RF) for the Eagle Ford Shale. Low recoveries in high volumetric areas suggests enhanced recovery methods (additional wells) are needed to optimize recovery; Talisman development area indicated by red star. Analogue published recovery factors in naturally fractured reservoirs are also shown.

Published examples of recovery factors in unconventional shale gas and oil reservoirs is limited, with authors attempting to predict it through various modeling techniques (Wan et al., 2013, Sierra et al., 2014). As such, it was decided to use naturally fractured reservoirs with similar matrix permeabilities as analogs to gain insight into the potential range and limits of recoveries. It is proposed that hydraulically stimulated unconventional reservoirs can be considered the "man-made" equivalent of Type II to III naturally fractured reservoir types. These reservoirs are defined as having dominate matrix storage, low matrix permeability, with natural fractures that provide the dominate fluid-flow pathway (Allan and Qing Sun, 2003). An extensive review of over 100 fractured fields was performed by Allan and Qing Sun (2003) that found typical oil recoveries for Type II/III solution gas drive reservoirs between 15-25% and total average Type II/III recoveries between 20-30%. Work by Aguilera (1999) establishes Type II/III gas recoveries at 75-85%, which is similar to modeling by Sierra et al. (2014) that predicts, given optimal completion strategies, shale gas recoveries of up to 70% can be achieved (Figure 1). The power of this exercise is to validate that further recovery enhancement can be achieved by implementing multi-zone (staggered) lateral placement.

The new realization of unconventional shale recoveries has fueled the search for "stranded resources" (Pioneer, Investor Presentation, 2014), as several operators look to test multi-zone vertical downspacing throughout the entire Eagle Ford trend (Figure 4). In all cases operators are focusing on areas with large in-place volumes; either achieved by thick sections containing Lower Eagle Ford, Upper Eagle Ford, and Austin Chalk. Within Talisman Energy's operated area the highest volumetrics are found dominantly in the Lower Eagle Ford section, with overall reservoir thickness ranging from 200-230ft and average field recoveries typically <15%. It was within this area that the initial staggered downspacing tests were to be implemented.

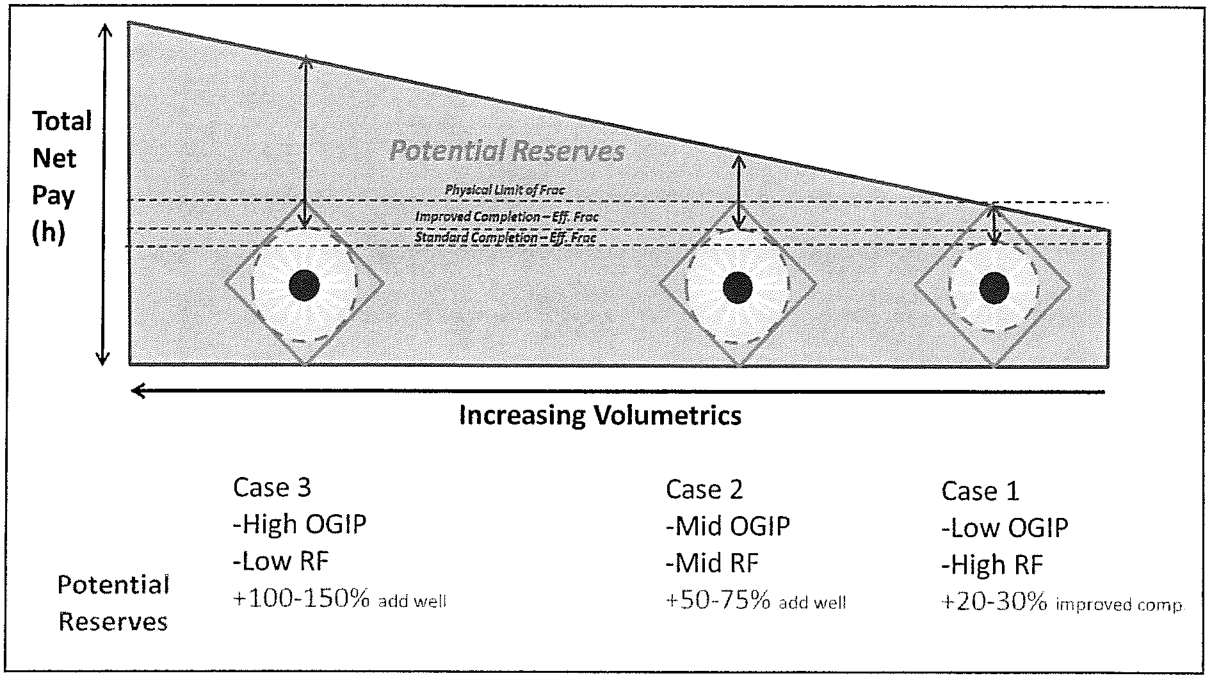
Total Net Pay (h)
Potential Reserves
Physical Limit of Frac
Improved Completion – Eff. Frac
Standard Completion – Eff. Frac
Increasing Volumetrics
Case 3
-High OGIP
-Low RF
+100-150% add well
Case 2
-Mid OGIP
-Mid RF
+50-75% add well
Case 1
-Low OGIP
-High RF
+20-30% improved comp.
Potential Reserves

Figure 2: Schematic illustrating the observed relationship between recovery factor and in-place volumetrics. It is proposed that this is largely dicated by the completion methods inability to access total reservoir height (net pay – h). Three potential scenarios are demostrated that exhibit that a greater amount of "potential reserves" exist as in-place volumes increase (net pay increases) and improved completions or additional wells are warrented.

Initial Reservoir Model

Reservoir HCIP, specifically reservoir height, and EUR were related through rate transient analysis (RTA). Utilizing the method outlined by Lalehrokh et al. (2013) and Miller et al. (2010), the contributing reservoir volume, related to the productivity index (PI), can be computed and kept constant by manipulating reservoir height (h), fracture half length (xf) and matrix permeability (km). This allowed sensitivities to be conducted given three potential drainage scenarios within a mile-by-mile development area; assuming a 200ft, 100ft and 75ft effective reservoir pay height (Figure 3). Given these assumptions, current type curve expectations (black line, Figure 3) could be achieved by: 1) access to total reservoir height (200ft) with an xf of 125ft; 2) access to 100ft of reservoir height with an xf of 168ft; or 3) a further reduced reservoir height (75ft) with an xf of 190ft (Figure 3). The results are profound, suggesting that long held spacing assumptions of 660ft (xf 330ft) and 200ft reservoir height results in a very unlikely fracture geometry; extremely small effective reservoir height (h) or extremely small xf for either end member to be achieved. Determining what case was most valid required the further integration of geoscience and engineering datasets.

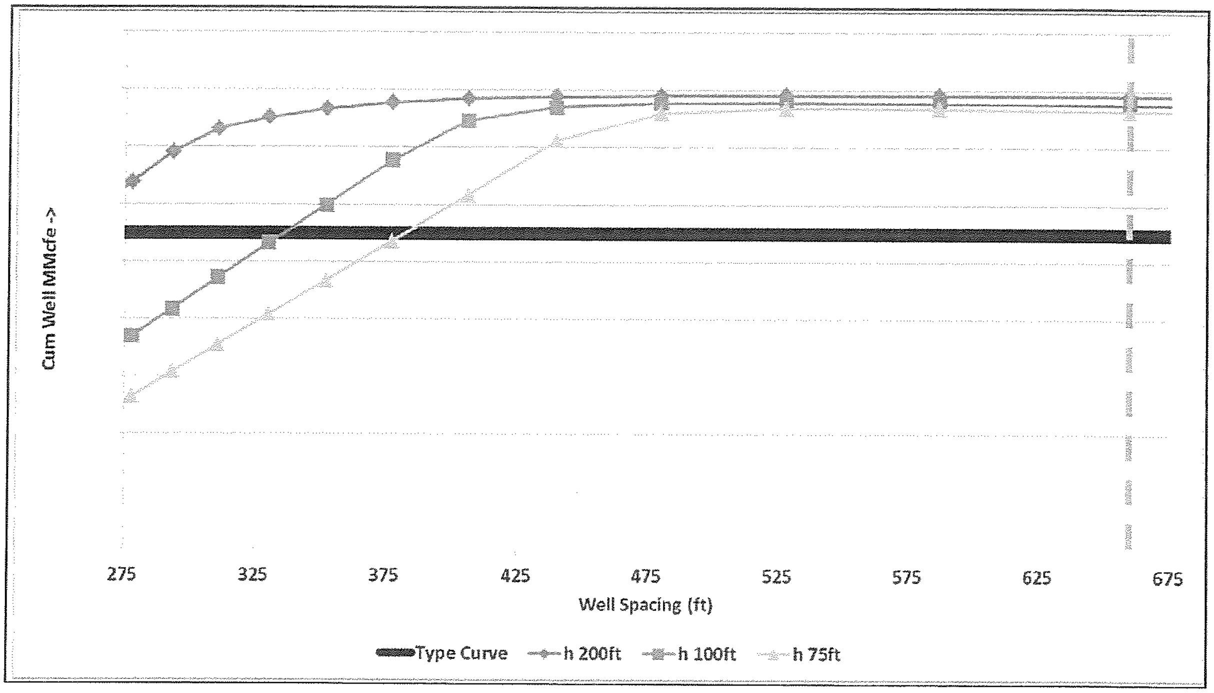

Figure 3: Rate transient (RTA) modeling estimated a drainage volume that can be realized through three xf and h assumptions: 1) h of 200ft, xf of 125ft (blue line), 2) h of 100ft, xf of 168ft (red line) and 3) h of 75ft, xf of 190ft (green line). Each scenario assumed a mile-by-mile development area, plotted is the cumulative EUR per well (y axis) versus well spacing (x axis), the intersection of each scenario and the black line (type curve) determines the well spacing needed to match average field EUR. Results suggested that long held well spacing assumptions (dashed grey line) were very unlikely given it would result in extremely small effective reservoir height (h) or extremely small xf.

Reservoir Characterization

In the development area where the initial staggered downspacing tests were to be executed, an extensive reservoir characterization program was conducted in order to quantify reservoir heterogeneity and establish/verify horizontal landing (target) zones. Datasets that were collected and analyzed included: a full wireline log suite with FMI log, surface logging (C1-C8 mudgas chromatography, X-ray fluorescence (XRF), Source Rock Analysis (SRA)), rotary side walls cores, unconventional core analysis and petrographic analysis (reflected light and scanning electron microscopy (SEM)).

The wireline log suite was calibrated via core analysis, XRF and SRA datasets. Specifically allowing for the calibration of porosities, fluid saturations, TOC (kerogen content), and bulk mineralogy (Figure 4). The calibrated wireline data suggested fairly uniform volumetric distribution throughout the Lower Eagle Ford section, with average total porosities ranging from 6-12% and TOC 4-7 wt%. Total volumetrics were computed at 120-140 bcf/640 acres or 0.6 bcf/ft/640 acres. Mineralogical variation within the Lower Eagle Ford is significant, with carbonate content ranging from 40-80% (cuttings and core samples). Overall computed mineralogical brittleness (internal developed ratio of competent minerals to non-competent minerals) is observed to decrease from the top to the bottom of the section. This is most consistent with the behavior of Young's modulus computed from dipole sonic logs (Figure 4 and 5).

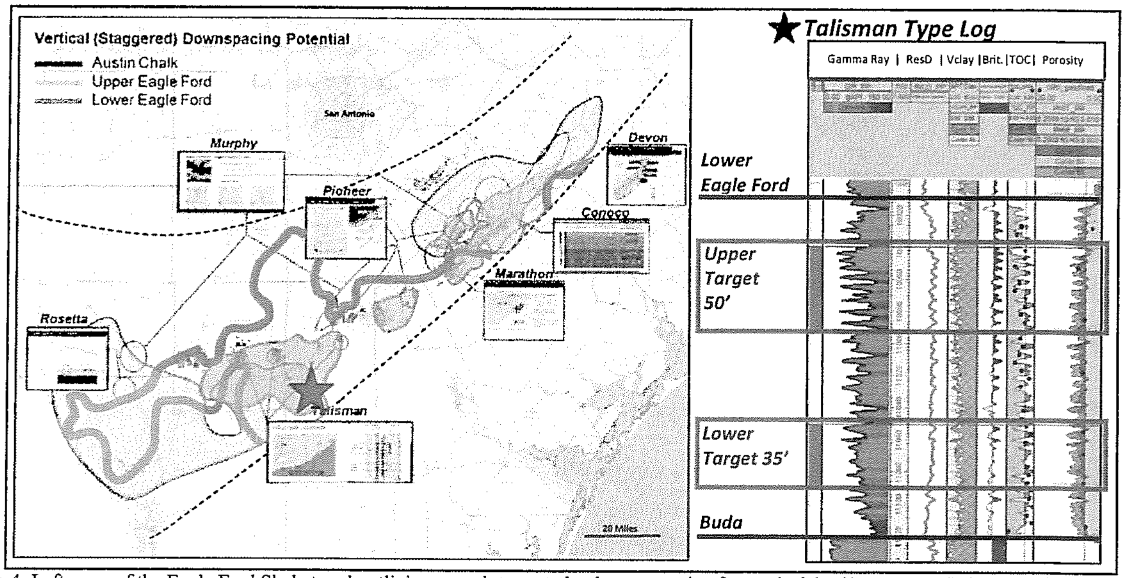
Vertical (Staggered) Downspacing Potential
Austin Chalk
Upper Eagle Ford
Lower Eagle Ford
San Antonio
Murphy
Pioneer
Devon
Conoco
Marathon
Rosetta
Talisman
20 Miles
Talisman Type Log
Gamma Ray | ResD | Vclay |Brit.|TOC| Porosity
Lower Eagle Ford
Upper Target 50'
Lower Target 35'
Buda

Figure 4: Left: map of the Eagle Ford Shale trend outlining areas interpreted to be prospective for vertical (and/or staggered) downspacing, also shown are areas were operators are currently testing (images modified from operator investor presentations, 2014); Talisman development area denoted by red star. Right: Type log displaying the over 200ft of Lower Eagle Ford section within Talisman's operated asset base within which two horizontal target (landing) zones have been identified. Log curves left to right: gamma ray, deep resistivity, bulk mineralogy (Vclay), XRF (mineralogical) brittleness, TOC, and porosity (red shaded effective porosity with 5% in dark red).

Mechanical stratigraphy, the layering of distinct geomechanical beds, has been demonstrated to have a major effect on fracture initiation, growth and complexity specifically in regards to the Eagle Ford (Ferrill and Morris, 2008, Ferrill et al., 2014, Smart et al., 2014). The continuum of various carbonate-rich lithologies (calcareous mudstone, marlstone and chalk) along with interbedded volcanic ash, creates a complex geomechanical framework that can be realized at several scales; from centimeter laminations to more simplified large mechanical units (Smart et al., 2014). Investigating these relationships within the study area involved the acquisition and pairing of dipole

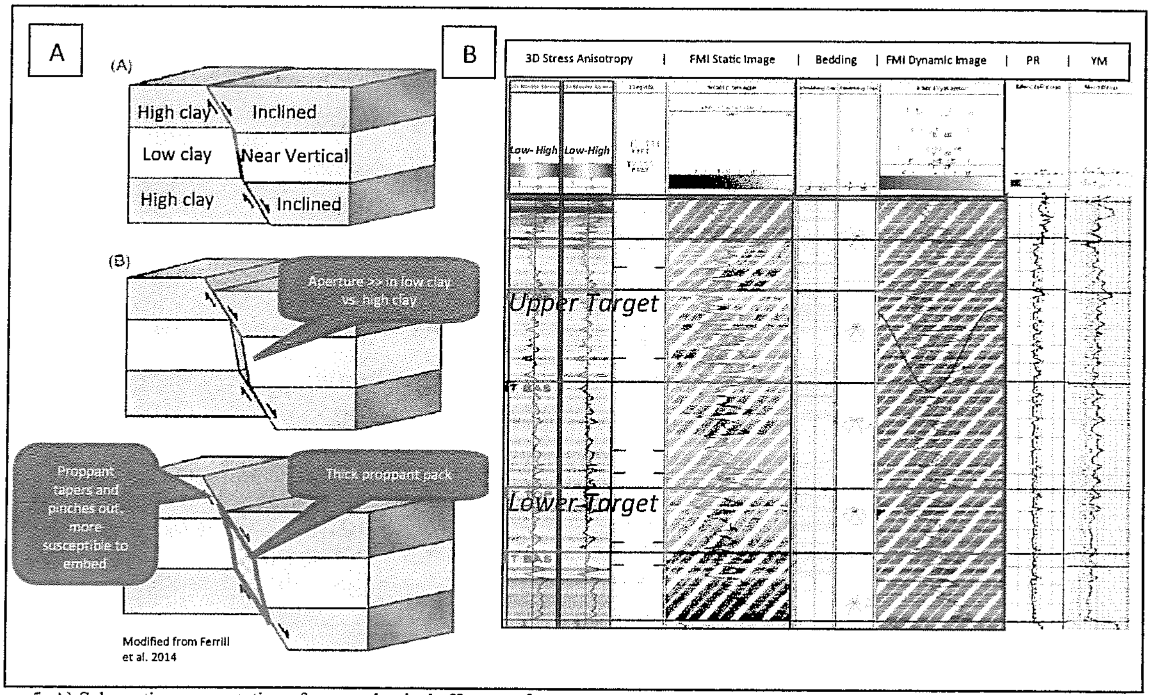
A
(A)
High clay
Inclined
Low clay
Near Vertical
High clay
Inclined
(B)
Aperture >> in low clay vs. high clay
Proppant tapers and pinches out, more susceptible to embed
Thick proppant pack
Modified from Ferrill et al. 2014
B
3D Stress Anisotropy | FMI Static Image | Bedding | FMI Dynamic Image | PR | YM
Low-High
Low-High
Upper Target
Lower Target

Figure 5: A) Schematic representation of geomechanical effects on fracture growth and subsequent proppant transport and connectivity (modified from Ferrill et al., 2014). B) Geomechanical log suite, left to right: 3D stress anisotropy, static FMI image, interpreted bedding planes and bedding angles, dynamic FMI image, directional Poisson's ratio and Young's modulus.

sonic logs with a formation micro-imaging (FMI) log. The main interpretation from this dataset is that similar continuous zones of favorable stress are present within the Lower Eagle Ford section, establishing that hydraulic fracture initiation can be achieved equally well at various locations within the section (i.e. upper and lower target zones) and that these initiation zones are separated by thicker continuous units of high stress (Figure 5). Secondly, the high resolution dynamic FMI images identify the smaller scale and more complex geomechanical features, with over 300 individual bed boundaries able to be quantified. These findings were incorporated into 3D hydraulic fracture modeling; by creating upscaled higher resolution lithologic dependent stress units. Several iterations of this model confirmed effective fracture initiation and propagation in both the upper and lower target zones, with vertical fracture growth limited by the imposed bed boundaries and high vertical stress anisotropy. Bed boundary and vertical stress changes have been shown to dictate vertical fracture growth and fracture failure type, specifically with weaker or more ductile zones forming more layer parallel or inclined shear dominated fracture planes versus competent mechanically brittle zones (Smart et al., 2014, Ferrill et al., 2014). It is proposed that this may be a major factor in limiting vertical proppant transport and subsequent fracture connectivity, therefore resulting in overall restrictions to effective reservoir pay thickness (h), as summarized by the schematic in Figure 5.

In recent years XRF, specifically its ability to differentiate numerous major and minor elements, has been used as a chemostratigraphic tool to predict TOC, paleoredox conditions, and overall stratigraphic "sweet spots" attributed to well deliverability (Rowe et al., 2009, Tinnin et al., 2013, Hashmy et al., 2012, Harbor, 2011). Under a similar methodology employed by Tinnin et al. (2013), key redox sensitive trace elements were correlated against core and log derived reservoir parameters including: TOC, porosity, mineralogy, gas chemistry (gas wetness), and SRA outputs (HI,OI,S1, S1/TOC, and S2). Overall enrichment of V, Ni, Mo, and Zn are observed in the upper section of the Lower Eagle Ford, with Cu and Cr enrichment in the lower section of the Lower Eagle Ford (Figure 6). There is a positive correlation (R^2 0.42-0.49) between Cr/Cu and TOC, as well as effective porosity and gas wetness. High Cr and Cu concentrations are also observed to be associated with P_2O_5 (phosphate), Zr, Y, FeO_2 and an overall higher clay proportion. S1/TOC, used as a proxy for mobile hydrocarbons (Jarvie, 2011), is seen to be most positively correlatable with V and Mo (R^2 0.38-0.49). The enrichment of V and Mo is also associated with the occurrence of Zn, Sr and Ni as well as with overall higher carbonate content (Figure 6). The relationship observed between geochemical indications of free (mobile) hydrocarbons and lithofacies is consistent with results presented by Fishman et al. (2013) from Eagle Ford samples with similar thermal maturities. The observed elemental associations are interpreted to correspond to similar associations described in modern upwelling pelagic shelf settings, which through space and time have been shown to record cyclic disoxic to euxinic conditions (Calvert and Price, 1983). It is therefore proposed that recorded within the Lower Eagle Ford section is an overall progression from disoxic to euxinic conditions, likely allowing for differing kerogen genesis and subsequently giving rise to the observed gas wetness variations. This also implies pore types and geometries, which involve the interplay of organic matter types (kerogen and bitumen) and lithofacies, should also vary; with certain developed pores being more inter-connected and conductive to flow versus others thereby favoring higher matrix deliverability into the induced hydraulic fracture network.

Scanning electron microscopy (SEM), particularly when paired with focused ion beam milling (FIB-SEM), has been shown to be a powerful tool in characterizing the diverse pore networks of the Eagle Ford as well as many other unconventional shale reservoirs (Driskill et al., 2013, Pommer, 2014, Loucks et al., 2010). Cuttings and rotary sidewall core plugs were examined following a similar methodology outlined by Driskill et al. (2013) producing over 150 2D SEM images, along with four 3D SEM volumes. The dominate pore network observed is organic associated spongy pores with pendular (bubble) pores being secondary. Inter and intragranular pores are typically created by disseminated coccolith tests and are most prevalent in carbonate rich intervals. The highest proportion of organic hosted porosity is seen to correspond with peaks in both Cr (Cu) and V (Mo and Ni). Additionally, pore distributions are observed to follow log-core computed porosity as well as many geochemical trends, including: S1, S2, sum of S1and S2 (S1+S2), HI (HI/OI) and TOC (Figure 6). The high frequency of geochemical data (acquired and sampled every 5ft) and its strong correlation to log-core parameters and SEM pore metrics enabled stratigraphic zones of what is proposed herein as relatively high versus low matrix deliverability units to be identified (Figure 6, SRA track "unit" log). From this interpretation the high degree of potential flow segregation or compartmentalization within the Lower Eagle Ford is evident, with relatively high deliverability units being no more then 10-50ft thick. Analyzing 3D digital volumes revealed mean pore diameters of 0.11-0.14 μm, maximum diameters of 0.53-0.58 μm, and computed permeabilities of 30-115 nD. The largest pores observed are associated with pendular organic and calcite inter and intragranular pores, both of which tend to dominate in the upper portion (upper target) of the Lower Eagle Ford. It is expected that a large quantity of pores exist below 2D/3D SEM resolution within sections of high TOC (Dong and Harris, 2013, Milliken et al., 2013). This is interpreted to account for the higher computed log (ELAN) derived/log-core porosity in the lower portion (lower target) of the Lower Eagle Ford, which is inferred to have the highest hydrocarbon storage capacity within the section.

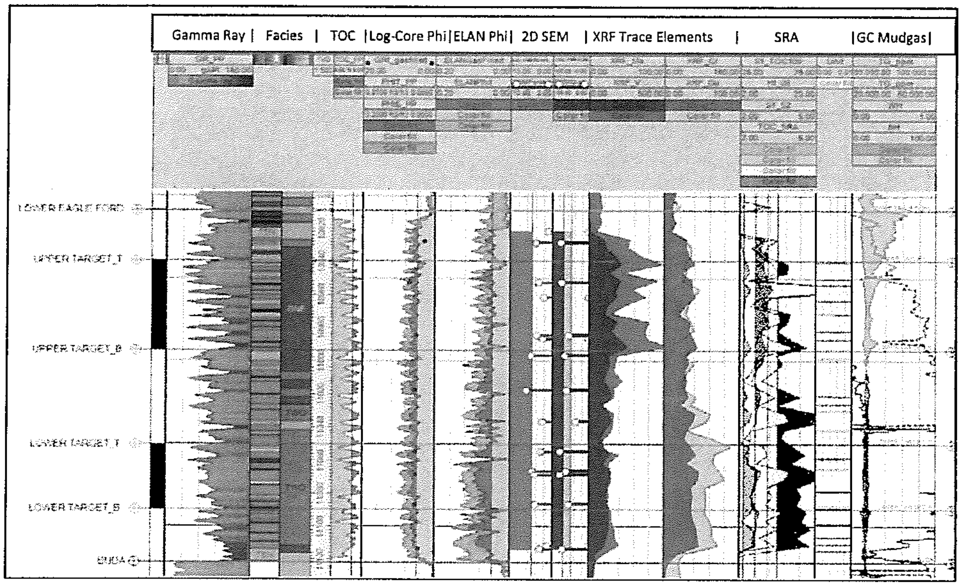

Figure 6: Log display summary of serveral datasets utilized to define upper and lower horizontal target zones. Log curves left to right: gamma ray, log derived and XRF facies, log-cuttings TOC, log porosities (log-core and ELAN with red shaded effective porosity), 2D SEM total porosity and percentage of porosity associated with organic matter, key XRF trace elements, SRA dataset utilized to describe "matrix deliverability" units and GC mudgas (total gas (TG) and gas wetness (WH/BH)).

Microseismic Results

Microseismic monitoring of hydraulic fracturing operations is considered to be a useful tool in gaining insight into fracture growth, particularly aiding in quantifying the distribution of complex fracture patterns which are characteristic of many unconventional shales (Maxwell et al., 2002, Fisher et al., 2002). Within the development area a permanent buried array was utilized to monitor the six well staggered test. The buried array consists of 90 stations, each with three channels at varying depth, for a total of 270 channels. The total area of the array is approximately 15 sq. miles.

The main deliverables from the deployed microseismic acquisition was to establish estimates of overall fracture geometry (height and length), specifically determining estimates of propped versus un-propped stimulated reservoir volume (SRV), and well to well interaction behavior. Propped versus un-propped SRV is determined by the microseismic contractor's proprietary workflow in which fractures are modeled per microseismic event, focal mechanism, seismic moment, rock rigidity, and injected fluid volume to create a discrete fracture network (DFN). The DFN modeled fractures are then filled utilizing a mass balance method which creates a propped DFN that can then be translated to a volume grid to create a propped SRV (PSRV).

Three wells drilled off of two pads constituted the six initial staggered test wells. The two groups of wells were drilled in mirrored staggered configurations, with wells within the same target zone spaced 500ft apart and vertical zone to zone spacing of approximately 100ft (Figure 7). Additionally, a new completion design was tested on pad 2 to determine completion effects on the staggered configuration. The microseismic derived PSRV shows similar propped to un-propped volume proportions on each pad, at roughly 40%. However, fracture growth is interpreted to change significantly between the two pads; from a propped xf of 290ft for pad 1, as compared to185ft for pad 2, and a propped h of 125ft for pad 1 as compared to 85ft for pad 2. Despite this roughly 30% decrease in height and length, both pads were able to generate near identical productive fracture surface areas of approximately 11 MMsqft. From both tests it is also clear that having staggered wells drastically increases the vertical coverage (SRV and

PSRV) within the entire Lower Eagle Ford section, with minimal PSRV overlap seen in wells within the same target zone (Figure 7).

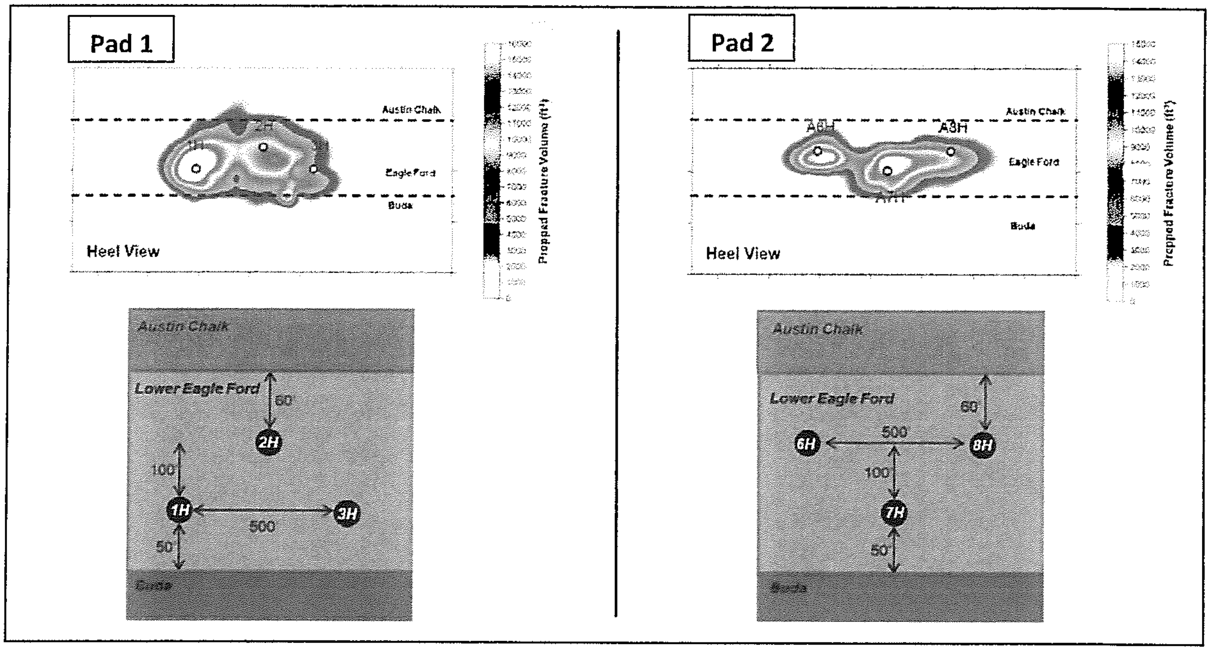

Figure 7: Microseimic "gun barrel" (lateral heal to toe) view displays of propped fracture volume (PSRV) for pad 1 and pad 2. Microseismic demonstrated that having staggered wells drastically increased the vertical coverage (SRV) within the entire Lower Eagle Ford section, with minimal PSRV overlap seen in wells within the same target zone

Discussion

An initial reservoir model was fundamental in establishing the expected geometries and limits of reservoir drainage; implying that enhanced field recovery was viable, but given the limits of the model it did not explicitly suggest how. Understanding the extents of reservoir drainage involved relating geologic attributes to fracture growth/connectivity and better quantifying overall reservoir heterogeneity. From this analysis, it is proposed that numerous bed boundaries and a complex geomechanical stratigraphy creates major restraints to fracture growth, specifically limiting proppant transport, placement and ultimate fracture conductivity, suggesting a clear disconnect between the fractures you can generate and the fractures that can actually produce. This is reflected in the microseismic PSRV, which despite the inherent limitations of the mass balance model, demonstrates that a small portion of the total stimulated volume is propped (roughly 40%) and likely contributing to production.

Wireline, core data and geochemical datasets were utilized in identifying two distinct target zones within the Lower Eagle Ford, each of which displaying geologic properties that are interpreted to yield high matrix to fracture deliverability and overall greater effective matrix drainage of the reservoir. By targeting multiple zones within the same reservoir volume vertical coverage (SRV and PSRV) within the entire Lower Eagle Ford section is maximized allowing access to numerous compartmentalized flow units that are interpreted to be prevalent throughout the section.

Reservoir engineering studies are the link in aiding to justify these claims. Flow analysis from many ultra-low permeability reservoirs suggests that much of the economic productive time of the well is dominated by linear flow from adjacent matrix which surrounds the productive fractures (Bello and Wattenbarger, 2008, Lalehrokh et al., 2013, Miller et al., 2010). This fracture area and matrix can be accounted for by calculating a RTA derived parameter known as Arootk (Sqrt(km)*Acm), being defined as the product of total fracture surface area draining the matrix (Acm) and the square root of matrix permeability (km) (Bello and Wattenbarger, 2008). The Arootk was calculated for the six staggered test wells, with propped surface area estimates from microseismic or SEM derived permeabilities substituted into the equation to solve for km or Acm. The results show that both estimates of Acm and km are within the same order of magnitude as predicted by either variable (Table 1). This suggests that both estimates are reliable in predicting reasonable well deliverability parameters. The Arootk parameter also implies that well delivery is dictated by surface area and not volume, which is important to recognize when interpreting the microseismic results of the two pads with different completions designs. Despite a smaller SRV, pad 2 achieved similar surface area to pad 1 which implies that pad 2 should achieve similar well productivity as pad 1 with the potential of near term/early production enhancement given the likelihood of more near-wellbore fractures. This demonstrates a clear connection between well spacing and completion design.

	Independently Computed Parameters			km Calculated from MS PSRV-A	Acm Calculated from SEM km
	RTA	Microseismic	SEM	Arootk Method	Arootk Method
	Arootk (md*sf)	PSRV-A (sf)	km (nD)	km (nD)	Acm (sf)
Arithmetic Average	77,680	11,344,667	55	60	10,474,392
Median	67,597	11,478,000	38	35	9,114,710

Abbreviations/Nomenclature

**Arootk method; km (matrix permeability) and Acm (total matrix surface area draining into fracture system) solved via equation,*

**Arootk = Sqrt(km)*Acm (Bello and Wattenbarger, 2008)*

**Microseismic (MS), PSRV-A (Propped Stimulated Rock Volume - Surface Area)*

Table 1: Comparison between independently computed parameters for Acm and km and calculated Acm and km via substitution of microseismic and SEM values into the Arootk equation.

Production and production forecasting (decline curve analysis (DCA) and rate transient analysis (RTA)) were used to understand long term productivity and its implications on ultimate field recovery. Currently pad 1 wells have been producing for over 4 months, with pad 2 wells producing for 2 months. Early results are encouraging; all wells are performing similarly or better than offset standalone single zone wells with no clear productivity loss evident between upper and lower target wells (Figure 8). Decline rates and drawdown are stable with an interpreted b factor of 1.2 and average yearly decline rates estimated at 55-65%. Of the two pads, pad 2 is displaying better early time productivity than pad 1, interpreted to be associated with the completion design as described above. Both pads are also producing well above expected condensate rates, with condensate-gas ratios (CGR) averaging 218 bbl/mmcf as compared to direct offsets of less than 180 bbl/mmcf and the computed field average of 85 bbl/mmcf. DCA and RTA estimates indicate an improvement in recovery factor by 4 times compared to the field average assuming similar area assumptions. Completion optimization yielding 185ft well spacing, as indicated by microseismic on pad 2, would see an additional 3 fold (7 times vs. field average) potential improvement.

Future expected production behavior was further investigated by utilizing a multi-well 3D DFN planar fracture model through the use of a commercial simulation software package. The assumptions of the model included: two phase flow (gas and condensate), pressure dependent fracture permeability through time, and no direct fracture communication (each well has independent SRVs) with inter-well communication only being possible through the matrix. A base case run of the model was used to gain insight into what the authors believe is a representative drainage scenario; which assumes a 200ft xf, 100ft h and km of 80 nD in the x and y direction and one tenth km in the z direction within a 20x30 ft cell grid. This was run for the case of: A) single well, B) two wells in the same stratigraphic target zone, and C) three wells in a staggered configuration (Figure 9). The results show that for the two well single zone case interference is observed after 20 years. This is shown to be accelerated to 7 years in the three well staggered case (Figure 9). After the aforementioned time periods, cumulative production begins to deviate from the single well case, with the most drastic effect seen in the three well staggered scenario. Despite the loss in EUR, both cases display minimal loss compared to the single well drainage scenario over 30 years; the two well single zone case is 2% less per well, and the three well staggered case is 7% less per well (Figure 9). It is interpreted that increasing xf, potentially having more fracture planes at identical xf or increasing km would further accelerate interference time. This interpretation can be applied to explain the early time production behavior from pad 2, reflecting more fractures (higher surface area) at a similar xf as compared to pad 1.

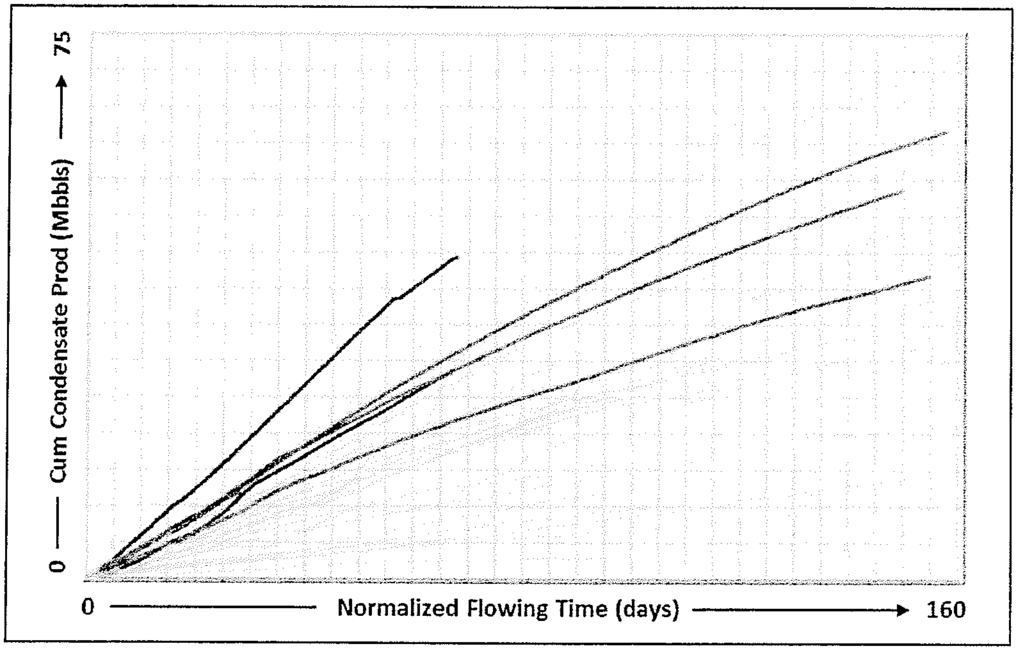

Figure 8: Cumulative condensate production versus time for pad 1 (green) and pad 2 (red) wells, all other wells in the field shown in grey.

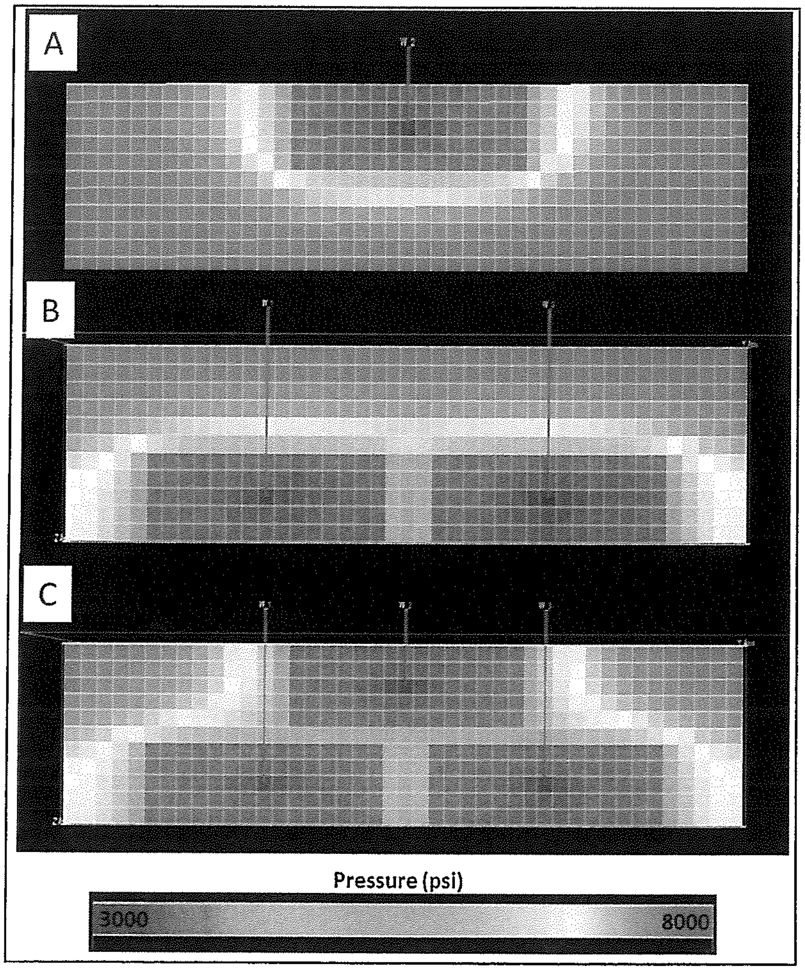
A
B
C
Pressure (psi)
3000
8000

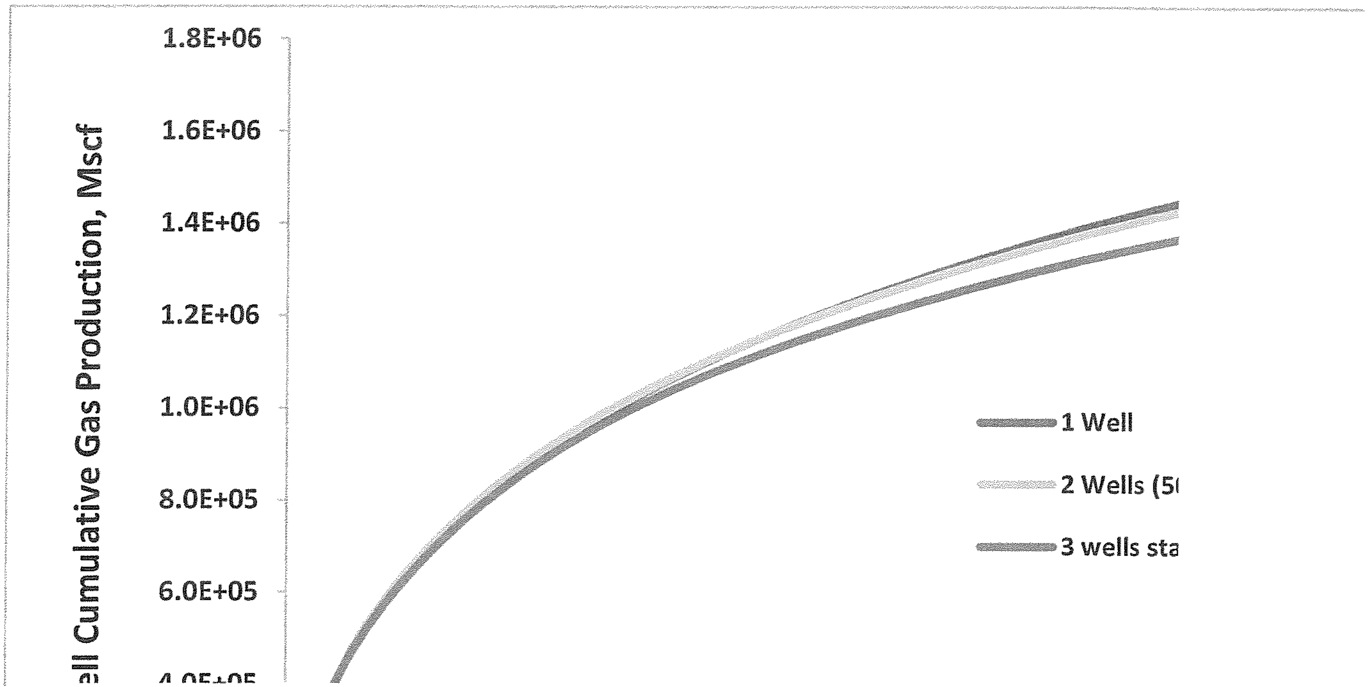

Figure 9: Pressure-time grid display from multi-well 3D DFN planar fracture model. Three cases are shown A) single well, B) two wells within the same stratigraphic target zone and C) three wells in a staggered configuration. The model suggests that despite a loss in EUR for case B and C the loss is minimal compared to the single well case over 30 years.

Conclusions

The immense resource of the Eagle Ford Shale continues to drive efforts for improved field development and optimization. This study has demonstrated that long held recovery factor assumptions within the play are not accurate and fail to capture the realization that the recovery method is dynamic and reliant on geological, technological and economic drivers. This understanding resulted in an extensive evaluation of the implementation of enhanced field recovery methods within the Eagle Ford development area, specifically the use of multi-zone (staggered) lateral downspacing. The analysis and integration of various geoscience and engineering datasets presented herein were crucial in the decision making and technical justification of an initial six well test program. Early production results are extremely encouraging, with forecasted volumes expected to be comparable to standalone single zone wells. Ultimately, these results are expected to have a drastic impact on the future development of the field by dramatically increasing field recoveries and doubling the economic value of the project.

In summary the key findings of this study include:

- Recovery factor in hydraulically stimulated reservoirs is dynamic and limited largely by the technological/economic limits of the stimulation method.
- Geologic heterogeneity must be taken into account in defining potential multi-zone targets and the corresponding differences in generated stimulated rock volume.
- Multi-zone (staggered) downspacing tests have a profound implication on future field development in unconventional reservoirs.

References

Aguilera R., 1999, Recovery Factors and Reserves in Naturally Fractured Reservoirs. Journal of Canadian Petroleum Technology, v. 38, No. 7, pp.15-18.

Allan J., and S. Qing Sun, 2003, Controls on Recovery Factor in Fractured Reservoirs: Lesson Learned from 100 Fractured Fields. SPE 84590 presented at the SPE Annual Technical Conference and Exhibition. Denver, Colorado, USA, October 5-8.

Bello. R.O., and R.A. Wattenbarger, 2008, Rate Transient Analysis in Naturally Fractured Shale Reservoirs. SPE 114591 presented at the CIPC/SPE Gas Technology Symposium 2008 Joint Conference, Calgary, Alberta, Canada, June 16-19.

Calvert S.E., and N.B. Price, 1983, Geochemistry of Namibian Shelf Sediments. In: E. Suess et al. (eds.), Coastal Upwelling its Sediment Record: Plenum Press, New York, USA, p.337-375.

Dong T., and N. B. Harris, 2013, Pore size distribution and morphology in the Horn River Shale, Middle and Upper Devonian, northeastern British Columbia, Canada, In: W. Camp, E. Diaz, and B. Wawak, eds., Electron microscopy of shale hydrocarbon reservoirs: AAPG Memoir 102, p. 67–79.

Driskill B., J. Walls, S. W. Sinclair, and J. DeVito, 2013, Applications of SEM imaging to reservoir characterization in the Eagle Ford Shale, south Texas, U.S.A., In: W. Camp, E. Diaz, and B. Wawak, eds., Electron microscopy of shale hydrocarbon reservoirs: AAPG Memoir 102, p. 115–136.

EIA, 2014, U.S. Crude Oil and Natural Gas Proved Reserves. Accessed 03/10/15
http://www.eia.gov/naturalgas/crudeoilreserves/pdf/usreserves.pdf

EIA, 2015, Eagle Ford Region: Drilling Productivity Report March 2015. Accessed 03/10/15
http://www.eia.gov/petroleum/drilling/pdf/eagleford.pdf

Fisher, M.K., C.A. Wright, B.M. Davidson, A.K. Goodwin, E.O. Fielder, W.S. Buckler and N.P. Steinsberger, 2002, Integrating Fracture Mapping Technologies to Optimize Stimulation in the Barnett Shale. SPE 77441-MS presented at the SPE Annual Technical Conference and Exhibition, San Antonio, Texas, USA, September 29-October 2.

Fishman N., J.M. Guthrie and M. Honarpour, 2013, Development of Organic and Inorganic Porosity in the Cretaceous Eagle Ford Formation, South Texas. Presented at the AAPG Annual Convention and Exhibition, Pittsburg Pennsylvania, May 19-22, Search and Discovery Article #50928 (2014).

Harbor R.L., 2011, Facies Characterization and Stratigraphic Architecture of Organic-Rich Mudrocks, Upper Cretaceous Eagle Ford Formation, South Texas: Master of Science Thesis, The University of Texas at Austin, 184 p.

Hashmy K.H., D. Tonner, S. Abueita, and J. Jonkers, 2012, Shale Reservoirs: Improved Production from Stimulation of Sweet Spots. SPE 158881 presented at the SPE Asia Pacific Oil and Gas Conference and Exhibition, Perth, Australia, October 22-24.

Jarvie D., 2011, Unconventional Oil Petroleum Systems: Shales and Shale Hybrids. Presented at the AAPG International Conference and Exhibition, Calgary, Alberta, Canada, September 12-15, Search and Discovery Article #80131 (2011).

Lalehrokh, F., R. Jayakumar, and R. Yalavarthi, 2013, Multiple Interpretations of Unconventional Well Performance Using Analytical Solutions: A Marcellus Case Study. SPE 168841.

Loucks, R. G., R. M. Reed, S. C. Ruppel, and U. Hammes, 2010, Preliminary classification of matrix pores in mudrocks: Gulf Coast Association of Geological Societies Transactions, v. 60, p. 435–441.

Maxwell, S.C., T.I. Urbancic, N. Steinsberger and R. Zinno, 2002. Microseismic Imaging of Hydraulic Fracture Complexity in the Barnett Shale. SPE 77440 presented at the SPE Annual Technical Conference and Exhibition, San Antonio, Texas, USA, September 29-October 2.

Miller, M.A., C. Jenkins, and R. Rai, 2010, Applying Innovative Production Modeling Techniques to Quantify Fracture Characteristics, Reservoir Properties, and Well Performance in Shale Gas Reservoirs. SPE 139097-MS presented at the Eastern Regional Meeting, Morgantown, West Virginia, October 12-14.

Milliken, K.L., M. Rudnicki, D.N. Awwiller, and T. Zhang, 2013, Organic matter-hosted pore system, Marcellus Formation (Devonian), Pennsylvania: AAPG Bulletin, v.97, No.2 (February 2013) p.177—200.

Pioneer Natural Resources, 2014, Investor Presentation: Accessed on 10/14/14 http://investors.pxd.com/phoenix.zhtml?c=90959&p=irol-presentations

Pommer M.E., 2014. Quantitative Assessment of Pore Types and Pore Size Distribution Across Thermal Maturity, Eagle Ford Formation, South Texas: Master of Science Thesis, The University of Texas at Austin, 208 p.

Rowe, H., S. Ruppel, S. Rimmer, and R. Loucks, 2009, Core-based chemostratigraphy of the Barnett Shale, Permian Basin, Texas. Gulf Coast Association of Geological Societies Transactions, v. 59, p. 675-686.

Shepherd, M., 2009, Factors influencing recovery from oil and gas fields, In: M. Shepherd, Oil field production geology: AAPG Memoir 91, p. 37– 46.

Sierra L., R. Sahai, and M. Mayerhofer, 2014, Quantification of Proppant Distribution Effect on Well Productivity and Recovery Factor of Hydraulically Fractured Unconventional Reservoirs. SPE 171594-MS presented at the SPE/CSUR Unconventional Resources Conference, Calgary, Alberta, Canada, September 30 – October 2.

Smart, K. J., G. I., Ofoegbu, A. P. Morris, R. N. McGinnis, and D. A. Ferrill, 2014, Geomechanical modeling of hydraulic fracturing: Why mechanical stratigraphy, stress state, and pre-existing structure matter. AAPG Bulletin, v. 98, no. 11 (November 2014), pp. 2237–2261.

Tinnin B., G. Hildred, and N.Martinez, 2013, Expanding the Application of Chemostratigraphy within Cretaceous Mudrocks: Estimating Total Organic Carbon and Paleoredox Facies using Major, Minor and Trace Element Geochemistry. SPE 168748/URTeC 1579472 presented at the Unconventional Resources Technology Conference, Denver, Colorado, USA., August 12-14.

Wan J., R.S. Barnum, D.C. DiGloria A. Leahy-Dios, R. Missman, and J. Hemphill, 2013, Factors Controlling Recovery in Liquids Rich Unconventional Systems. IPTC 17103 presented at the International Petroleum Technology Conference, Beijing, China, March 26-28.

Staggered Development Strategy Overview

- Initial staggered and downspacing results encouraging
- TLM kicked off evaluation of downspacing potential in 2012
- First pilot initiated in 2013
- In line with industry views

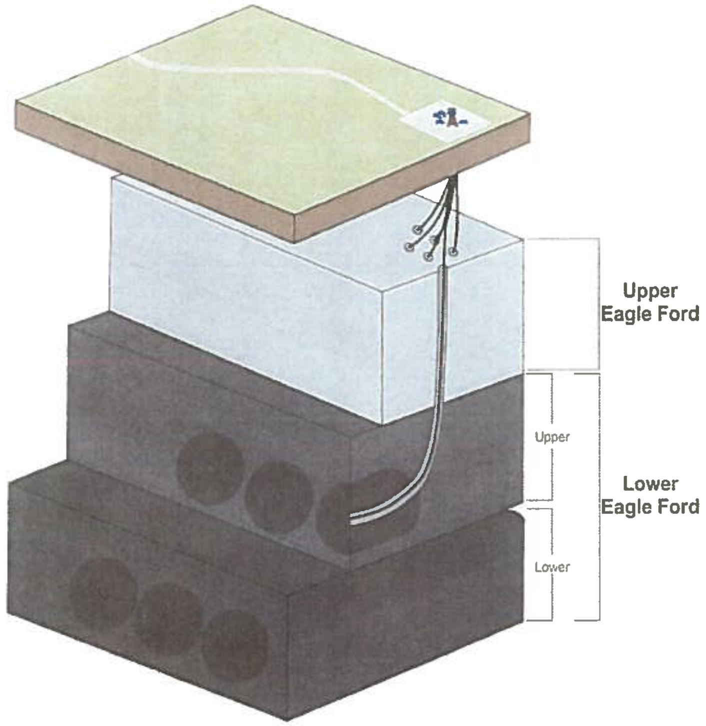
Upper Eagle Ford
Upper
Lower Eagle Ford
Lower

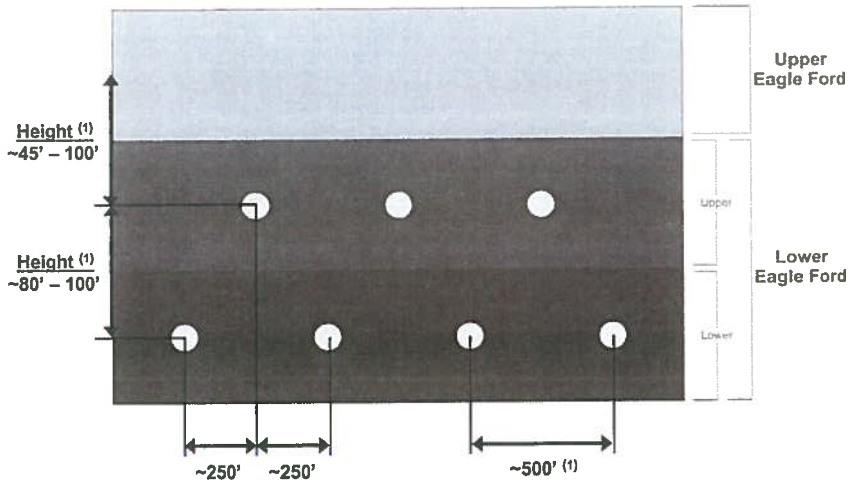
Upper Eagle Ford
Height (1) ~45' – 100'
Upper
Lower Eagle Ford
Height (1) ~80' – 100'
Lower
~250'
~250'
~500' (1)

Note: Illustrations not drawn to scale.
(1) Spacing illustration based on condensate phase window.

Attachment 3

TALISMAN ENERGY USA INC.
DOCKET NO.: 01-0297078, et al.
September 09, 2015

Exhibit 42

Cooke Ranch Lease
Estimated Ultimate Recoveries

Well	Lateral Length (ft)	EUR (MMcf)	Mcf / ft
Cooke Ranch A 1H	5,848	3,232	552.7
Cooke Ranch A 2H	5,858	3,322	567.1
Cooke Ranch A 3H	6,024	2,950	489.7
Cooke Ranch B 2H	4,407	3,118	707.5
Cooke Ranch B 5H	5,232	4,020	768.3
Cooke Ranch C 2H	4,245	1,536	361.8
Cooke Ranch C 3H	3,813	1,904	499.3
Cooke Ranch D 1H	6,475	5,304	819.2
Cooke Ranch D 3H	6,040	3,891	644.2
Cooke Ranch F 1H	5,280	4,084	773.5
Cooke Ranch F 3H	5,341	3,484	652.3
Cooke Ranch C 1H	4,722	1,231	260.7
	Median Mcf/ft =		644.2
	Mean Mcf/ft =		621.4

Did not include C 1H in median / mean due to lost portion of lateral

Proposed Wells	Lateral Length (ft)	Mcf / ft	EUR (MMcf)
Cooke Ranch C 4H	8,270	644.2	5,328
Cooke Ranch C 5H	5,248	644.2	3,381
Cooke Ranch C 6H	5,513	644.2	3,552
Cooke Ranch C 7H	5,512	644.2	3,551
Cooke Ranch C 8H	5,681	644.2	3,660
Cooke Ranch C 9H	5,679	644.2	3,659
Cooke Ranch A 4H	5,476	644.2	3,528
Cooke Ranch A 5H	5,476	644.2	3,528
Cooke Ranch A 6H	5,476	644.2	3,528
Cooke Ranch A 7H	5,476	644.2	3,528
Cooke Ranch A 8H	5,475	644.2	3,527
Cooke Ranch A 9H	5,476	644.2	3,528

Attachment 4

Oil and Gas Docket No. 01-0297078, et al
Talisman Energy USA, Inc.
September 9, 2015 Exhibit No. 54

THE SHALE EVOLUTION:

Zipper Fracture Takes Hold

Trent Jacobs, *JPT* Technology Writer

Attachment 5

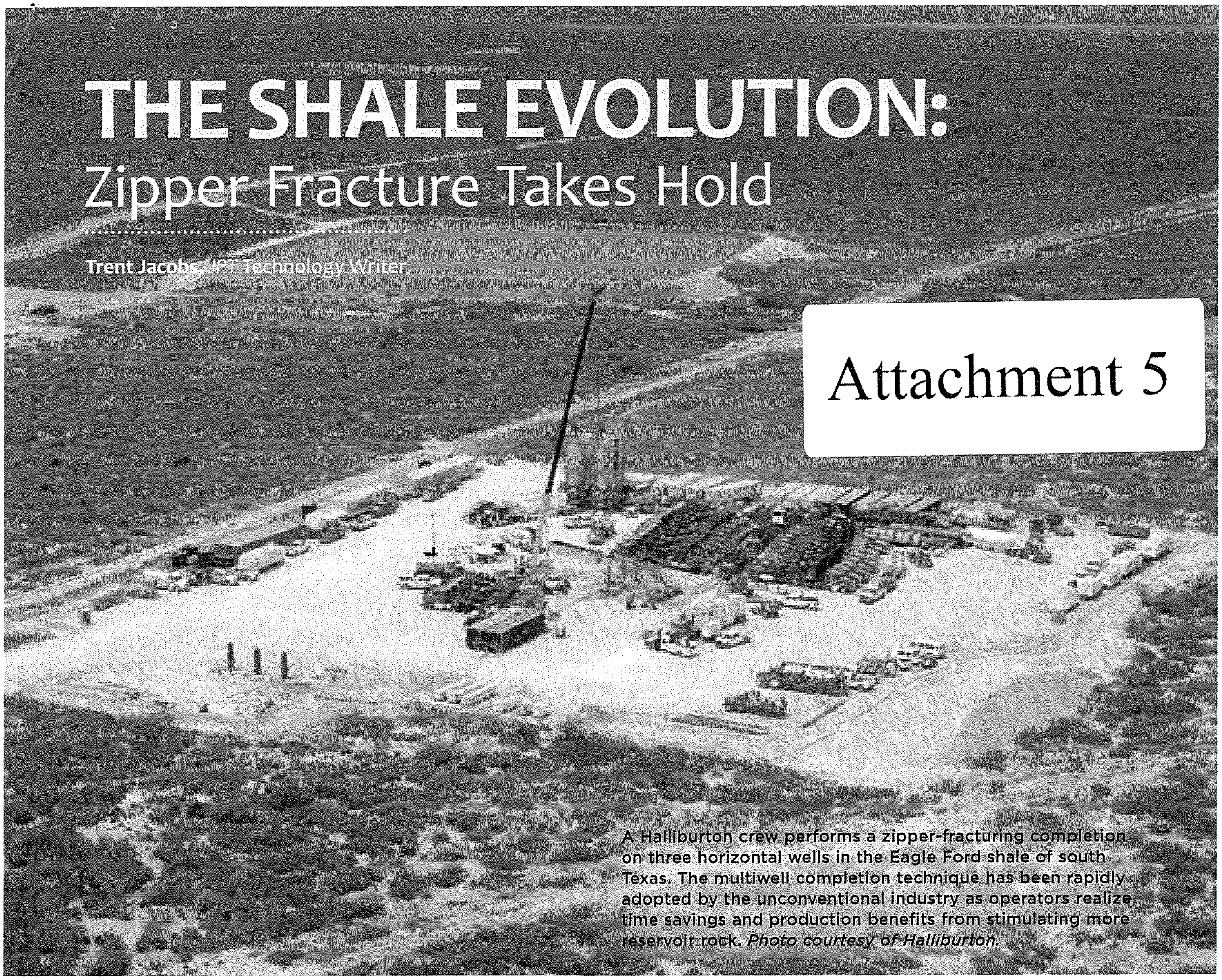

A Halliburton crew performs a zipper-fracturing completion on three horizontal wells in the Eagle Ford shale of south Texas. The multiwell completion technique has been rapidly adopted by the unconventional industry as operators realize time savings and production benefits from stimulating more reservoir rock. *Photo courtesy of Halliburton.*

A horizontal well completion method known as zipper fracturing has been rapidly adopted over the last couple of years by companies in the Eagle Ford shale of south Texas. Instead of drilling and hydraulically fracturing one well at a time, the zipper method involves drilling multiple wells from a pad site and then hydraulically fracturing a stage in one well, while getting ready for the next, as wireline and perforation operations take place in another. The multiwell completion method earns its name from the zipper-like configuration of the fracture stages from wells drilled with relatively tight spacing.

This shaves days off the time it takes to complete a multiwell pad. Many companies in south Texas are now using the completion method on almost every new pad site they drill into, saving tens of millions of dollars per year while accelerating the development of their well inventories.

But the big prize may be that zipper fractures are increasing initial production and estimated ultimate recovery rates when designed so that the fractures stimulate the most reservoir volume possible. Tulsa-based WPX Energy, an independent operator of 160,000 acres in the San Juan Basin of New Mexico, told investors this summer that when the company switched to zipper fracturing, it averaged 420 B/D of oil production compared with 388 B/D from single-well completions. While not entirely sure if zipper fracturing is the direct cause of improved production, WPX said it expects that is the case.

Mukul Sharma, a professor and chair in the petroleum department at the University of Texas at Austin [UT], said field data from Eagle Ford wells make it clear to him that zipper fractures are indeed improving initial production rates and the estimated ultimate recovery. Sharma said operators in south Texas have reported improved initial production rates ranging from 20% to 40% using the zipper method. "I would say that this is definitely the way people are going to be doing a lot of their fractures in the future," he said. "What I think we need to do is understand better how it works—why it works. Once we understand that, we can apply it much more efficiently."

Exhibit No. 83
DOCKET NO. 01-0297078, et al.
Talisman Energy USA, Inc.
January 7, 2016

Marathon Oil first tested the zipper method in the Eagle Ford shale 2 years ago. Today, at least 95% of the company's pad wells are being completed with zipper fractures. This is saving Marathon an average of 4 days in completion time per pad. "Anything with two or more wells, we will zipper frac," said Richie Catlett, completions engineering supervisor at Marathon. "From a completions standpoint, for us the main thing is efficiency. It cuts days off our operations, and that is the big reason we went to zipper fracs."

The Eagle Ford is also where Schlumberger is doing its highest share of zipper fractures, but the company said there is significant momentum behind its adoption outside south Texas, including in the Permian Basin of west Texas and Williston basin in North Dakota. "Nearly half of the completions that we do today in North America are completed with what we call the zipper-fracturing method," said Alejandro Peña, global chemistry and materials portfolio manager at Schlumberger.

As the use of this method spreads, the Eagle Ford shale remains the uncontested zipper-fracturing capital of the world. Two-and-a-half years ago, less than 25% of Halliburton's completion operations in the Eagle Ford were zipper fractures. Since then, that share has grown to 85%. Bill Melton, a completions sales manager at Halliburton, said operators have been inspired to adopt the method more for its completion efficiencies than for its potential production benefits.

"By doing zipper fracs," he said, "a customer can do six to eight frac stages a day. Whereas if they did each well for the entire length, and then switched over to the next well, they could only do three-and-a-half to four stages a day."

Halliburton has even taken the zipper method south of the US border into Mexico for Petróleos Mexicanos, more commonly known as Pemex, where unconventional shale exploration remains in its infancy. The company believes that this could help develop Mexican shale fields, and those elsewhere, relatively quickly compared with the Texas experience, which took years of trial and error to achieve the near-record production levels seen today. "It takes advantage of all the learning that has already been done, and it accelerates their development cycle time," Melton said. "Where it may have taken a year for a US operator to get to a 50-well volume, if they are doing pad drilling and pad completions," non-US operators could be there in a third of the time.

Changes and Challenges

Companies using the zipper method have had to make a few operational considerations that do not apply to single-well completions. When completing horizontal wells one at a time, once the fracturing job in an individual stage is finished, the wireline operation to set plugs and perforate the next stage in the wellbore normally takes 2 to 3 hours, though it can last for as long as 5 hours between stages.

Clifford Phillips, an advanced drilling engineer at Marathon, said when doing zipper fracturing the break in stimulation operations may only last 15 minutes as workers switch from one well to another. "It is a big change operationally for the frac crew," he said. "They go from having a huge amount of dead time in between fracs to almost no time at all."

The constant rate of high-horsepower pumping has a downside for service companies; their pumping trucks are lasting about half as long when working on zipper fractures. Catlett also said zipper fracturing allows service companies fewer opportunities to perform maintenance on in-between jobs. "They have to either provide more pumps, which is getting to be a problem with the industry right now, or they are going to have to provide more efficient pumps that can last longer," he said. "It is a challenge."

With a lot of the extra workload shouldered by the service companies, one challenge for the operator is to make sure that a steady stream of sand or proppant is arriving to the pad site to keep up with the continuous fracturing. Marathon engineers said they like to keep enough proppant on site for at least four or five stages so that if there is an interruption in deliveries, the fracturing crew can keep moving, which increases truck traffic into and out of the pad site substantially.

There are some limitations to deploying the zipper method. On a five-well pad Marathon will only zipper fracture three wells at a time, and then the next two. This is because the crane it uses for the wireline operations only has a radius of 90 ft while the wells are spaced out at approximately 25 ft to 30 ft.

In terms of extra equipment, the only added system requirement is what is called a zipper manifold, which Dennis Donovan, completions engineer at Marathon, described as a "frac stack" turned on its side that redirects the fracturing

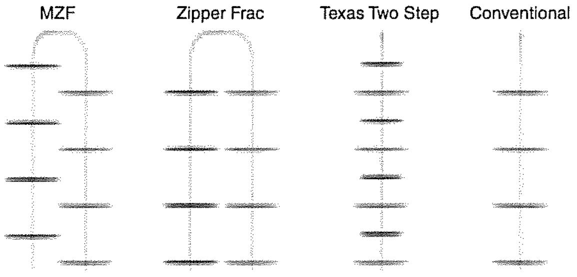

As seen from above, the various types of completion methods that are used to develop shale formations. The modified zipper fracturing (MZF) is the latest evolutionary step taken by the industry to yield more production compared with the regular zipper fracturing and "Texas Two Step," also known as alternating fracturing, where stages are stimulated out of sequence. *Image courtesy of Mohamed Soliman/Texas Tech University.*

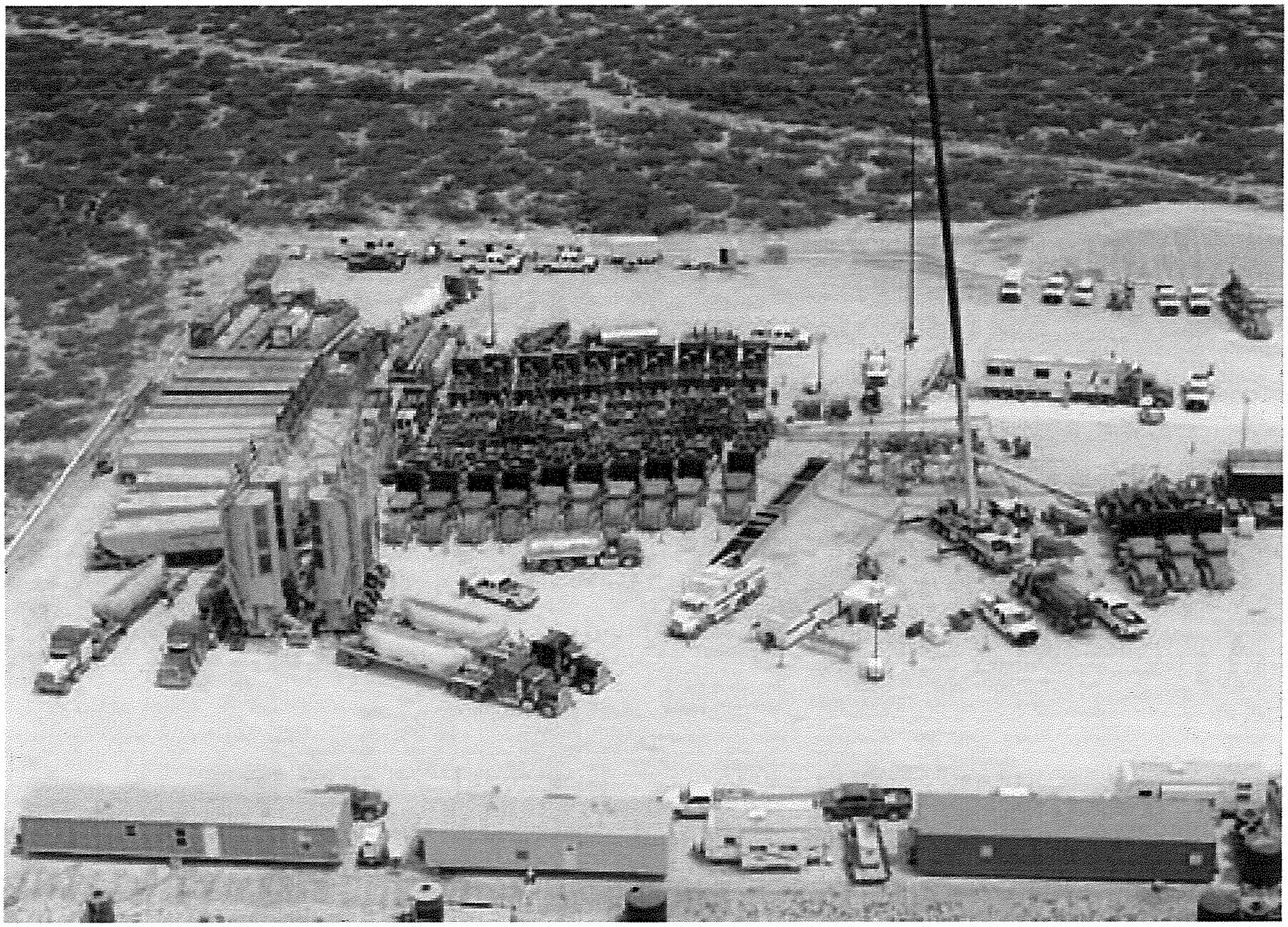

A closer view of a Halliburton zipper-fracturing treatment shows the tight arrangement of pressure pumping trucks, wellheads, and wireline crane. The company said that in less than 3 years, the proportion of zipper-fracturing completions it does in the Eagle Ford shale of Texas has increased threefold to 85%. *Photo courtesy of Halliburton.*

fluids into different wells. "That way we are going down the line from one well to the next," he said. And the cost of the manifold is easily offset by the money saved in rig time and other rental equipment.

Time Delay Critical

When hydraulic fractures propagate into a formation, a stress shadow is created inside the rock that acts like a force field, hindering the fracturing of another stage. As the fracture closes, the spatial extent and the magnitude of the stress shadow is reduced.

Sharma has been studying the role that induced unpropped fractures play in unconventional development for years and has found evidence suggesting that they not only exist, which has been a subject of debate, but they also penetrate into the rock farther than the propped fractures do. He said production history matching, tracer technology, and microseismic monitoring all indicate that induced unpropped fractures tend to form around the propped fractures and then close in a relatively short period of time.

This is important because Sharma believes it is the reason why zipper fractures work. "The stress shadow you see right after you frac the well can have a fairly large spatial extent, but over time this stress shadow will become confined to a region around the main fracture as the induced unpropped fractures close," he said.

Allowing the stress shadow to shrink is believed to make fracturing the subsequent stage in a horizontal well more effective because there will be far less stress interference in the rock from the previous fracture blocking the new fractures.

When hydraulic fractures are closely spaced, the stress shadow effect can lead the fractures to grow away from one another and towards areas of lower stress, which may mean less rock is stimulated. To reduce the effect of the stress shadow, Sharma said some operators are doing four-well zipper fracturing instead of two-well.

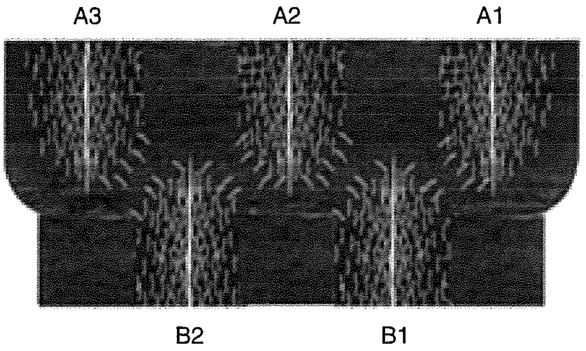

This example shows zipper-fracturing treatments for two wells in the sequence of A1, B1, A2, B2, A3, and so on. ***Image courtesy of Petróleos Mexicanos.***

"You can do Well 1, then 4, come back and do 2, and then do Well 3," he said. "People have tried that and it seems to work." By applying the method to four wells instead of just two, Sharma said the time delay between two adjacent fractures in the wellbore can be extended by a factor of five or six.

One way operators can plan and design for this is by using modeling software that includes the stress shadow effect from adjacent wells. In the past, most commercially available fracturing software modeled one well at a time. Over the past 2 years, Sharma said companies have realized that modeling horizontal well fractures in isolation is insufficient when planning for a zipper-fracturing program. As a result, UT now offers operators software that is able to model more than 100 fracturing stages in a multiwell pad.

Zipper Mechanics

Neal Nagel, chief engineer and principal at Houston-based OilField Geomechanics, started studying zipper fractures several years ago when operators needed help in figuring out why the completion method has increased production for some, but not for others. He said the big question that operators want to know is why does the interaction between two wells potentially increase production?

"There is a strong link between a hydraulic fracture and the natural fractures, and from a geomechanical perspective, we were looking at that," he said. Using a series of numerical tools, called discrete element models, Nagel simulated and evaluated the interaction of hydraulic fracturing with natural fractures. Instead of doing this with a single horizontal well, the simulation was run with a dual-well configuration. What Nagel concluded from his geomechanical evaluations is that there are three primary factors that dictate how well a zipper fracture may perform. They are:

- Existence and conductivity of the natural fractures
- The impact the stress shadow may have on hydraulic fracturing between two wells
- Ability to change the pressure within the natural fractures between two wells

SAFETY CONSIDERATIONS

From the service company's perspective, Halliburton said that the technical hurdles to move from a single-well completion to a multiwell completion, such as in zipper fracturing, are not all that high. Although, the fast-paced operations, extra equipment, and personnel do increase the level of planning needed for a zipper fracturing. "It is really a tremendous exercise in collaboration and optimization to pull some of these very massive jobs off at a very intense rate," Bill Melton, a completions sales manager at Halliburton, said.

Regarding safety, there are other considerations to make as well. One involves preventing a radio signal from errantly inducing an electrical current that might prematurely fire one of the perforating guns used to punch through the casing and into the formation using an explosive shape charge. Halliburton developed its own radio-safe detonators and perforation guns to minimize the risk of an accidental detonation. In a zipper fracture, there are multiple guns that might go off because of an errant radio signal.

Clifford Phillips, an advanced drilling engineer at Marathon, said the company has also implemented its own safety practices at its pad sites to protect workers. After testing the zipper method, the company realized that it could be done safely but it wanted workers to pay even closer attention to the increased number of high-pressure lines to ensure that they are not near people while they are working. "You have to make sure that the wireline guys who are working together with the frac guys are never around each other when there is pressure in the lines," he said.

"It is those three issues combined that we think are the foundational and important issues when zipper fracs work," he said. "When they do not work, one of those three things is essentially missing."

Without natural fractures, Nagel believes that zipper fractures will have zero impact on production. He said one of the reasons that the zipper-fracturing method has taken off in the Eagle Ford shale more than in other areas is because of the prevalence of natural fractures. Unlike in the Barnett, Bakken, Marcellus, and Haynesville shales, operators in the Eagle Ford have reported more pressure communication between adjacent wells. This suggests that natural fractures in the Eagle Ford tend to exhibit greater communication over a longer range than in many other shale plays.

"For those situations like the Marcellus and Haynesville, where it is very uncommon to see operators report pressure communication between wells—that tells you the natural fracture system is not as pervasive or not as connected," Nagel said. "That would mean that you are not

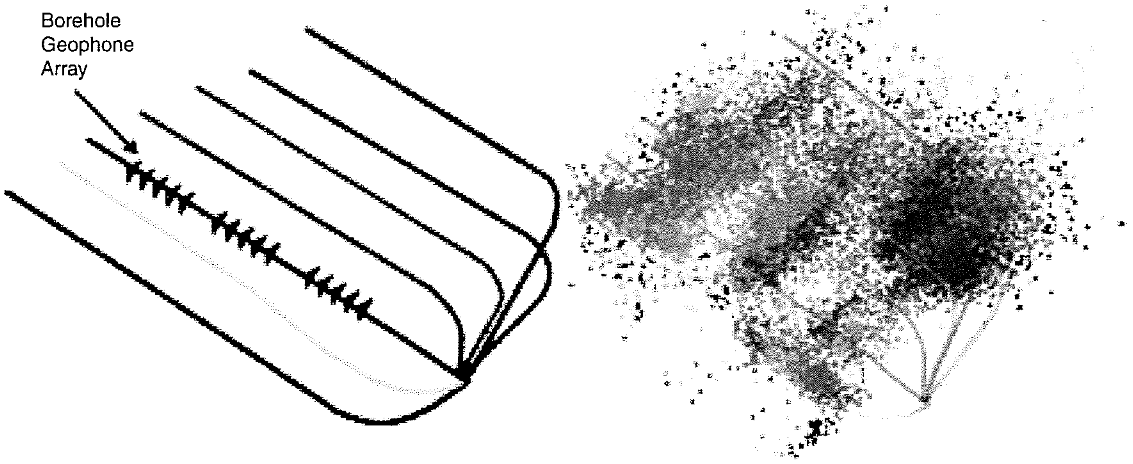

The image on the left shows the position of microseismic geophones and on the right are the microseismic events recorded during a zipper-fracturing sequence. *Image courtesy of Research Partnership to Secure Energy for America, and Gas Technology Institute.*

going to be able to change the pressure between two wells. And without that pressure change, a zipper frac is unlikely to show much benefit."

Also, to achieve a positive production outcome, the wells must be properly spaced, and the fractures need to be long enough so that they touch and overlap with one another, thus ensuring there is communication between adjacent wells.

An SPE paper published by Halliburton this year, which evaluated the benefit of zipper fractures in unconventional reservoirs ran simulations that showed when zipper fractures overlap the incremental recovery factor was in the range of 15% to 20%, compared with zipper fractures that do not overlap.

Based on the field data and case study work he has done, Nagel is convinced that pore pressure is the most important factor leading to a zipper fracture that nets higher stimulated reservoir volume and thus production. "When I create a hydraulic fracture, I am injecting at a pressure higher than the minimum in-situ stress, which, by definition, has to be greater than my pore pressure," he said.

The effect of the increased pore pressure is that the natural fractures are induced to slip more, thereby increasing the permeability and flow capacity of the source rock, as Nagel's research suggests, and is responsible for the higher productivity in zipper-fractured wells. He said these subsurface events can be detected and observed using microseismic technology.

"When zipper fracs work, we have a configuration where the pressure increase from the first well increases the pressure in the region of the second well," Nagel said. "When we frac that second well, what it [increased pressure] does is make it easier for the natural fractures and weakness planes to slip; we see greater microseismicity, we see increase in flow capacity, and we see an increase in production."

Modified Zipper Fracture

Before Mohamed Soliman became the chair at Texas Tech University's petroleum engineering department in 2011, he worked for Halliburton for 32 years and holds 26 patents on hydraulic-fracturing technology. One of the patents that Soliman received while at the company was for the alternating fracturing, a precursor to the more efficient modified zipper fracture, which also was designed to breakup as much rock to create more complex fracture networks.

"We came up with alternating fracturing which is done from one well. You create a fracture, then you create another

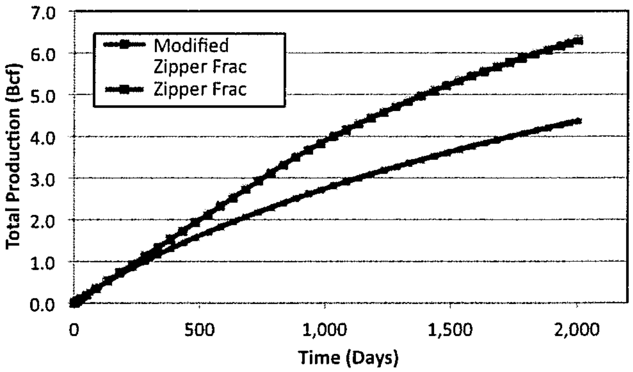

Simulation results of two wells show the modified zipper fracture (MZF) increasing gas production by 44% more than the original zipper fracture due to the increased fracture complexity. *Graph courtesy of Mohamed Soliman/ Texas Tech University.*

DIVERSION TECHNOLOGY COMPLEMENTS ZIPPER FRACTURES

A primary driver behind the adoption of zipper fractures has been to reduce the money and time spent completing a series of wells. Service companies such as Schlumberger are now incorporating ancillary technologies, such as diverting agents to boost the efficiency of zipper fractures even more. The fracturing technology is called BroadBand Sequence by Schlumberger, and involves a diverting agent made of biodegradable composite particles and fibers, and is also used in refracturing operations where it is difficult or impossible to re-enter an older well to set and remove plugs.

In most fracturing operations, be they multiwell or single-well, mechanical devices such as bridge plugs are used to isolate each stage so that the hydraulic pressure flows into the targeted interval. The process is continued systematically along the length of a horizontal well. By using a diverting agent operators save several trips in and out of the well with wireline and coiled tubing units to set and then mill out the plugs. Other service companies, including Weatherford, Halliburton, and Baker Hughes have also developed their own diversion fluids for stimulation operations.

In addition to saving on completion time, Schlumberger touts its ability to help improve oil and gas production by increasing the reservoir contact of the stimulation operation. This year Marathon and Schlumberger co-authored an SPE technical paper detailing a case study of a zipper-fracturing operation in the Eagle Ford shale, which showed the incorporation of a diverting agent improved production by about 20% compared with an adjacent well that used the same completion parameters, minus the use of the BroadBand Sequence technique. Alejandro Peña, global chemistry and materials portfolio manager at Schlumberger, said that the net production gain seen in the case study is an average result for horizontal completions.

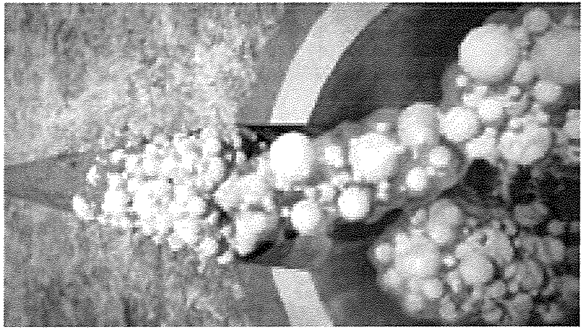

Designed to increase the effectiveness of hydraulic fracturing, Schlumberger's biodegradable composite diverting agent is one technology that has the ability to further improve the efficiency of zipper fractures. *Image courtesy of Schlumberger.*

When using its newly commercialized technology, the company follows a prescribed workflow to assess how much composite material is needed and then the crew pumps it downhole. "We have at the wellsite a dedicated pump, which connects at the discharge of the fracturing fleet before you enter the wellbore," said Peña. "We inject the [composite material] right at the end of the fracturing treatment to basically provide temporary isolation in the fractures that have just been stimulated."

The company introduced BroadBand Sequence in February and reported that the proportion of completions that it is used in is already in the "double digits." It did not provide a figure.

fracture, and then you go in the middle to create another fracture," he said. "Needless to say, operationally this is not exactly what you would want to do."

Soliman explained that technology has been created to lessen the complications involved with fracturing stages out of sequence but there are too many operational complexities to work through. "It can be done, but it is a headache," he said.

When Soliman got to Texas Tech he and his research students took a look back at alternating fracturing and also the emerging zipper-fracture method to see if there was a way to net similar production results from alternating fracturing, but without the operational complexity.

What they ended up inventing was the modified zipper fracture that differs from a normal zipper fracture. Rather than having the fractures of two adjacent wells pointing toward one another, they are staggered so the fractures will overlap with one another. Soliman said that with the modified zipper fracturing operators get the benefits of alternating fracturing without all the extra work.

"You probably will have to have your horizontal wells a little closer than you would have in a regular zipper frac, or you create a fracture that is a little longer," he said. "Another issue is that it will require more engineering work ahead of the drilling. You need to acquire some data, and do your homework."

Soliman said he and a graduate student have created a simulation software to further study fracture attraction. The software has not yet been commercialized but Soliman said he expects to present it at future SPE conferences.

One of the most intriguing aspects of the overlapping fractures that Soliman has observed is that

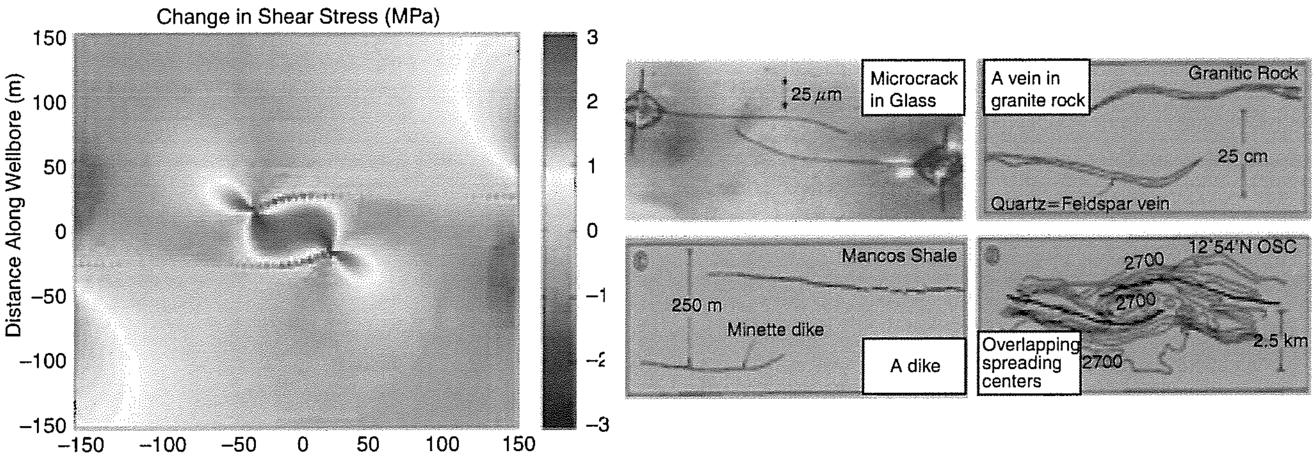

To verify their fracture model (left), which showed that as two fractures propagate towards one another they begin to demonstrate a physical attraction, researchers from Texas Tech University looked for other examples and found that the phenomenon is ubiquitous in the natural world. ***Image courtesy of Mohamed Soliman/Texas Tech University.***

as the fractures propagate towards one another, once they are in very close proximity, they begin to show an attraction. Soliman said he has recently completed research work on this phenomenon and will publish the results later this year.

"If you have fractures coming fairly close to one another, they will actually turn around towards each other," he said. "It is very interesting. It looks almost as if it does not make sense, but when you think about the calculations of how stresses change—it does." **JPT**

INNOVATIVE SOLUTIONS FOR AN EVOLVING WORLD.

NORTH AMERICA | EUROPE | MIDDLE EAST | SOUTH AMERICA | SOUTHEAST ASIA

We have been busy—aggressively on the move to meet the growing needs of energy customers around the world with the solutions and services they have come to expect. That includes the highest quality tubular connection and hydraulic power equipment, like our weCATT™ wireless torque sub. Onshore or offshore, rest assured that wherever you are, we are there.

/// WWW.MCCOYGLOBAL.COM

MCCOY GLOBAL

MOVING GLOBAL ENERGY FORWARD

Oil and Gas Docket No. 01-0297078, et al
Talisman Energy USA, Inc.
September 9, 2015 Exhibit No. 52

Cooke Ranch A1 History Match

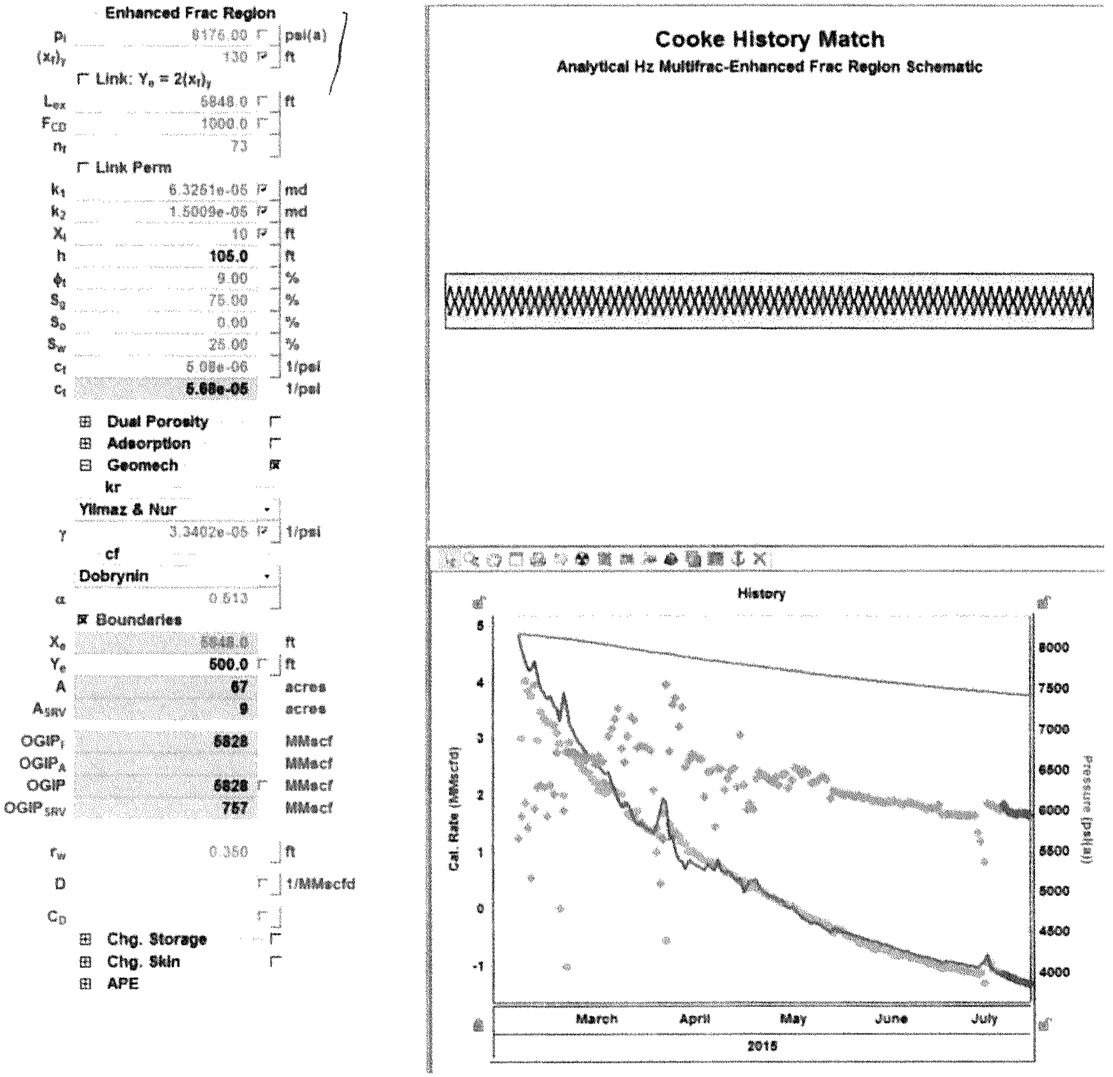

Enhanced Frac Region

p_i	8175.00	☐	psi(a)
$(x_f)_y$	130	☑	ft
☐ Link: $Y_e = 2(x_f)_y$			
L_{ex}	5848.0	☐	ft
F_{CD}	1000.0	☐	
n_f	73		
☐ Link Perm			
k_1	6.3251e-06	☑	md
k_2	1.5009e-05	☑	md
X_i	10	☑	ft
h	**105.0**		ft
ϕ_t	9.00		%
S_g	75.00		%
S_o	0.00		%
S_w	25.00		%
c_f	5.08e-06		1/psi
c_t	**5.68e-05**		1/psi
⊞ Dual Porosity		☐	
⊞ Adsorption		☐	
⊟ Geomech		☒	
kr	Yilmaz & Nur		
γ	3.3402e-05	☑	1/psi
cf	Dobrynin		
α	0.613		
☒ Boundaries			
X_e	5848.0		ft
Y_e	**500.0**	☐	ft
A	**67**		acres
A_{SRV}	**9**		acres
$OGIP_f$	**5828**		MMscf
$OGIP_A$			MMscf
OGIP	**5828**	☐	MMscf
$OGIP_{SRV}$	**757**		MMscf
r_w	0.350		ft
D		☐	1/MMscfd
C_D		☐	
⊞ Chg. Storage		☐	
⊞ Chg. Skin		☐	
⊞ APE			

Cooke History Match
Analytical Hz Multifrac-Enhanced Frac Region Schematic
History
Cal. Rate (MMscfd)
5
4
3
2
1
0
-1
Pressure (psi(a))
8000
7500
7000
6500
6000
5500
5000
4500
4000
March
April
May
June
July
2015

Attachment 6

Cooke Ranch A1 Forecast

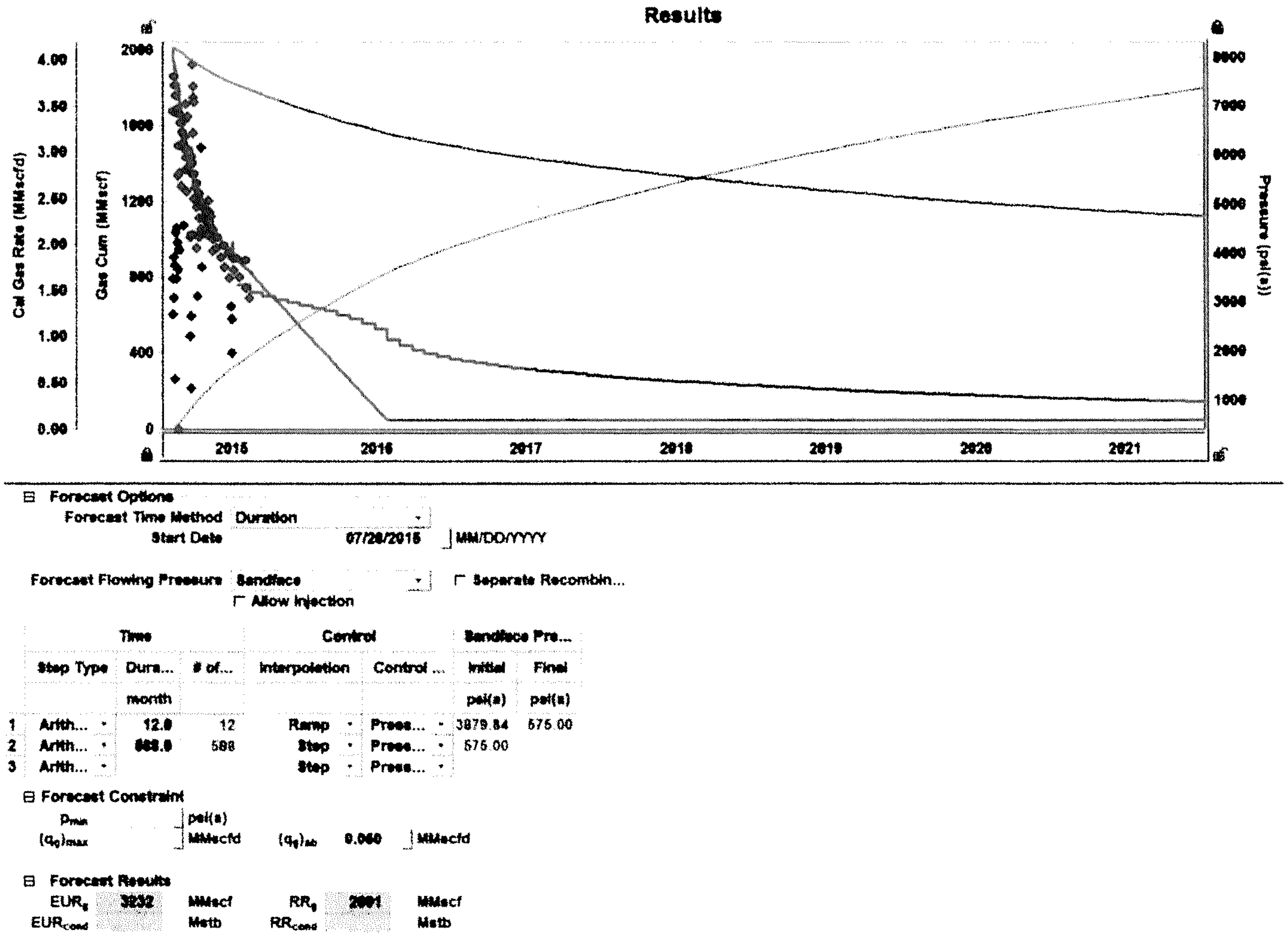
Results
Cal Gas Rate (MMscfd)
4.00
3.50
3.00
2.50
2.00
1.50
1.00
0.50
0.00
Gas Cum (MMscf)
2000
1600
1200
800
400
0
Pressure (psi(a))
8000
7000
6000
5000
4000
3000
2000
1000
2015
2016
2017
2018
2019
2020
2021

⊟ **Forecast Options**

Forecast Time Method Duration

Start Date 07/28/2015 MM/DD/YYYY

Forecast Flowing Pressure Sandface ☐ Separate Recombin...

☐ Allow Injection

	Time			Control		Sandface Pre...	
	Step Type	Dura...	# of...	Interpolation	Control ...	Initial	Final
		month				psi(a)	psi(a)
1	Arith...	12.0	12	Ramp	Press...	3879.84	575.00
2	Arith...	588.0	588	Step	Press...	575.00	
3	Arith...			Step	Press...		

⊟ **Forecast Constraint**

p_{min} psi(a)

$(q_g)_{max}$ MMscfd $(q_g)_{ab}$ 0.060 MMscfd

⊟ **Forecast Results**

EUR_g 3232 MMscf RR_g 2001 MMscf

EUR_{cond} Mstb RR_{cond} Mstb

Cooke Ranch A2 History Match

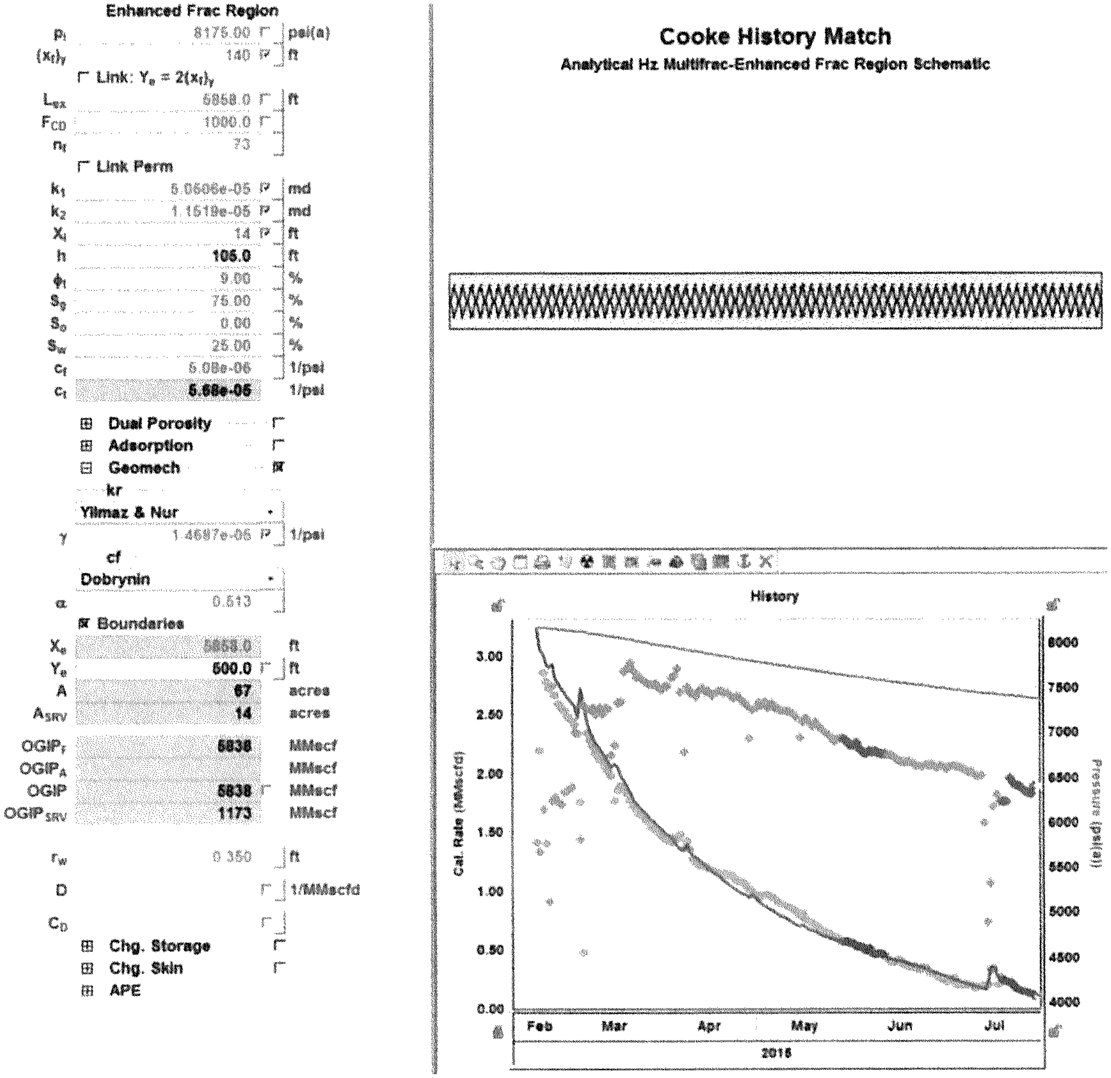

Enhanced Frac Region

p_i	8175.00	☐	psi(a)
$(x_f)_y$	140	☑	ft

☐ Link: $Y_e = 2(x_f)_y$

L_{ex}	5858.0	☐	ft
F_{CD}	1000.0	☐	
n_f	73		

☐ Link Perm

k_1	5.0606e-05	☑	md
k_2	1.1519e-05	☑	md
X_i	14	☑	ft
h	**105.0**		ft
ϕ_t	9.00		%
S_g	75.00		%
S_o	0.00		%
S_w	25.00		%
c_f	5.08e-06		1/psi
c_t	**5.68e-05**		1/psi

⊞ **Dual Porosity** ☐
⊞ **Adsorption** ☐
⊟ **Geomech** ☒

kr

Yilmaz & Nur

γ	1.4687e-06	☑	1/psi

cf

Dobrynin

α	0.513		

☒ **Boundaries**

X_e	5858.0		ft
Y_e	**500.0**	☐	ft
A	**67**		acres
A_{SRV}	**14**		acres
$OGIP_f$	**5838**		MMscf
$OGIP_A$			MMscf
OGIP	**5838**	☐	MMscf
$OGIP_{SRV}$	**1173**		MMscf
r_w	0.350		ft
D		☐	1/MMscfd
C_D		☐	

⊞ **Chg. Storage** ☐
⊞ **Chg. Skin** ☐
⊞ **APE**

Cooke History Match

Analytical Hz Multifrac-Enhanced Frac Region Schematic

History
Cal. Rate (MMscfd)
0.00
0.50
1.00
1.50
2.00
2.50
3.00
Pressure (psi(a))
4000
4500
5000
5500
6000
6500
7000
7500
8000
Feb
Mar
Apr
May
Jun
Jul
2016

Cooke Ranch A2 Forecast

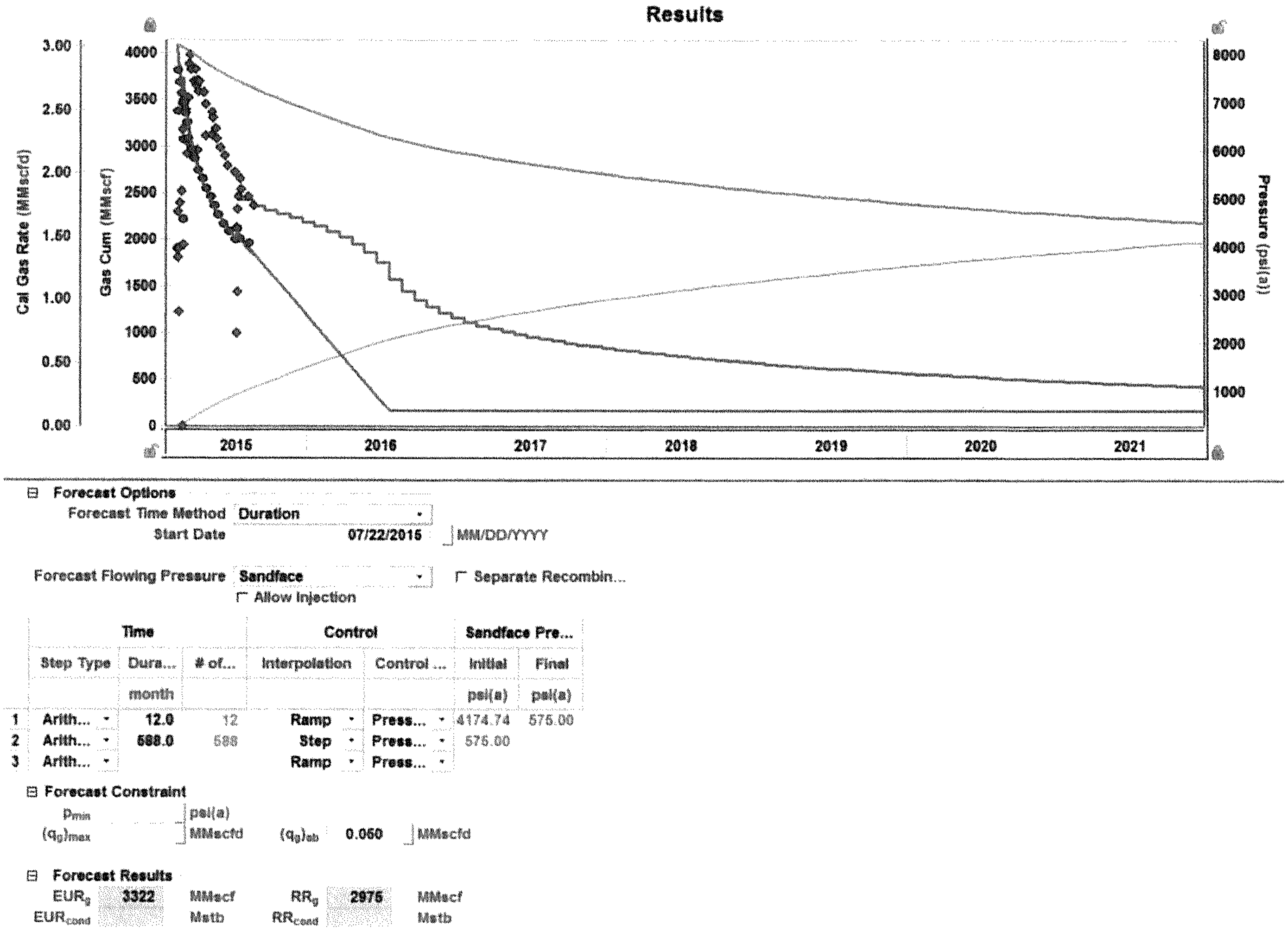
Results
Cal Gas Rate (MMscfd)
3.00
2.50
2.00
1.50
1.00
0.50
0.00
Gas Cum (MMscf)
4000
3500
3000
2500
2000
1500
1000
500
0
Pressure (psi(a))
8000
7000
6000
5000
4000
3000
2000
1000
2015
2016
2017
2018
2019
2020
2021

⊟ **Forecast Options**

Forecast Time Method: Duration

Start Date: 07/22/2015 MM/DD/YYYY

Forecast Flowing Pressure: Sandface

☐ Separate Recombin...

☐ Allow Injection

	Time			Control		Sandface Pre...	
	Step Type	Dura...	# of...	Interpolation	Control ...	Initial	Final
		month				psi(a)	psi(a)
1	Arith...	12.0	12	Ramp	Press...	4174.74	575.00
2	Arith...	588.0	588	Step	Press...	575.00	
3	Arith...			Ramp	Press...		

⊟ **Forecast Constraint**

p_{min} psi(a)

$(q_g)_{max}$ MMscfd $(q_g)_{ab}$ 0.050 MMscfd

⊟ **Forecast Results**

EUR_g 3322 MMscf RR_g 2975 MMscf

EUR_{cond} Mstb RR_{cond} Mstb

Cooke Ranch A3 History Match

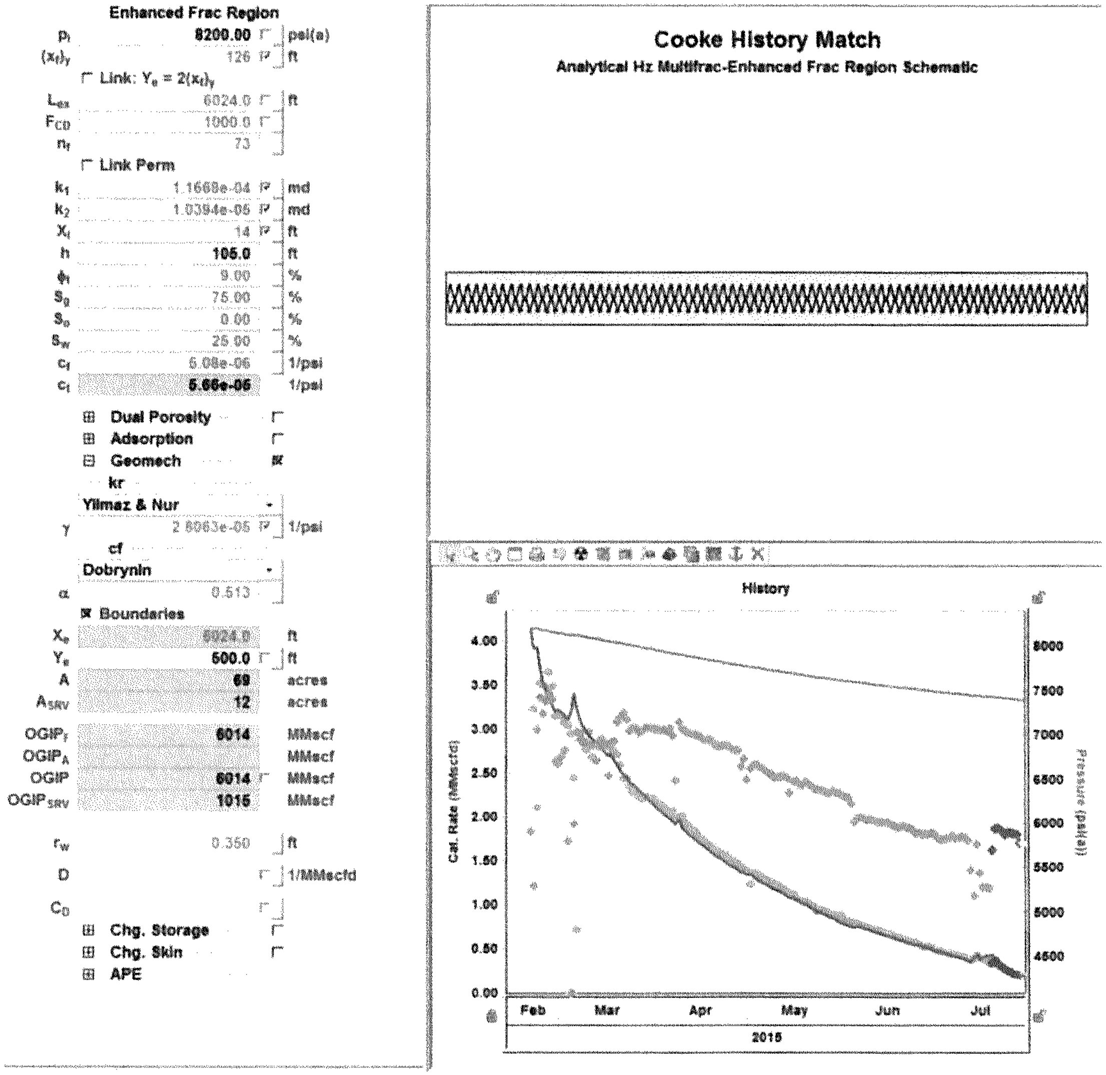

Enhanced Frac Region

p_i	8200.00	☐	psi(a)
$(x_f)_y$	126	☑	ft

☐ Link: $Y_e = 2(x_f)_y$

L_{ex}	6024.0	☐	ft
F_{CD}	1000.0	☐	
n_f	73		

☐ Link Perm

k_1	1.1668e-04	☑	md
k_2	1.0394e-05	☑	md
X_i	14	☑	ft
h	106.0		ft
ϕ_t	9.00		%
S_g	75.00		%
S_o	0.00		%
S_w	25.00		%
c_f	6.08e-06		1/psi
c_t	5.66e-05		1/psi

⊞ Dual Porosity ☐
⊞ Adsorption ☐
⊟ Geomech ☒

kr
Yilmaz & Nur

γ	2.8063e-05	☑	1/psi

cf
Dobrynin

α	0.513		

☒ Boundaries

X_e	6024.0		ft
Y_e	500.0	☐	ft
A	69		acres
A_{SRV}	12		acres
$OGIP_f$	6014		MMscf
$OGIP_A$			MMscf
OGIP	6014	☐	MMscf
$OGIP_{SRV}$	1016		MMscf
r_w	0.350		ft
D		☐	1/MMscfd
C_D		☐	

⊞ Chg. Storage ☐
⊞ Chg. Skin ☐
⊞ APE

Cooke History Match

Analytical Hz Multifrac-Enhanced Frac Region Schematic

History
Cal. Rate (MMscfd)
4.00
3.50
3.00
2.50
2.00
1.50
1.00
0.50
0.00
Pressure (psi(a))
8000
7500
7000
6500
6000
5500
5000
4500
Feb
Mar
Apr
May
Jun
Jul
2015

Cooke Ranch A3 Forecast

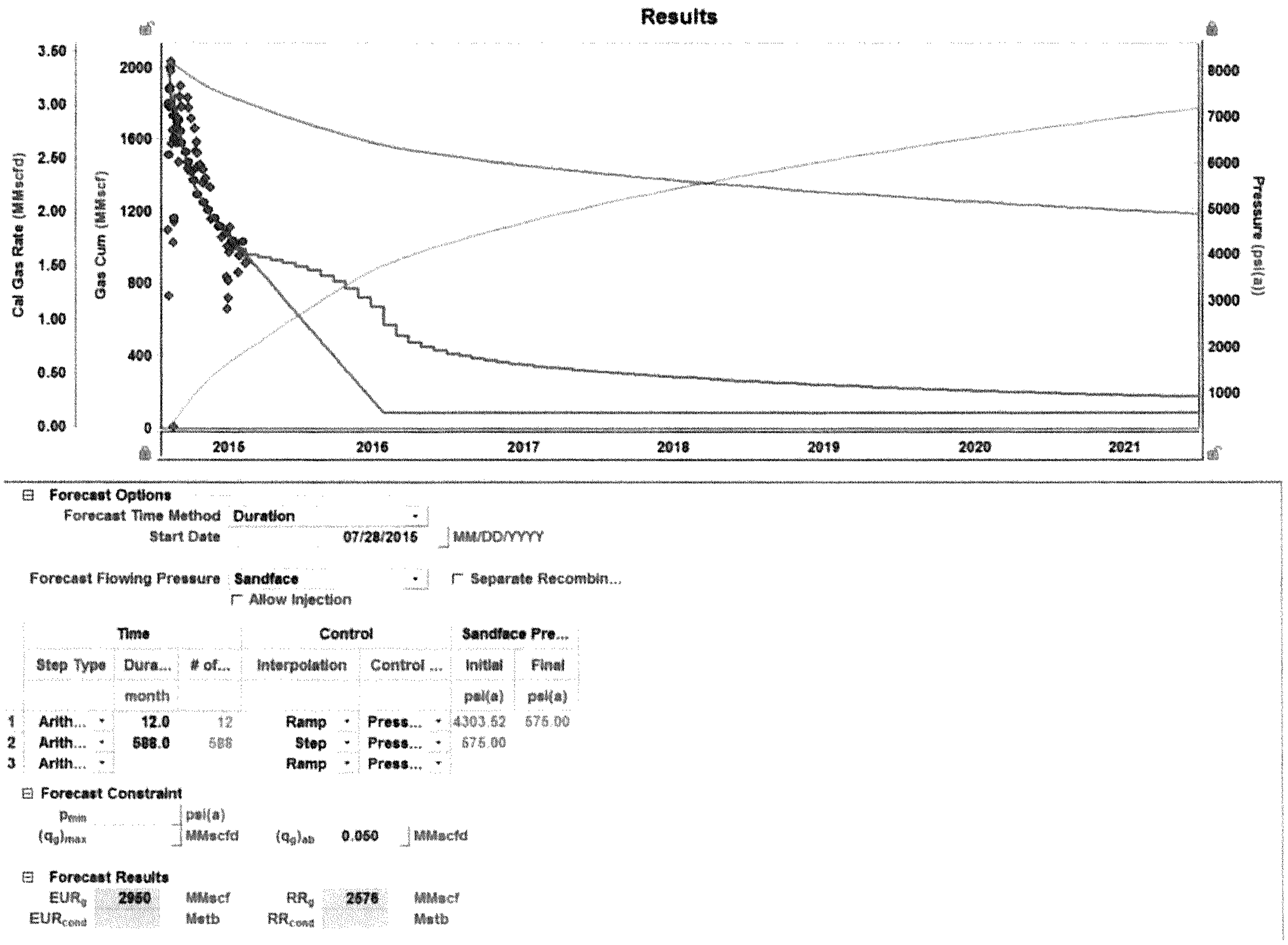
Results
Cal Gas Rate (MMscfd)
3.50
3.00
2.50
2.00
1.50
1.00
0.50
0.00
Gas Cum (MMscf)
2000
1600
1200
800
400
0
Pressure (psi(a))
8000
7000
6000
5000
4000
3000
2000
1000
2015
2016
2017
2018
2019
2020
2021

⊟ **Forecast Options**

Forecast Time Method: **Duration**

Start Date: **07/28/2015** MM/DD/YYYY

Forecast Flowing Pressure: **Sandface**

☐ Separate Recombin...

☐ Allow Injection

	Time			Control		Sandface Pre...	
	Step Type	Dura...	# of...	Interpolation	Control ...	Initial	Final
		month				psi(a)	psi(a)
1	Arith...	12.0	12	Ramp	Press...	4303.52	575.00
2	Arith...	588.0	588	Step	Press...	575.00	
3	Arith...			Ramp	Press...		

⊟ **Forecast Constraint**

p_{min} psi(a)

$(q_g)_{max}$ MMscfd $(q_g)_{ab}$ 0.050 MMscfd

⊟ **Forecast Results**

EUR_g 2950 MMscf RR_g 2576 MMscf

EUR_{cond} Mstb RR_{cond} Mstb

Cooke Ranch B2H History Match

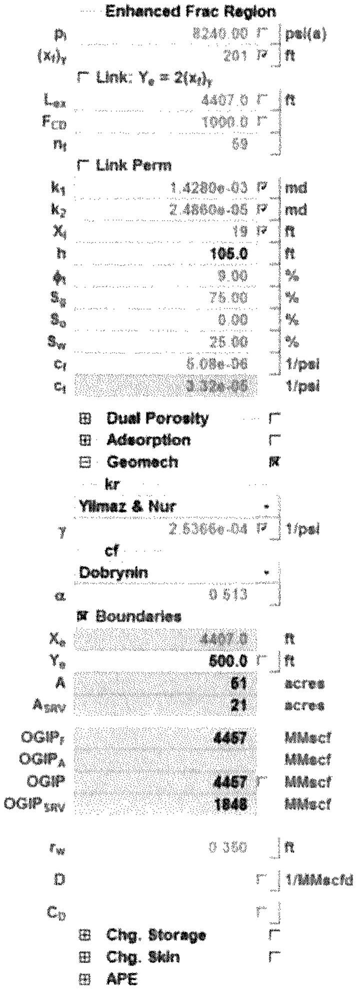

Enhanced Frac Region

p_i	8240.00	☐	psi(a)
$(x_f)_y$	201	☑	ft
☐ Link: $Y_e = 2(x_f)_y$			
L_{ex}	4407.0	☐	ft
F_{CD}	1000.0	☐	
n_f	59		
☐ Link Perm			
k_1	1.4280e-03	☑	md
k_2	2.4860e-05	☑	md
X_i	19	☑	ft
h	**105.0**		ft
ϕ_i	9.00		%
S_g	75.00		%
S_o	0.00		%
S_w	25.00		%
c_f	5.08e-06		1/psi
c_t	3.32e-05		1/psi
⊞ **Dual Porosity**		☐	
⊞ **Adsorption**		☐	
⊟ **Geomech**		☒	
kr			
Yilmaz & Nur			
γ	2.5366e-04	☑	1/psi
cf			
Dobrynin			
α	0.513		
☒ **Boundaries**			
X_e	4407.0		ft
Y_e	**500.0**	☐	ft
A	**51**		acres
A_{SRV}	**21**		acres
$OGIP_F$	**4457**		MMscf
$OGIP_A$			MMscf
OGIP	**4457**	☐	MMscf
$OGIP_{SRV}$	**1848**		MMscf
r_w	0.350		ft
D		☐	1/MMscfd
C_D		☐	
⊞ **Chg. Storage**		☐	
⊞ **Chg. Skin**		☐	
⊞ **APE**			

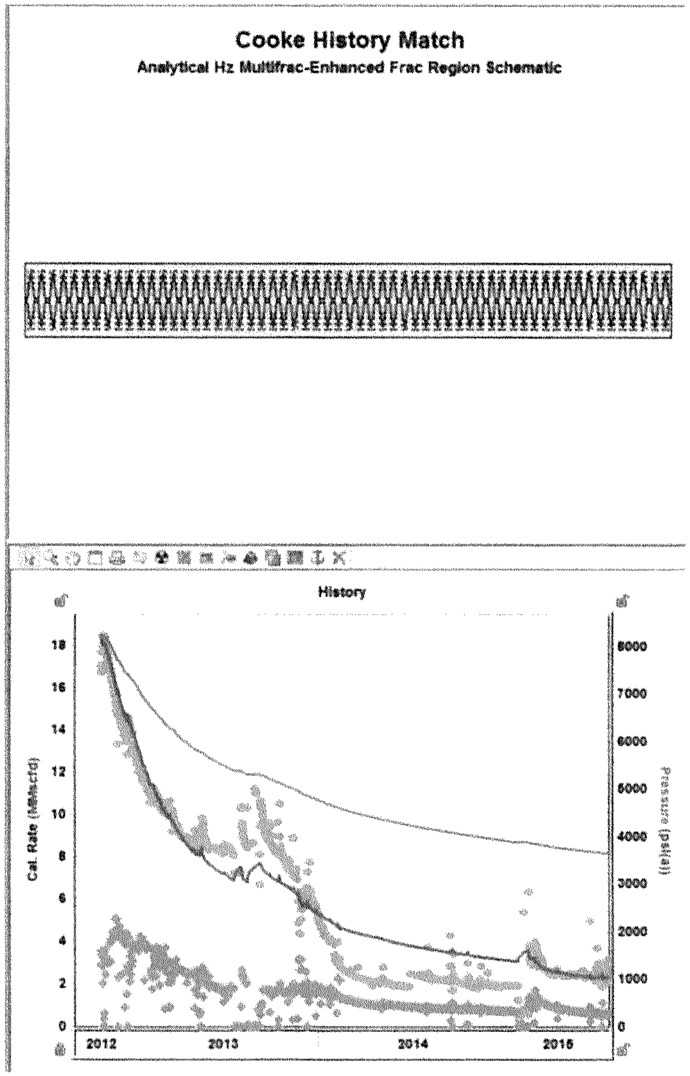

Cooke Ranch B2H Forecast

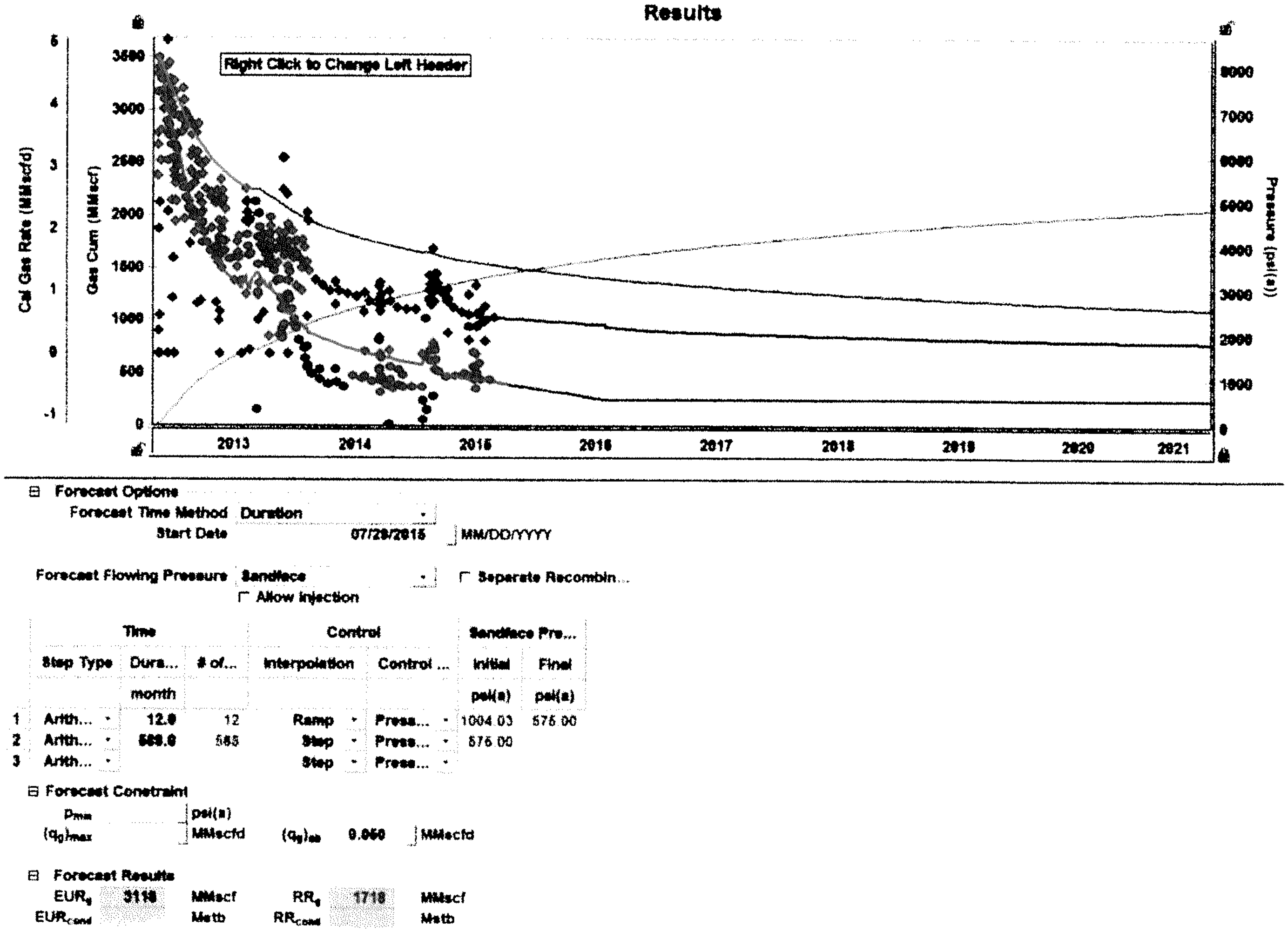
Results
Right Click to Change Left Header
Cal Gas Rate (MMscfd)
5
4
3
2
1
0
-1
Gas Cum (MMscf)
3500
3000
2500
2000
1500
1000
500
0
Pressure (psi(a))
8000
7000
6000
5000
4000
3000
2000
1000
0
2013
2014
2015
2016
2017
2018
2019
2020
2021

⊟ **Forecast Options**

Forecast Time Method: Duration

Start Date: 07/29/2015 MM/DD/YYYY

Forecast Flowing Pressure: Sandface

☐ Separate Recombin...

☐ Allow injection

	Time			Control		Sandface Pre...	
	Step Type	Dura...	# of...	Interpolation	Control ...	Initial	Final
		month				psi(a)	psi(a)
1	Arith...	12.0	12	Ramp	Press...	1004.03	576.00
2	Arith...	585.0	585	Step	Press...	576.00	
3	Arith...			Step	Press...		

⊟ **Forecast Constraint**

p_{min} psi(a)

$(q_g)_{max}$ MMscfd $(q_g)_{ab}$ 0.050 MMscfd

⊟ **Forecast Results**

EUR_g	3118	MMscf	RR_g	1718	MMscf
EUR_{cond}		Mstb	RR_{cond}		Mstb

Cooke Ranch B5 History Match

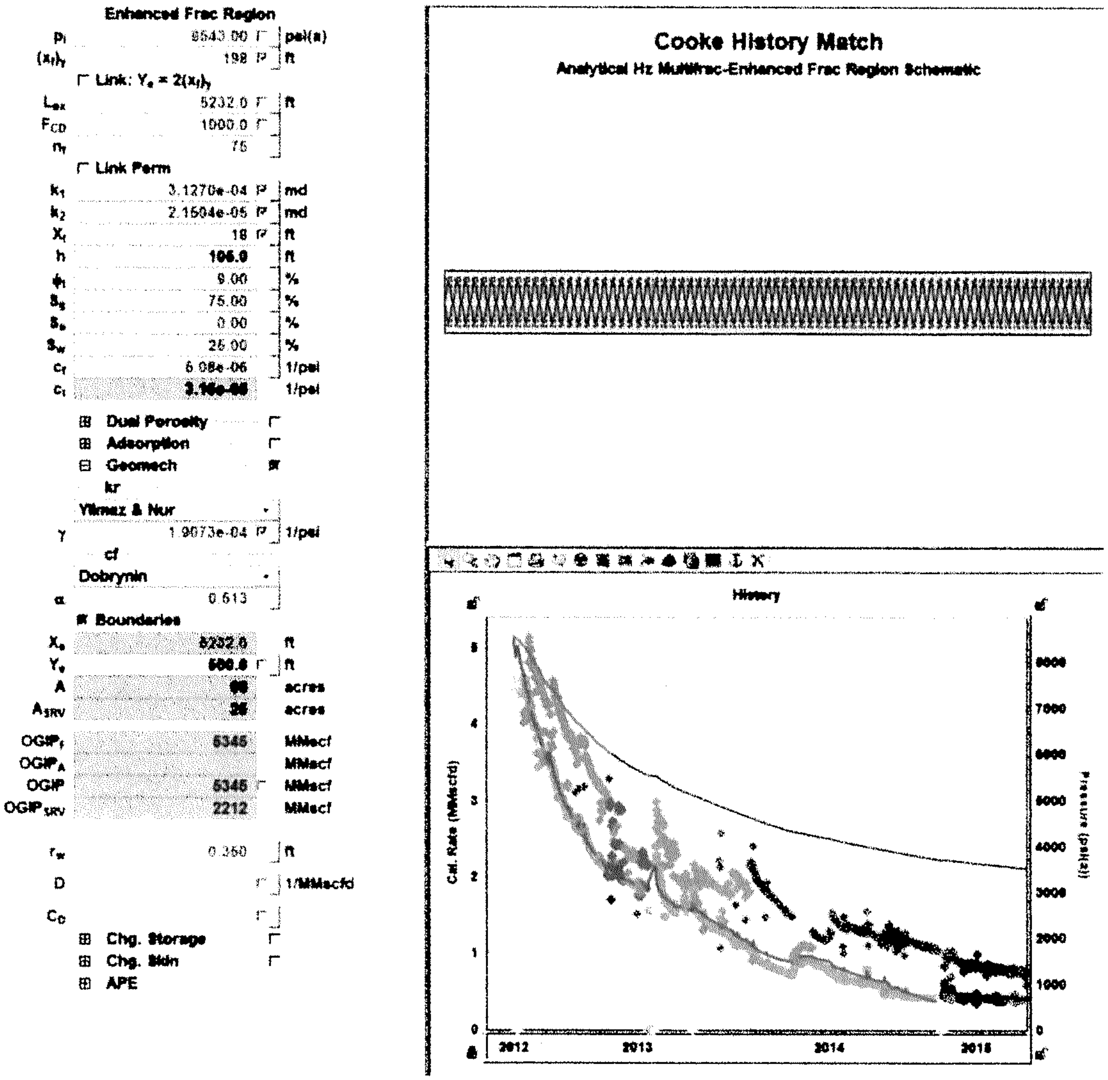

Enhanced Frac Region

p_i	8543.00 ☐	psi(a)
$(x_f)_y$	198 ☑	ft
☐ Link: $Y_e = 2(x_f)_y$		
L_{ex}	5232.0 ☐	ft
F_{CD}	1000.0 ☐	
n_f	75	
☐ Link Perm		
k_1	3.1270e-04 ☑	md
k_2	2.1504e-05 ☑	md
X_f	18 ☑	ft
h	106.0	ft
ϕ_t	9.00	%
S_g	75.00	%
S_o	0.00	%
S_w	25.00	%
c_f	6.08e-06	1/psi
c_t	[illegible]	1/psi
⊞ Dual Porosity	☐	
⊞ Adsorption	☐	
⊟ Geomech	☑	
kr		
Yilmaz & Nur		
γ	1.9073e-04 ☑	1/psi
cf		
Dobrynin		
α	0.613	
☑ Boundaries		
X_e	5232.0	ft
Y_e	600.0 ☐	ft
A	[illegible]	acres
A_{SRV}	25	acres
$OGIP_f$	5345	MMscf
$OGIP_A$		MMscf
OGIP	5345 ☐	MMscf
$OGIP_{SRV}$	2212	MMscf
r_w	0.350	ft
D	☐	1/MMscfd
C_D	☐	
⊞ Chg. Storage	☐	
⊞ Chg. Skin	☐	
⊞ APE		

Cooke History Match
Analytical Hz Multifrac-Enhanced Frac Region Schematic
History
Cal. Rate (MMscfd)
0
1
2
3
4
5
Pressure (psi(a))
0
1000
2000
3000
4000
5000
6000
7000
8000
2012
2013
2014
2015

Cooke Ranch B5 Forecast

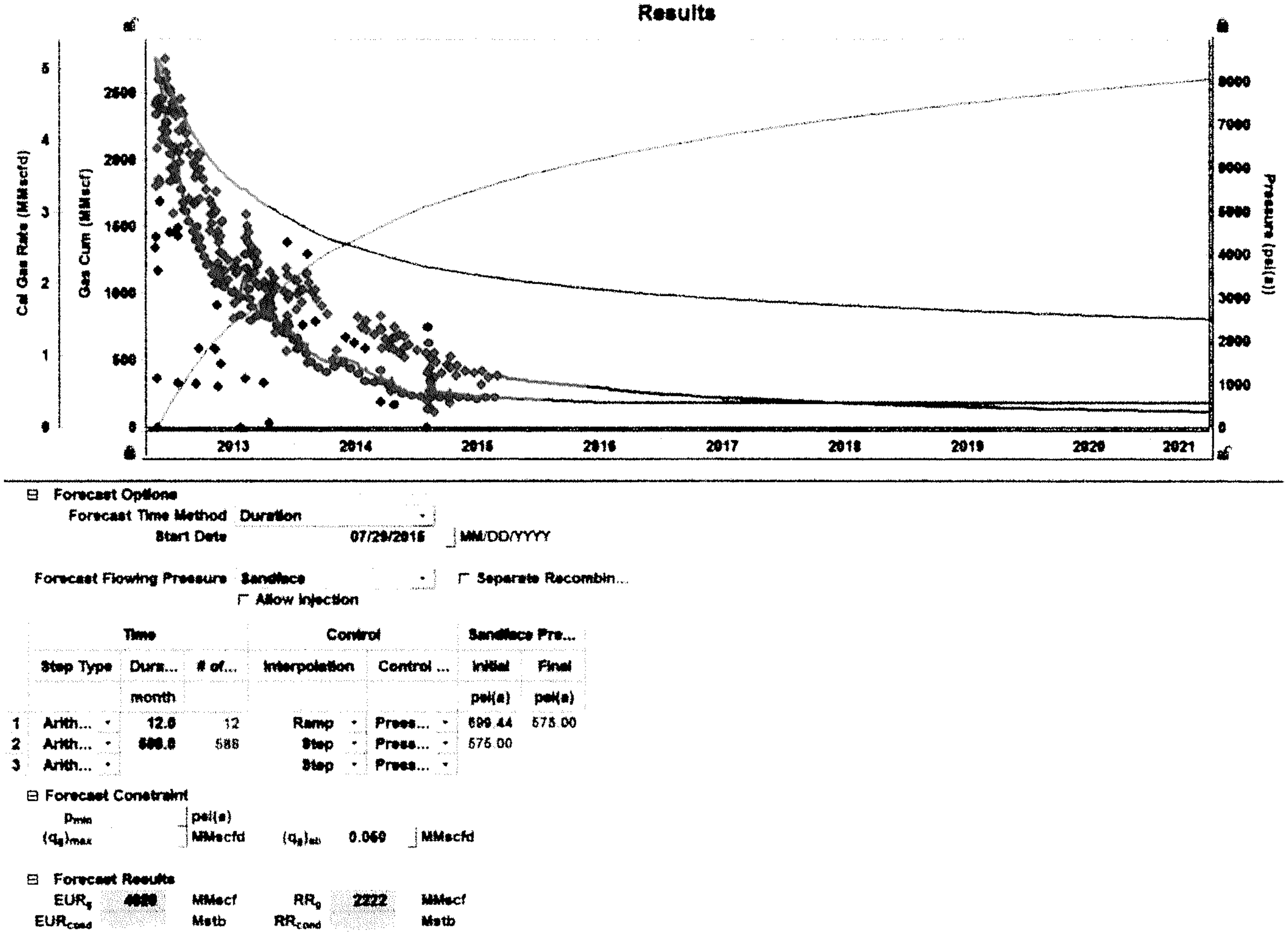
Results
Cal Gas Rate (MMscfd)
0
1
2
3
4
5
Gas Cum (MMscf)
0
500
1000
1500
2000
2500
Pressure (psi(a))
0
1000
2000
3000
4000
5000
6000
7000
8000
2013
2014
2015
2016
2017
2018
2019
2020
2021

⊟ Forecast Options

Forecast Time Method: Duration

Start Date: 07/29/2015 MM/DD/YYYY

Forecast Flowing Pressure: Sandface

☐ Separate Recombin...

☐ Allow Injection

	Time			Control		Sandface Pre...	
	Step Type	Dura...	# of...	Interpolation	Control ...	Initial	Final
		month				psi(a)	psi(a)
1	Arith...	12.0	12	Ramp	Press...	699.44	575.00
2	Arith...	588.0	588	Step	Press...	575.00	
3	Arith...			Step	Press...		

⊟ Forecast Constraint

p_{min} psi(a)

$(q_g)_{max}$ MMscfd $(q_g)_{ab}$ 0.060 MMscfd

⊟ Forecast Results

EUR_g [illegible] MMscf RR_g 2222 MMscf

EUR_{cond} Mstb RR_{cond} Mstb

Cooke Ranch C2 History Match

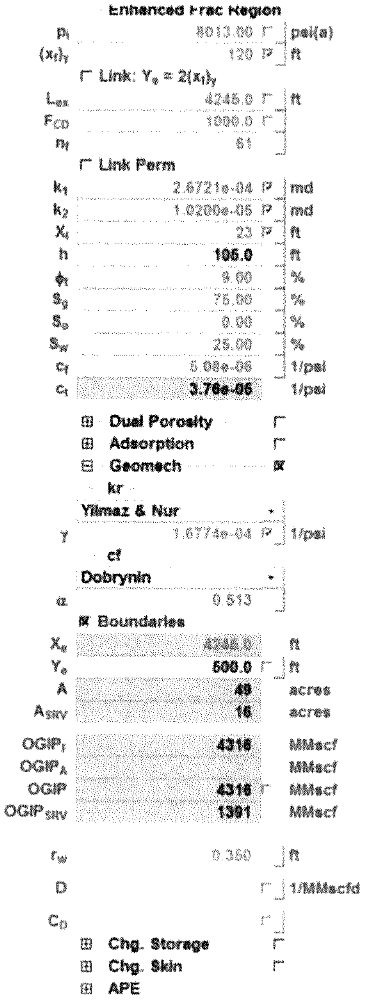

Enhanced Frac Region

p_i	8013.00	☐	psi(a)
$(x_f)_y$	120	☑	ft
☐ Link: $Y_e = 2(x_f)_y$			
L_{ex}	4245.0	☐	ft
F_{CD}	1000.0	☐	
n_f	61		
☐ Link Perm			
k_1	2.6721e-04	☑	md
k_2	1.0200e-05	☑	md
X_i	23	☑	ft
h	**106.0**		ft
ϕ_t	9.00		%
S_g	75.00		%
S_o	0.00		%
S_w	25.00		%
c_f	5.08e-06		1/psi
c_t	**3.76e-05**		1/psi
⊞ **Dual Porosity**		☐	
⊞ **Adsorption**		☐	
⊟ **Geomech**		☒	
kr			
	Yilmaz & Nur		
γ	1.6774e-04	☑	1/psi
cf			
	Dobrynin		
α	0.513		
☒ **Boundaries**			
X_e	4245.0		ft
Y_e	**500.0**	☐	ft
A	**49**		acres
A_{SRV}	**16**		acres
$OGIP_f$	**4316**		MMscf
$OGIP_A$			MMscf
OGIP	**4316**	☐	MMscf
$OGIP_{SRV}$	**1391**		MMscf
r_w	0.350		ft
D		☐	1/MMscfd
C_D		☐	
⊞ **Chg. Storage**		☐	
⊞ **Chg. Skin**		☐	
⊞ **APE**			

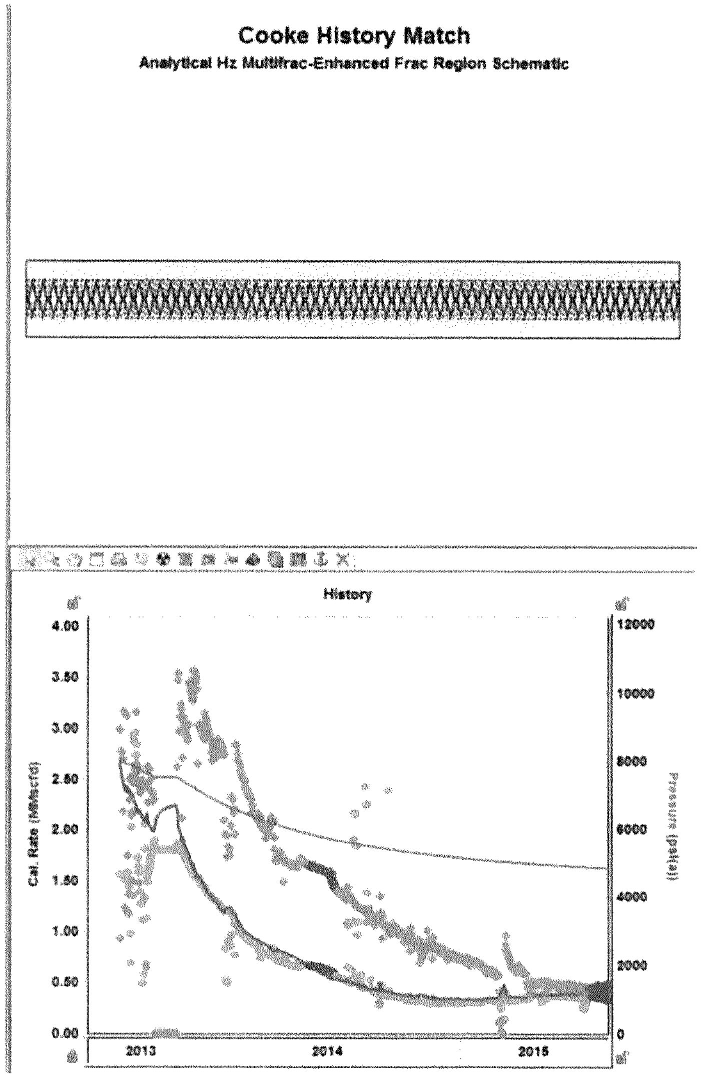

Cooke History Match

Analytical Hz Multifrac-Enhanced Frac Region Schematic

Cooke Ranch C2 Forecast

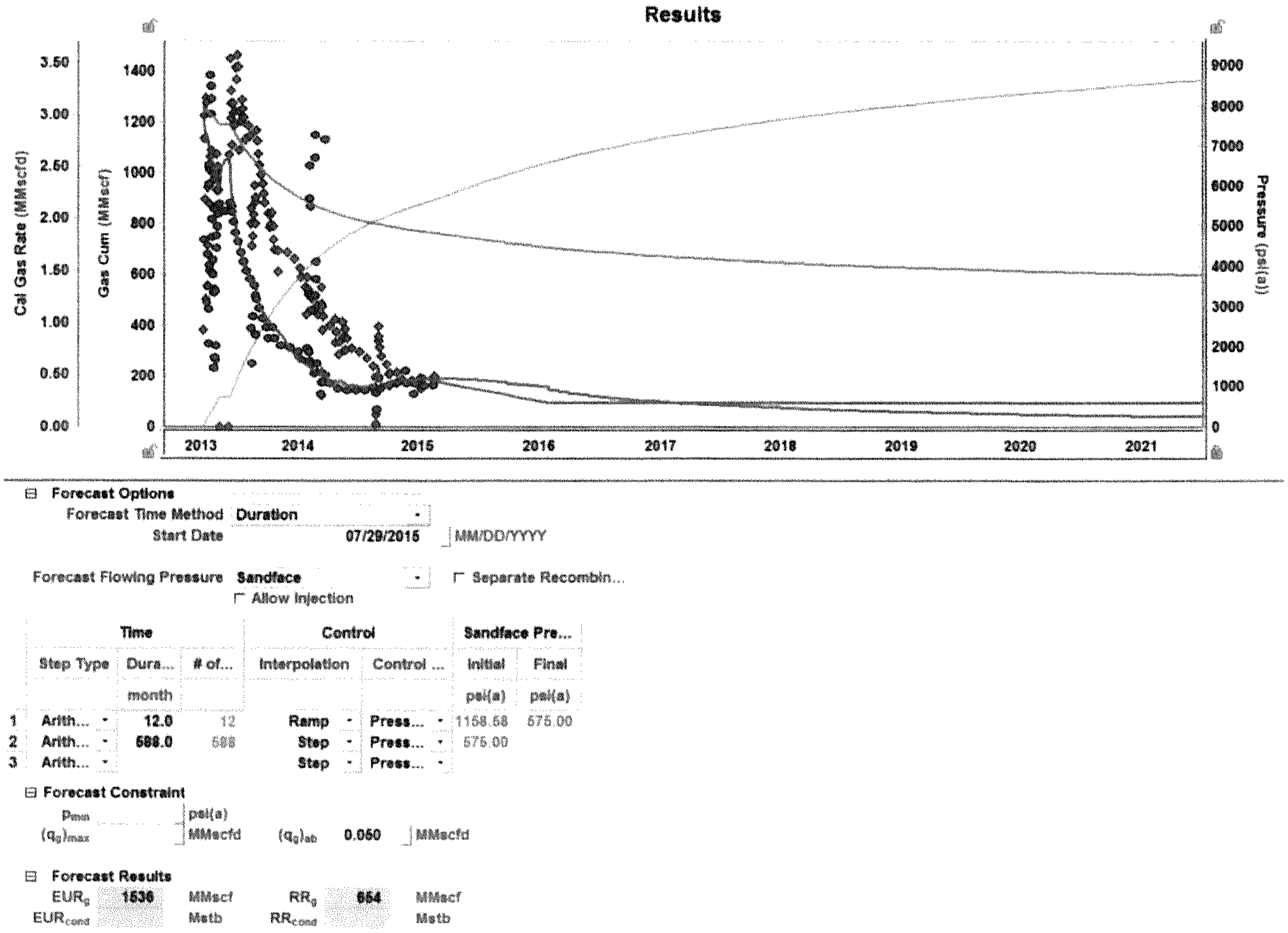
Results
Cal Gas Rate (MMscfd)
3.50
3.00
2.50
2.00
1.50
1.00
0.50
0.00
Gas Cum (MMscf)
1400
1200
1000
800
600
400
200
0
Pressure (psi(a))
9000
8000
7000
6000
5000
4000
3000
2000
1000
0
2013
2014
2015
2016
2017
2018
2019
2020
2021

⊟ Forecast Options

Forecast Time Method: Duration

Start Date: 07/29/2015 MM/DD/YYYY

Forecast Flowing Pressure: Sandface

☐ Separate Recombin...

☐ Allow Injection

	Time			Control		Sandface Pre...	
	Step Type	Dura...	# of...	Interpolation	Control ...	Initial	Final
		month				psi(a)	psi(a)
1	Arith...	12.0	12	Ramp	Press...	1158.68	575.00
2	Arith...	588.0	588	Step	Press...	575.00	
3	Arith...			Step	Press...		

⊟ Forecast Constraint

p_{min} psi(a)

$(q_g)_{max}$ MMscfd

$(q_g)_{ab}$ 0.050 MMscfd

⊟ Forecast Results

EUR_g 1536 MMscf

RR_g 654 MMscf

EUR_{cond} Mstb

RR_{cond} Mstb

Cooke Ranch C3 History Match

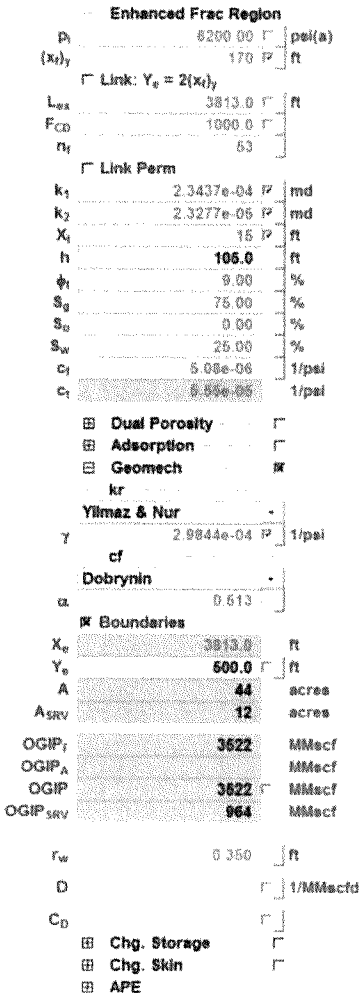

Enhanced Frac Region

p_i	6200.00	☐	psi(a)
$(x_f)_y$	170	☑	ft
☐ Link: $Y_e = 2(x_f)_y$			
L_{ex}	3813.0	☐	ft
F_{CD}	1000.0	☐	
n_f	63		
☐ Link Perm			
k_1	2.3437e-04	☑	md
k_2	2.3277e-06	☑	md
X_f	15	☑	ft
h	**105.0**		ft
ϕ_t	9.00		%
S_g	75.00		%
S_o	0.00		%
S_w	25.00		%
c_f	5.08e-06		1/psi
c_t	[illegible]		1/psi
⊞ **Dual Porosity**		☐	
⊞ **Adsorption**		☐	
⊟ **Geomech**		☒	
kr			
Yilmaz & Nur			
γ	2.9844e-04	☑	1/psi
cf			
Dobrynin			
α	0.613		
☒ **Boundaries**			
X_e	3813.0		ft
Y_e	**500.0**	☐	ft
A	**44**		acres
A_{SRV}	**12**		acres
$OGIP_f$	**3522**		MMscf
$OGIP_A$			MMscf
OGIP	**3522**	☐	MMscf
$OGIP_{SRV}$	**964**		MMscf
r_w	0.350		ft
D		☐	1/MMscfd
C_D		☐	
⊞ **Chg. Storage**		☐	
⊞ **Chg. Skin**		☐	
⊞ **APE**			

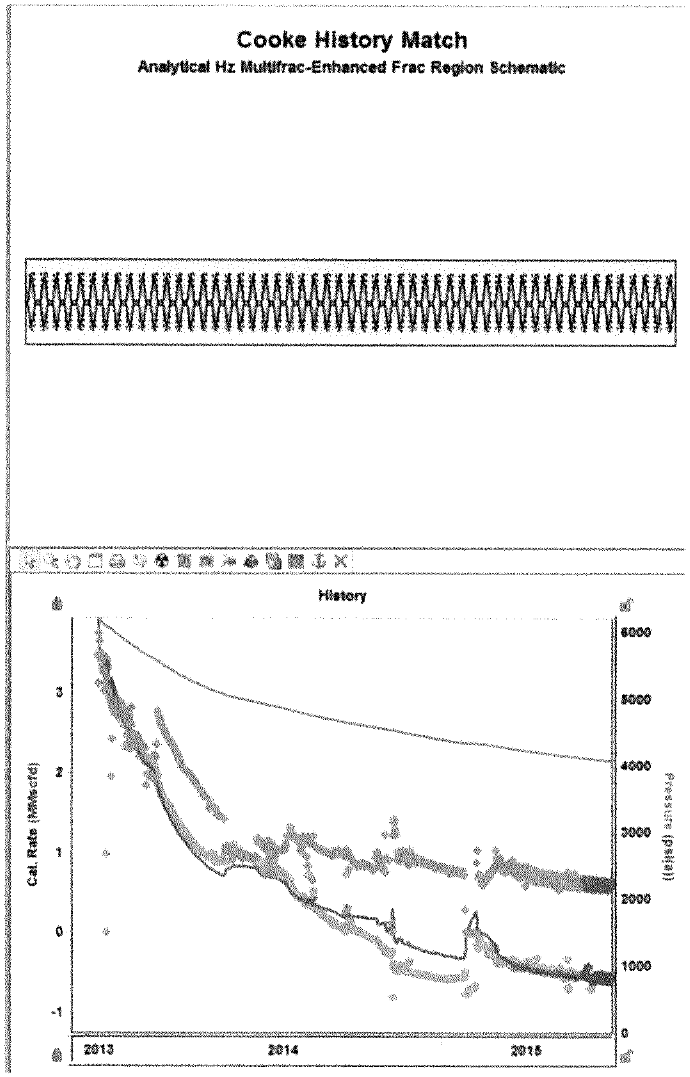

Cooke History Match

Analytical Hz Multifrac-Enhanced Frac Region Schematic

Cooke Ranch C3 Forecast

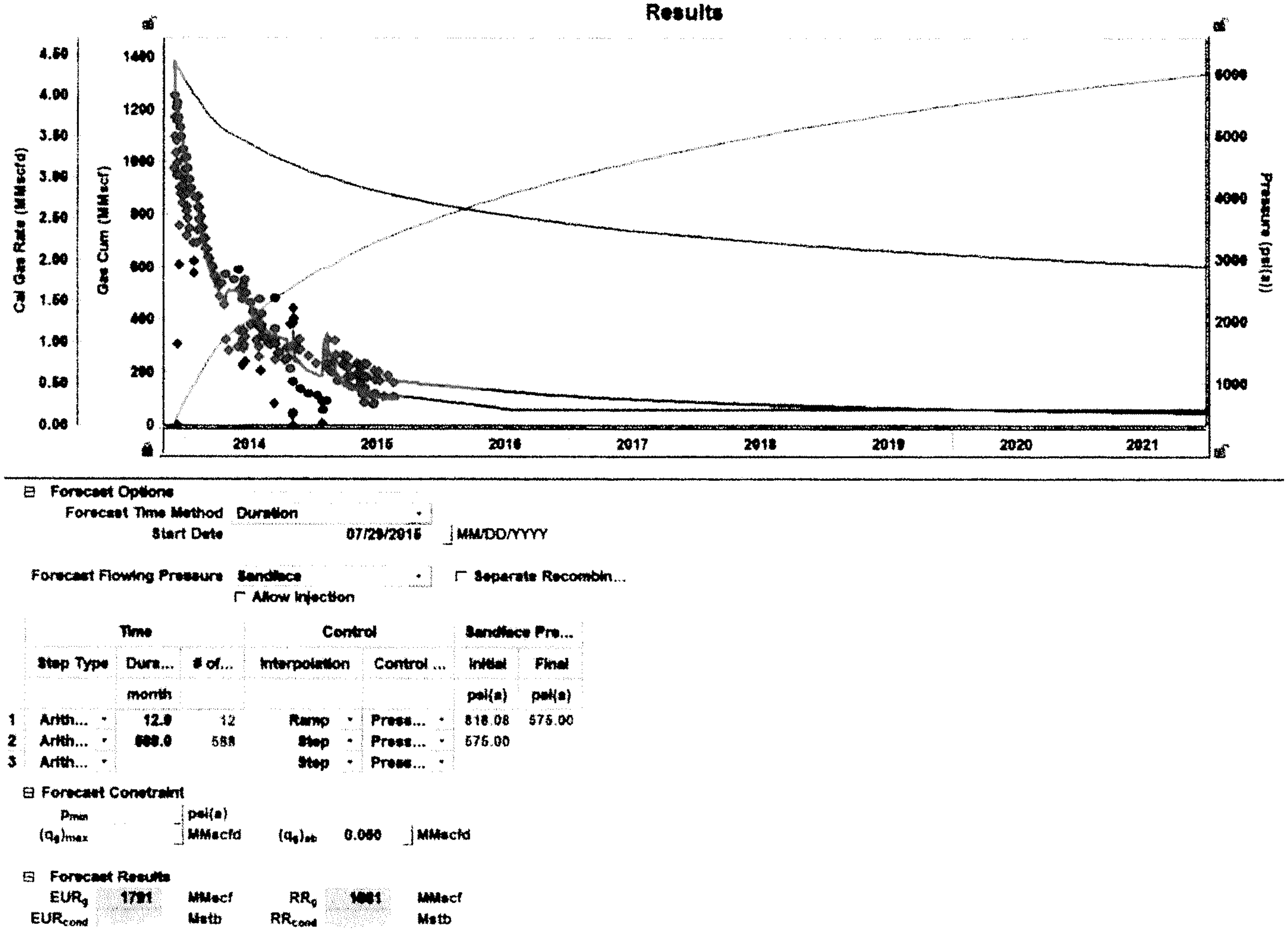
Results
Cal Gas Rate (MMscfd)
4.50
4.00
3.50
3.00
2.50
2.00
1.50
1.00
0.50
0.00
Gas Cum (MMscf)
1400
1200
1000
800
600
400
200
0
Pressure (psi(a))
6000
5000
4000
3000
2000
1000
2014
2015
2016
2017
2018
2019
2020
2021

⊟ Forecast Options

Forecast Time Method: Duration

Start Date: 07/29/2015 MM/DD/YYYY

Forecast Flowing Pressure: Sandface

☐ Separate Recombin...

☐ Allow Injection

	Time			Control		Sandface Pre...	
	Step Type	Dura...	# of...	Interpolation	Control ...	Initial	Final
		month				psi(a)	psi(a)
1	Arith...	12.0	12	Ramp	Press...	818.08	575.00
2	Arith...	588.0	588	Step	Press...	575.00	
3	Arith...			Step	Press...		

⊟ Forecast Constraint

P_{min} psi(a)

$(q_g)_{max}$ MMscfd $(q_g)_{ab}$ 0.060 MMscfd

⊟ Forecast Results

EUR_g 1791 MMscf RR_g 1081 MMscf

EUR_{cond} Mstb RR_{cond} Mstb

Cooke Ranch D1 History Match

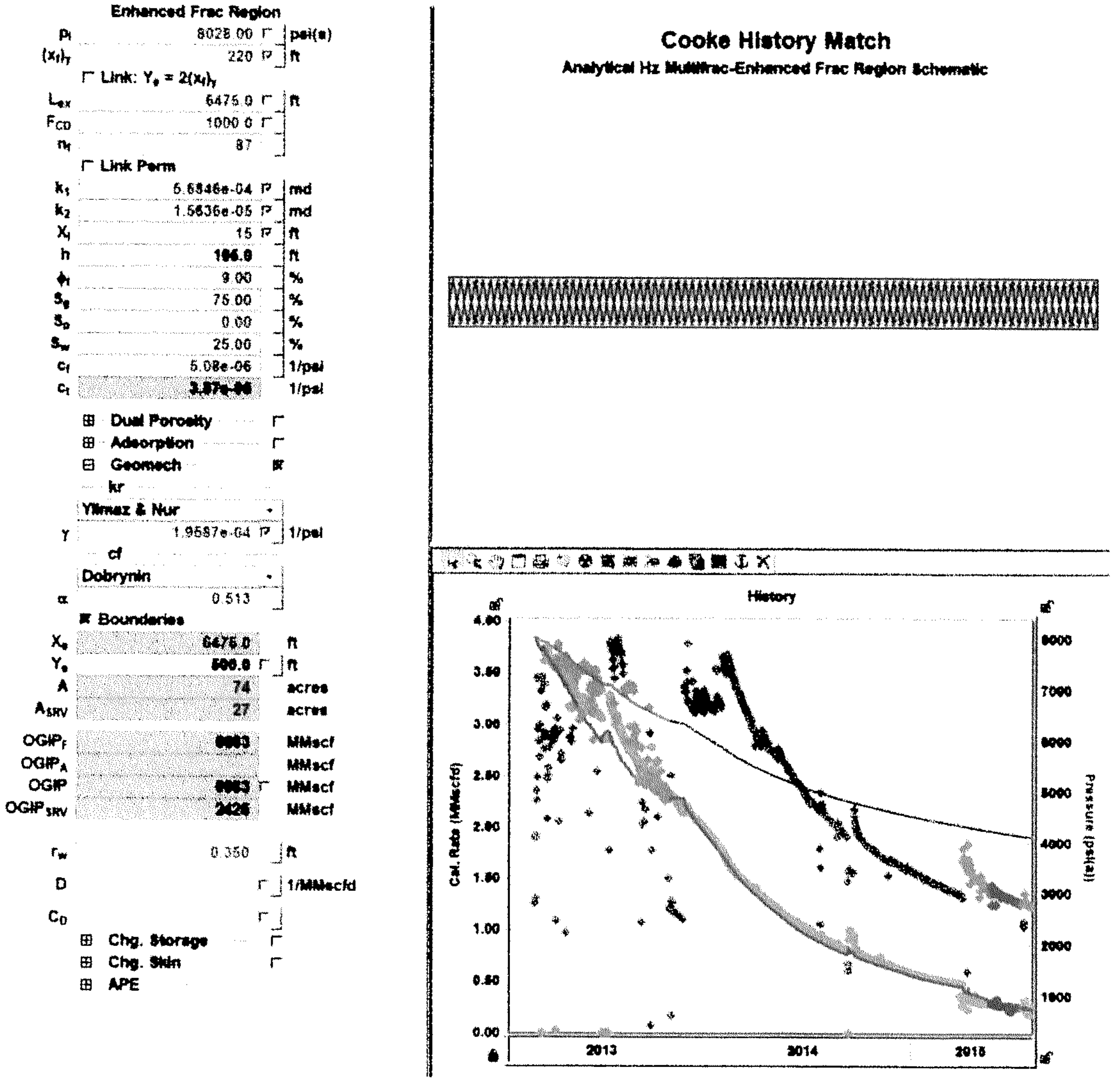

Enhanced Frac Region

p_i	8028.00	☐	psi(a)
$(x_f)_T$	220	☑	ft
☐ Link: $Y_e = 2(x_f)_T$			
L_{ex}	6475.0	☐	ft
F_{CD}	1000.0	☐	
n_f	87		
☐ Link Perm			
k_1	6.6846e-04	☑	md
k_2	1.5636e-05	☑	md
X_i	15	☑	ft
h	166.0		ft
ϕ_i	9.00		%
S_g	75.00		%
S_o	0.00		%
S_w	25.00		%
c_f	5.08e-06		1/psi
c_t	3.87e-06		1/psi
⊞ Dual Porosity		☐	
⊞ Adsorption		☐	
⊟ Geomech		☑	
kr			
	Yilmaz & Nur		
γ	1.9587e-04	☑	1/psi
cf			
	Dobrynin		
α	0.513		
☑ Boundaries			
X_e	6475.0		ft
Y_e	500.0	☐	ft
A	74		acres
A_{SRV}	27		acres
$OGIP_F$	[illegible]		MMscf
$OGIP_A$			MMscf
OGIP	[illegible]	☐	MMscf
$OGIP_{SRV}$	2426		MMscf
r_w	0.350		ft
D		☐	1/MMscfd
C_D		☐	
⊞ Chg. Storage		☐	
⊞ Chg. Skin		☐	
⊞ APE			

Cooke History Match
Analytical Hz Multifrac-Enhanced Frac Region Schematic
History
Cal. Rate (MMscfd)
4.00
3.50
3.00
2.50
2.00
1.50
1.00
0.50
0.00
Pressure (psi(a))
8000
7000
6000
5000
4000
3000
2000
1000
2013
2014
2015

Cooke Ranch D1 Forecast

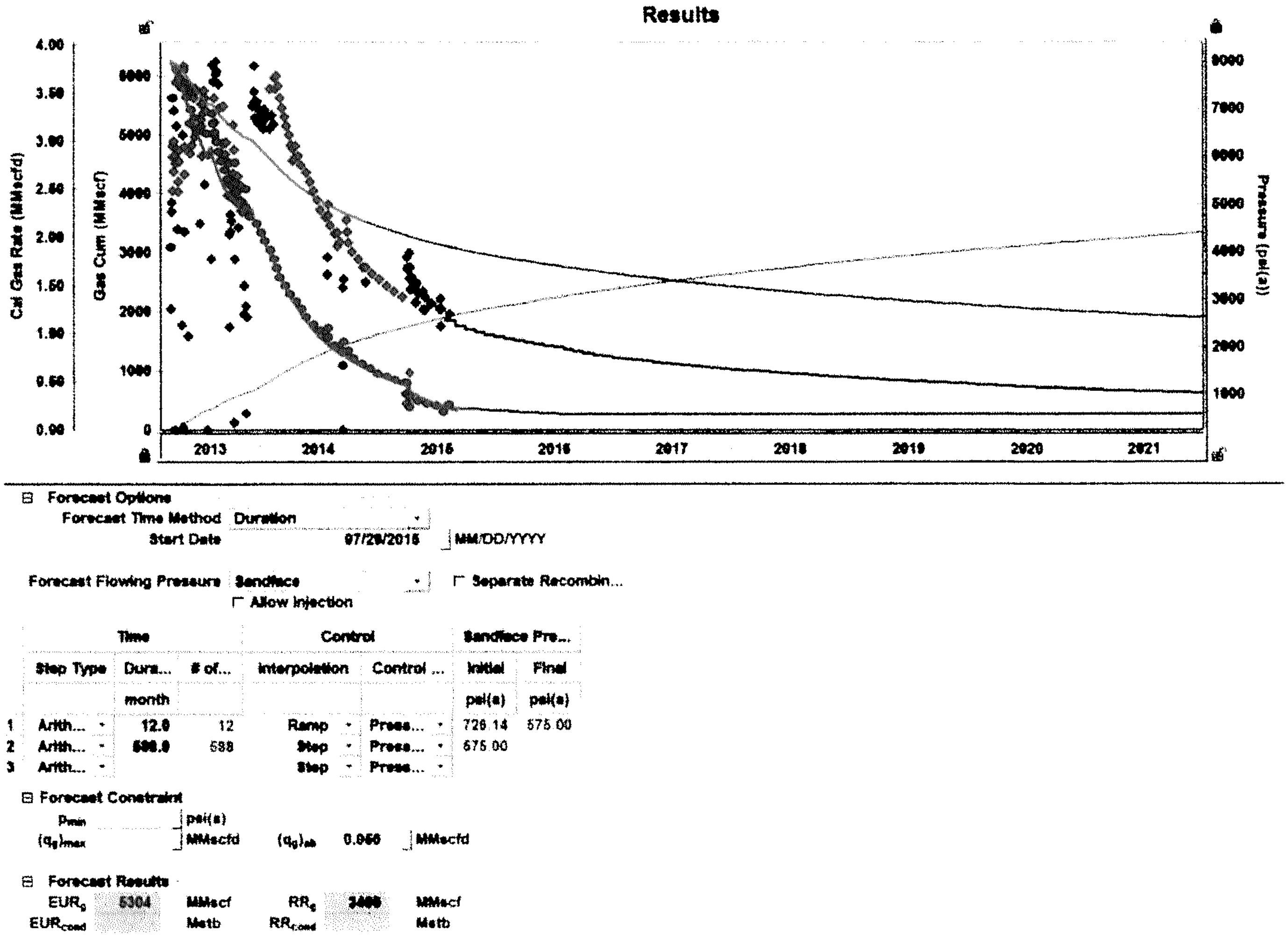
Results
Cal Gas Rate (MMscfd)
4.00
3.50
3.00
2.50
2.00
1.50
1.00
0.50
0.00
Gas Cum (MMscf)
6000
5000
4000
3000
2000
1000
0
Pressure (psi(a))
8000
7000
6000
5000
4000
3000
2000
1000
2013
2014
2015
2016
2017
2018
2019
2020
2021

⊟ **Forecast Options**

Forecast Time Method: Duration

Start Date: 07/29/2015 MM/DD/YYYY

Forecast Flowing Pressure: Sandface

☐ Separate Recombin...

☐ Allow injection

	Time			Control		Sandface Pre...	
	Step Type	Dura...	# of...	Interpolation	Control ...	Initial	Final
		month				psi(a)	psi(a)
1	Arith...	12.0	12	Ramp	Press...	726.14	575.00
2	Arith...	588.0	588	Step	Press...	575.00	
3	Arith...			Step	Press...		

⊟ **Forecast Constraint**

p_{min} psi(a)

$(q_g)_{max}$ MMscfd $(q_g)_{ab}$ 0.050 MMscfd

⊟ **Forecast Results**

EUR_g 5304 MMscf RR_g 3400 MMscf

EUR_{cond} Mstb RR_{cond} Mstb

Cooke Ranch D3 History Match

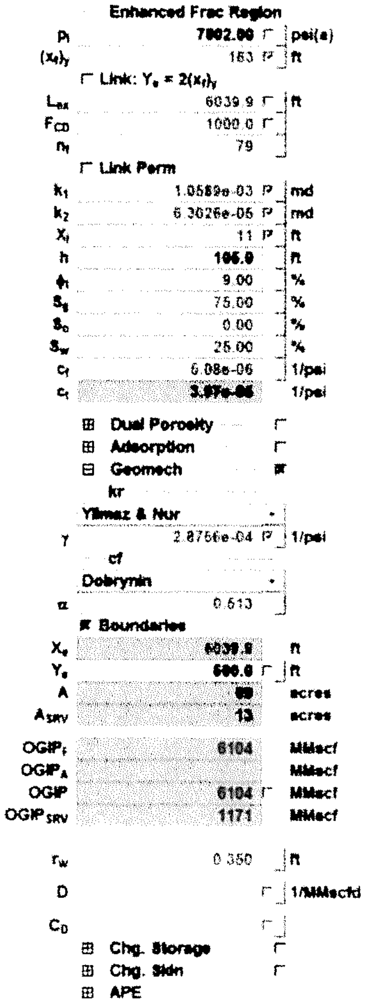

Enhanced Frac Region

p_i	7802.00	☐	psi(a)
$(x_f)_y$	163	☑	ft
☐ Link: $Y_e = 2(x_f)_y$			
L_{ex}	6039.9	☐	ft
F_{CD}	1000.0	☐	
n_f	79		
☐ Link Perm			
k_1	1.0589e-03	☑	md
k_2	6.3026e-05	☑	md
X_f	11	☑	ft
h	106.0		ft
ϕ_t	9.00		%
S_g	75.00		%
S_o	0.00		%
S_w	25.00		%
c_f	6.08e-06		1/psi
c_t	3.87e-05		1/psi
⊞ Dual Porosity		☐	
⊞ Adsorption		☐	
⊟ Geomech		☒	
kr			
Yilmaz & Nur			
γ	2.8756e-04	☑	1/psi
cf			
Dobrynin			
α	0.613		
☒ Boundaries			
X_e	6039.9		ft
Y_e	600.0	☐	ft
A	83		acres
A_{SRV}	13		acres
$OGIP_f$	6104		MMscf
$OGIP_A$			MMscf
OGIP	6104	☐	MMscf
$OGIP_{SRV}$	1171		MMscf
r_w	0.350		ft
D		☐	1/MMscfd
C_D		☐	
⊞ Chg. Storage		☐	
⊞ Chg. Skin		☐	
⊞ APE			

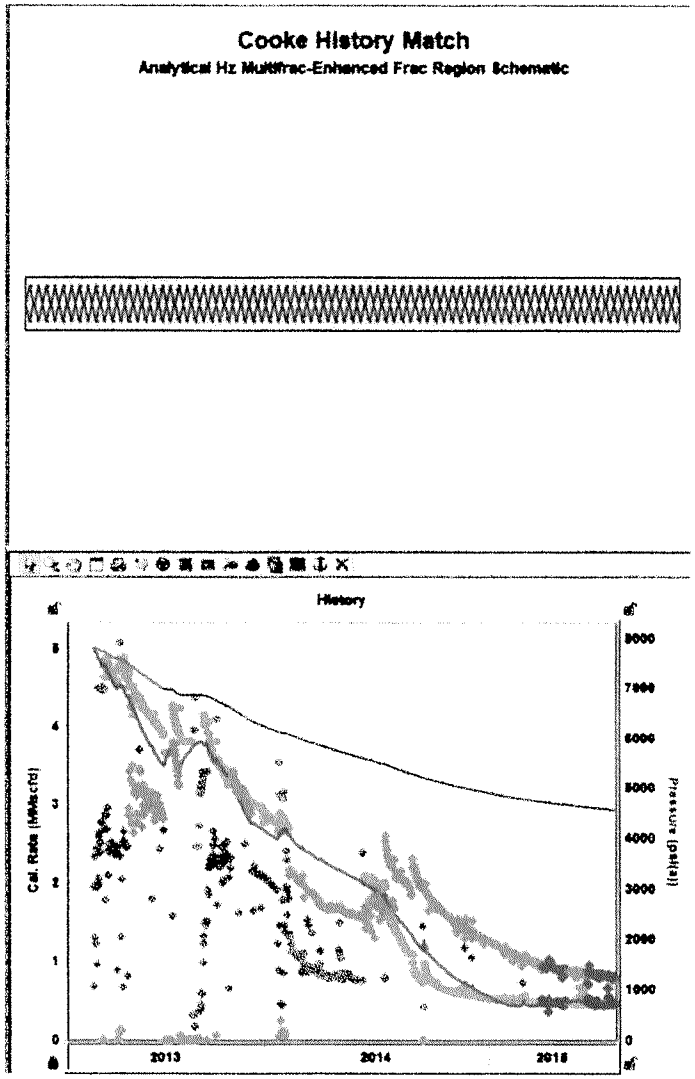

Cooke Ranch D3 Forecast

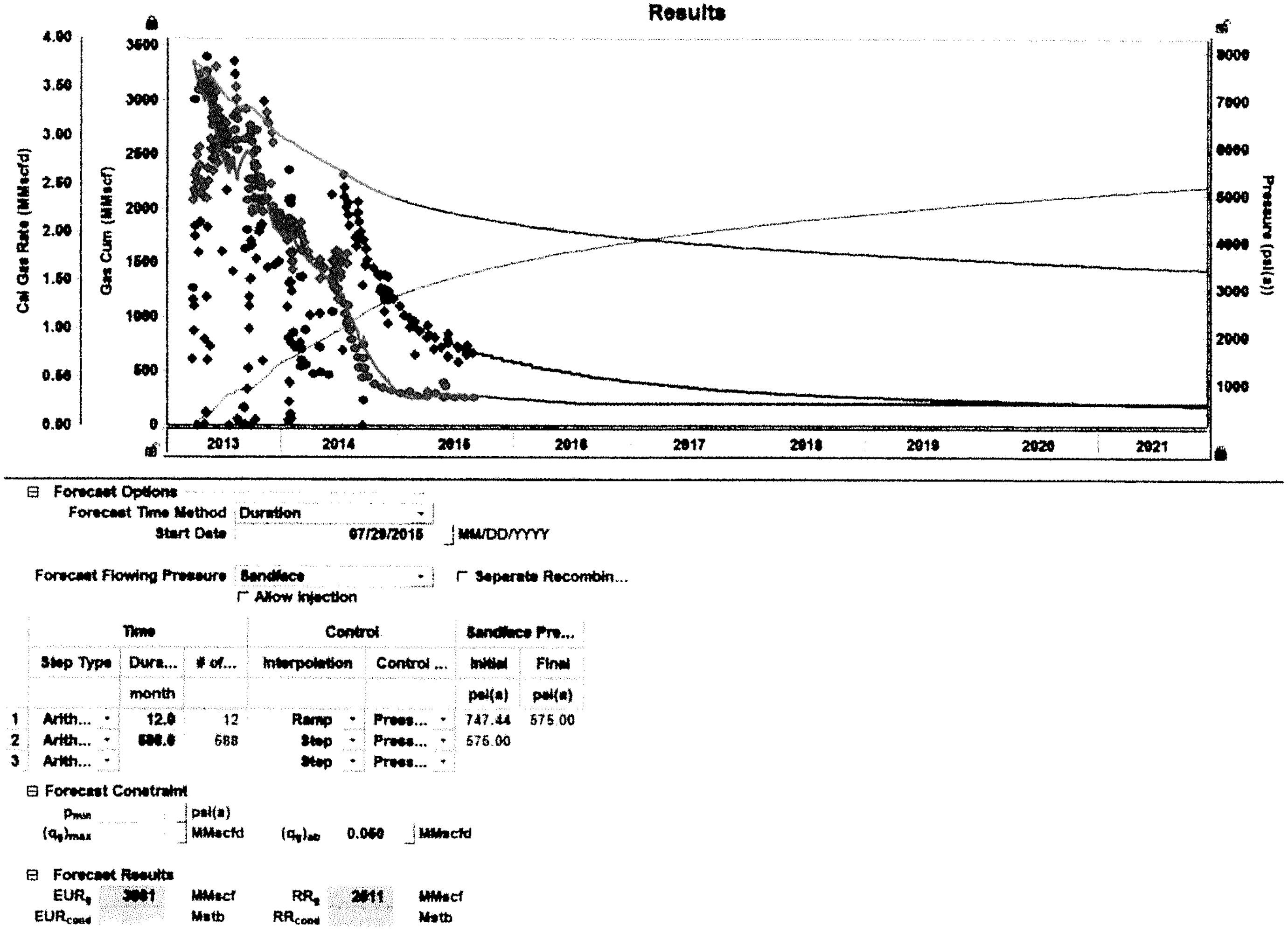
Results
Cal Gas Rate (MMscfd)
4.00
3.50
3.00
2.50
2.00
1.50
1.00
0.50
0.00
Gas Cum (MMscf)
3500
3000
2500
2000
1500
1000
500
0
Pressure (psi(a))
8000
7000
6000
5000
4000
3000
2000
1000
2013
2014
2015
2016
2017
2018
2019
2020
2021

⊟ Forecast Options

Forecast Time Method: Duration

Start Date: 07/29/2015 MM/DD/YYYY

Forecast Flowing Pressure: Sandface

☐ Separate Recombin...

☐ Allow Injection

	Time			Control		Sandface Pre...	
	Step Type	Dura...	# of...	Interpolation	Control ...	Initial	Final
		month				psi(a)	psi(a)
1	Arith...	12.0	12	Ramp	Press...	747.44	575.00
2	Arith...	588.0	588	Step	Press...	575.00	
3	Arith...			Step	Press...		

⊟ Forecast Constraint

p_{min} psi(a)

$(q_g)_{max}$ MMscfd $(q_g)_{ab}$ 0.050 MMscfd

⊟ Forecast Results

EUR_g 3061 MMscf RR_g 2611 MMscf

EUR_{cond} Mstb RR_{cond} Mstb

Cooke Ranch F1 History Match

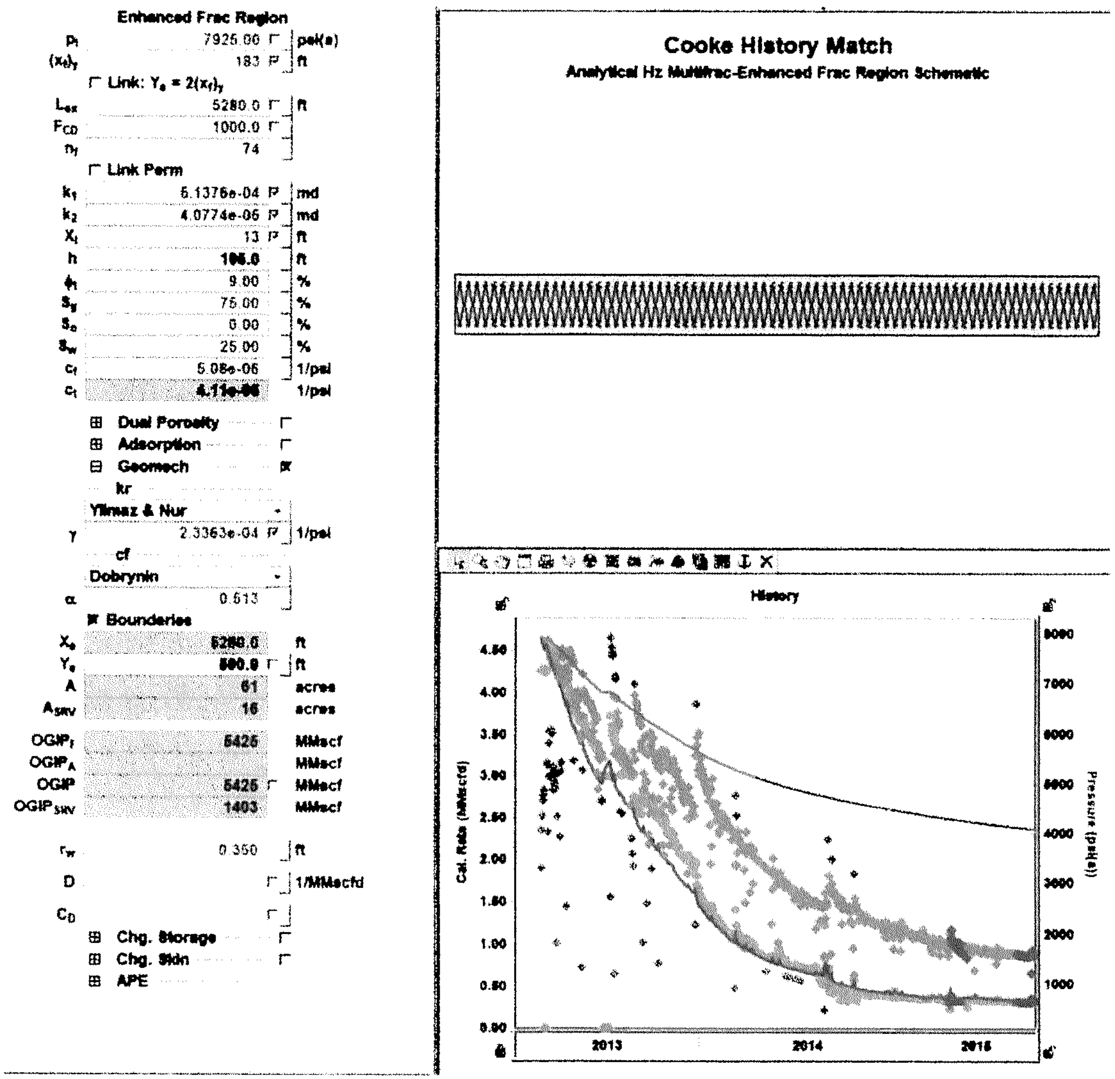

Enhanced Frac Region

p_i	7926.00	☐	psi(a)
$(x_f)_y$	183	☑	ft

☐ Link: $Y_e = 2(x_f)_y$

L_{ex}	5280.0	☐	ft
F_{CD}	1000.0	☐	
n_f	74		

☐ Link Perm

k_1	5.1376e-04	☑	md
k_2	4.0774e-06	☑	md
X_1	13	☑	ft
h	105.0		ft
ϕ_i	9.00		%
S_g	75.00		%
S_o	0.00		%
S_w	25.00		%
c_f	5.08e-06		1/psi
c_t	4.11e-06		1/psi

⊞ Dual Porosity ☐
⊞ Adsorption ☐
⊟ Geomech ☒
kr
Yilmaz & Nur

γ	2.3363e-04	☑	1/psi

cf
Dobrynin

α	0.613		

☒ Bounderies

X_e	5280.0		ft
Y_e	500.0	☐	ft
A	61		acres
A_{SRV}	16		acres
$OGIP_f$	5425		MMscf
$OGIP_A$			MMscf
OGIP	5425	☐	MMscf
$OGIP_{SRV}$	1403		MMscf
r_w	0.350		ft
D		☐	1/MMscfd
C_D		☐	

⊞ Chg. Storage ☐
⊞ Chg. Skin ☐
⊞ APE

Cooke History Match

Analytical Hz Multifrac-Enhanced Frac Region Schematic

History
Cal. Rate (MMscfd)
4.50
4.00
3.50
3.00
2.50
2.00
1.50
1.00
0.50
0.00
Pressure (psi(a))
8000
7000
6000
5000
4000
3000
2000
1000
2013
2014
2015

Cooke Ranch F1 Forecast

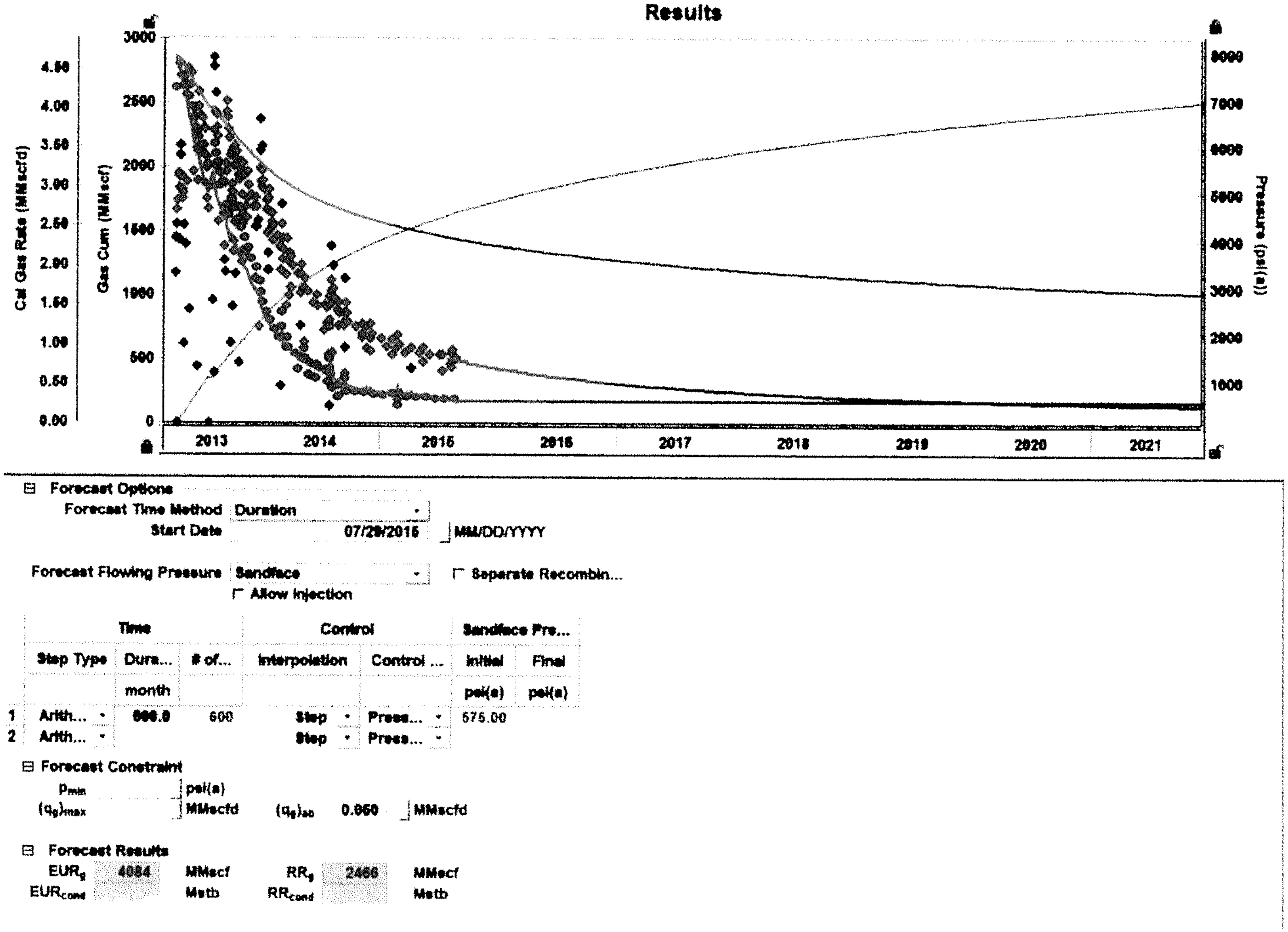
Results
Cal Gas Rate (MMscfd)
0.00
0.50
1.00
1.50
2.00
2.50
3.00
3.50
4.00
4.50
Gas Cum (MMscf)
0
500
1000
1500
2000
2500
3000
Pressure (psi(a))
1000
2000
3000
4000
5000
6000
7000
8000
2013
2014
2015
2016
2017
2018
2019
2020
2021

⊟ Forecast Options

Forecast Time Method: Duration

Start Date: 07/29/2015 MM/DD/YYYY

Forecast Flowing Pressure: Sandface

☐ Separate Recombin...

☐ Allow Injection

	Time			Control		Sandface Pre...	
	Step Type	Dura...	# of...	Interpolation	Control ...	Initial	Final
		month				psi(a)	psi(a)
1	Arith...	600.0	600	Step	Press...	575.00	
2	Arith...			Step	Press...		

⊟ Forecast Constraint

p_{min} psi(a)

$(q_g)_{max}$ MMscfd $(q_g)_{ab}$ 0.050 MMscfd

⊟ Forecast Results

EUR_g 4084 MMscf RR_g 2466 MMscf

EUR_{cond} Mstb RR_{cond} Mstb

Cooke Ranch F3 History Match

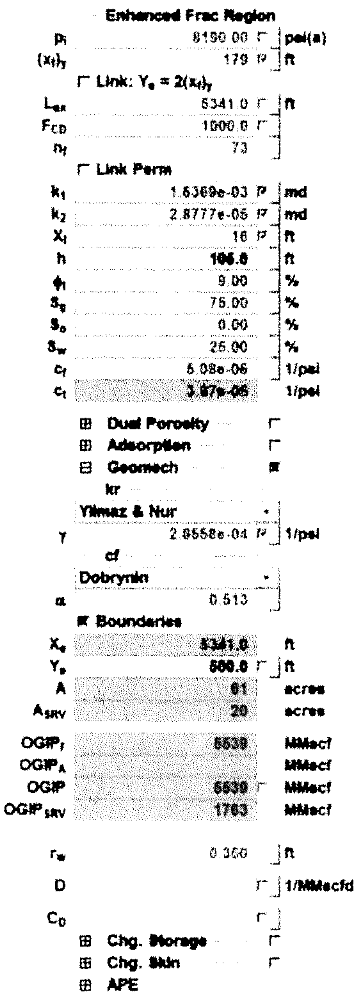

Enhanced Frac Region

p_i	8190.00	☐	psi(a)
$(x_f)_y$	179	☑	ft
☐ Link: $Y_e = 2(x_f)_y$			
L_{ex}	5341.0	☐	ft
F_{CD}	1000.0	☐	
n_f	73		
☐ Link Perm			
k_1	1.6369e-03	☑	md
k_2	2.8777e-05	☑	md
X_1	16	☑	ft
h	106.8		ft
ϕ_t	9.00		%
S_g	75.00		%
S_o	0.00		%
S_w	25.00		%
c_f	5.08e-06		1/psi
c_t	3.87e-05		1/psi
⊞ Dual Porosity		☐	
⊞ Adsorption		☐	
⊟ Geomech		☒	
kr	Yilmaz & Nur		
γ	2.8558e-04	☑	1/psi
cf	Dobrynin		
α	0.513		
☒ Boundaries			
X_e	5341.0		ft
Y_e	500.0	☐	ft
A	61		acres
A_{SRV}	20		acres
$OGIP_f$	5539		MMscf
$OGIP_A$			MMscf
OGIP	5539	☐	MMscf
$OGIP_{SRV}$	1763		MMscf
r_w	0.350		ft
D		☐	1/MMscfd
C_D		☐	
⊞ Chg. Storage		☐	
⊞ Chg. Skin		☐	
⊞ APE			

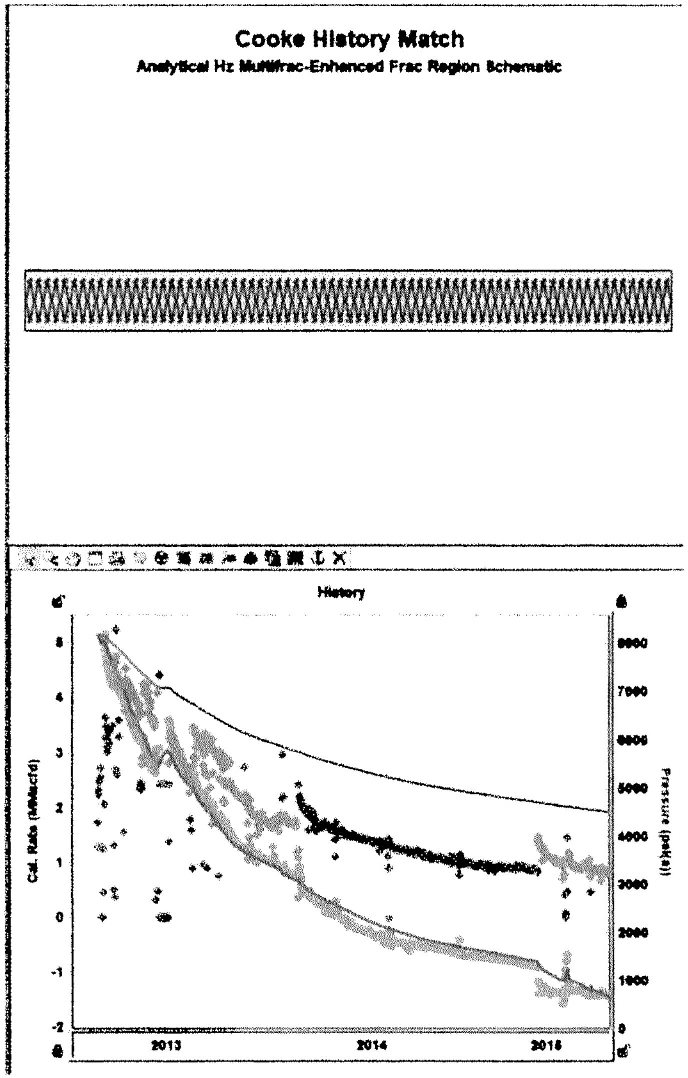

Cooke History Match

Analytical Hz Multifrac-Enhanced Frac Region Schematic

Cooke Ranch F3 Forecast

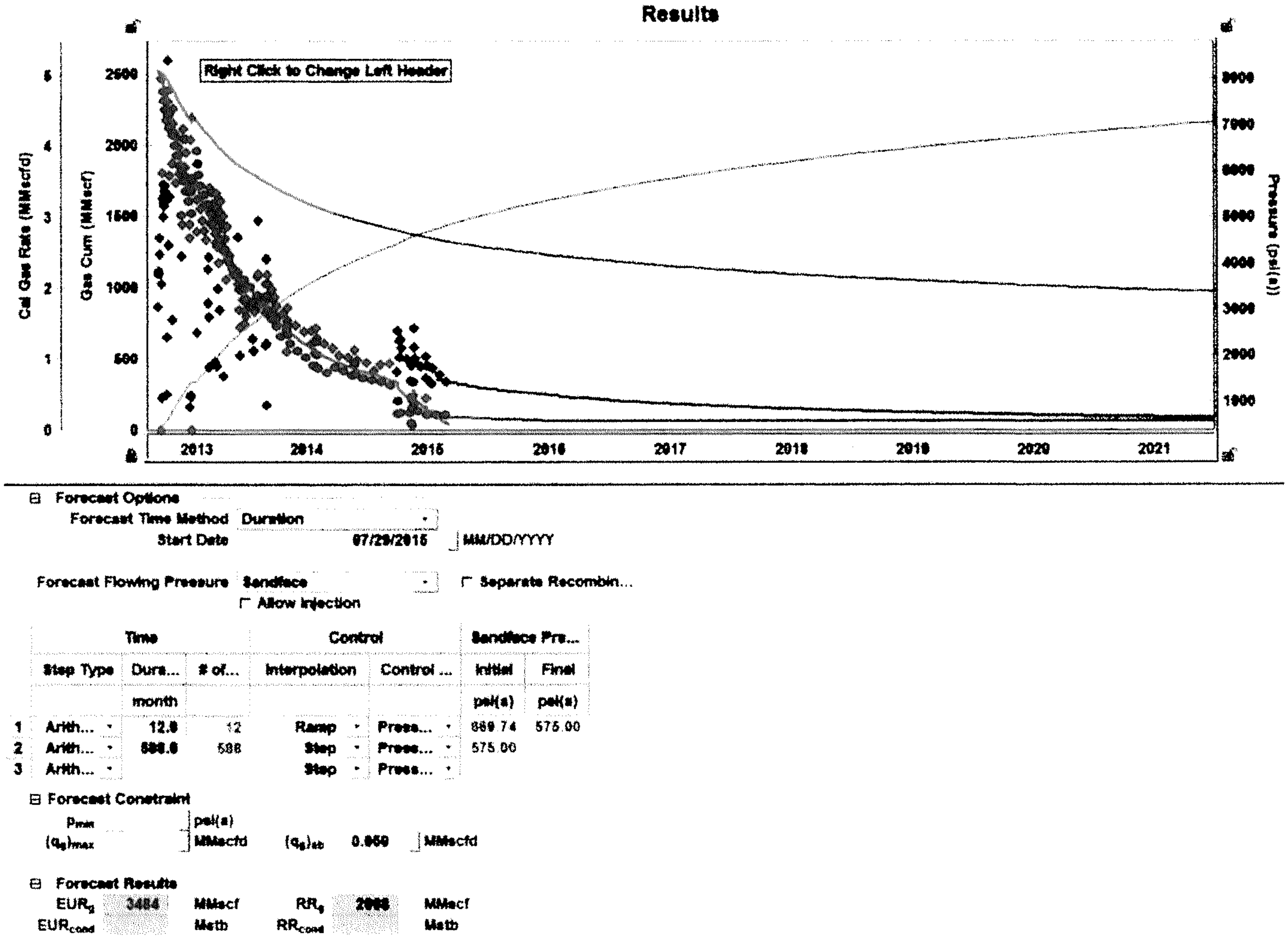
Results
Right Click to Change Left Header
Cal Gas Rate (MMscfd)
Gas Cum (MMscf)
Pressure (psi(a))
0
1
2
3
4
5
0
500
1000
1500
2000
2500
1000
2000
3000
4000
5000
6000
7000
8000
2013
2014
2015
2016
2017
2018
2019
2020
2021

⊟ Forecast Options

Forecast Time Method: Duration
Start Date: 07/29/2015 MM/DD/YYYY

Forecast Flowing Pressure: Sandface
☐ Separate Recombin...
☐ Allow Injection

	Time			Control		Sandface Pre...	
	Step Type	Dura...	# of...	Interpolation	Control ...	Initial	Final
		month				psi(a)	psi(a)
1	Arith...	12.0	12	Ramp	Press...	869.74	575.00
2	Arith...	588.0	588	Step	Press...	575.00	
3	Arith...			Step	Press...		

⊟ Forecast Constraint

p_{min} psi(a)
$(q_g)_{max}$ MMscfd $(q_g)_{ab}$ 0.050 MMscfd

⊟ Forecast Results

EUR_g	3484	MMscf	RR_g	2006	MMscf
EUR_{cond}		Mstb	RR_{cond}		Mstb

Deterministic vs. Probabilistic RTA

Cooke Ranch F1H

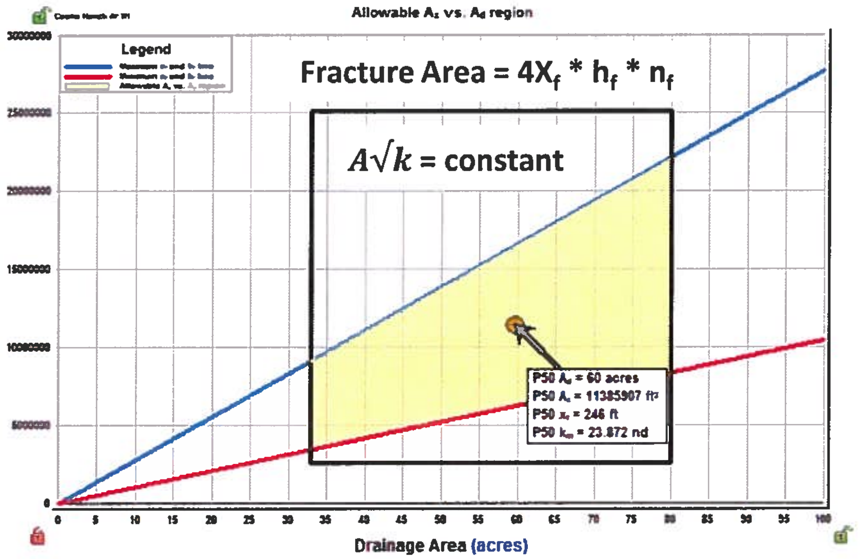

Fracture Area = $4X_f * h_f * n_f$

$A\sqrt{k}$ = constant

P50 A_d = 60 acres
P50 A_x = 11385907 ft²
P50 x_f = 246 ft
P50 k_m = 23.872 nd

- Every point inside the shaded area is a valid answer based on the well production and pressure history.
- Deterministic approach is a single solution among several possible solutions.

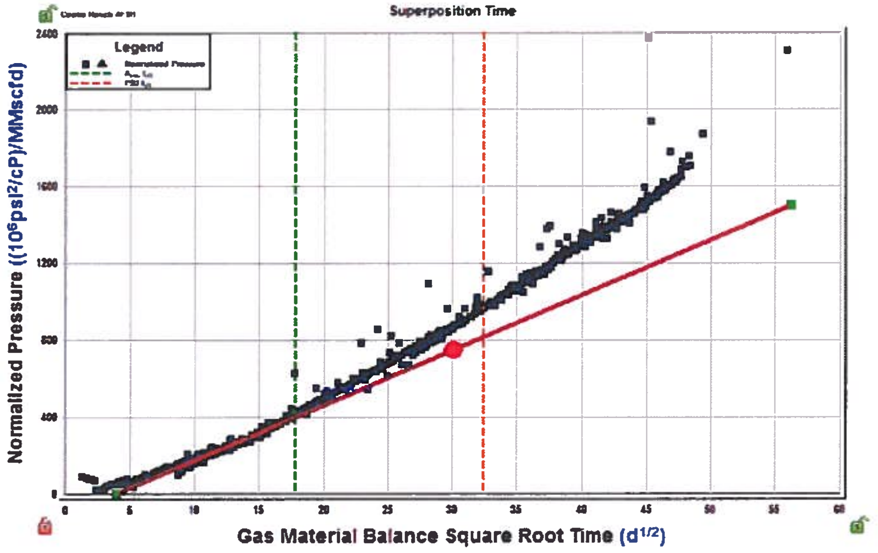

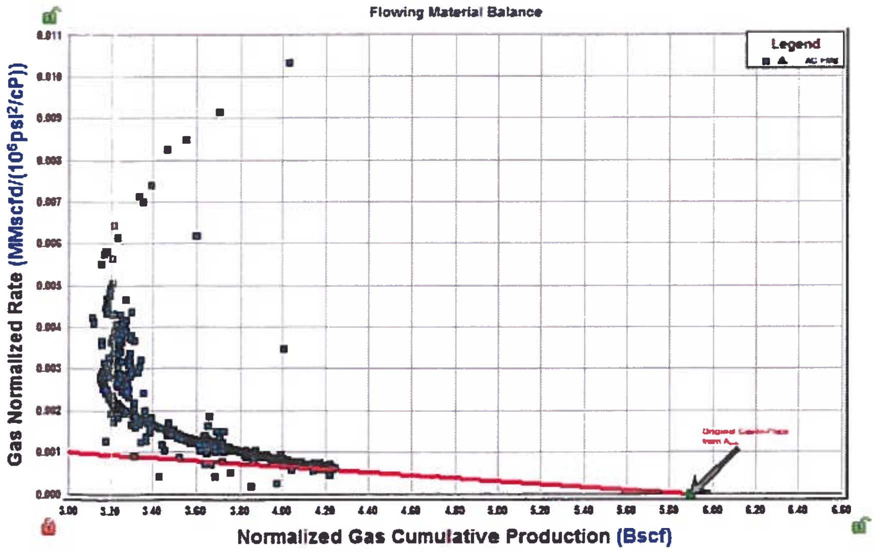

Exhibit No. 74
DOCKET NO. 01-0297078, et al.
Talisman Energy USA, Inc.
January 7, 2016

Attachment 7

Cooke Ranch F1H RTA

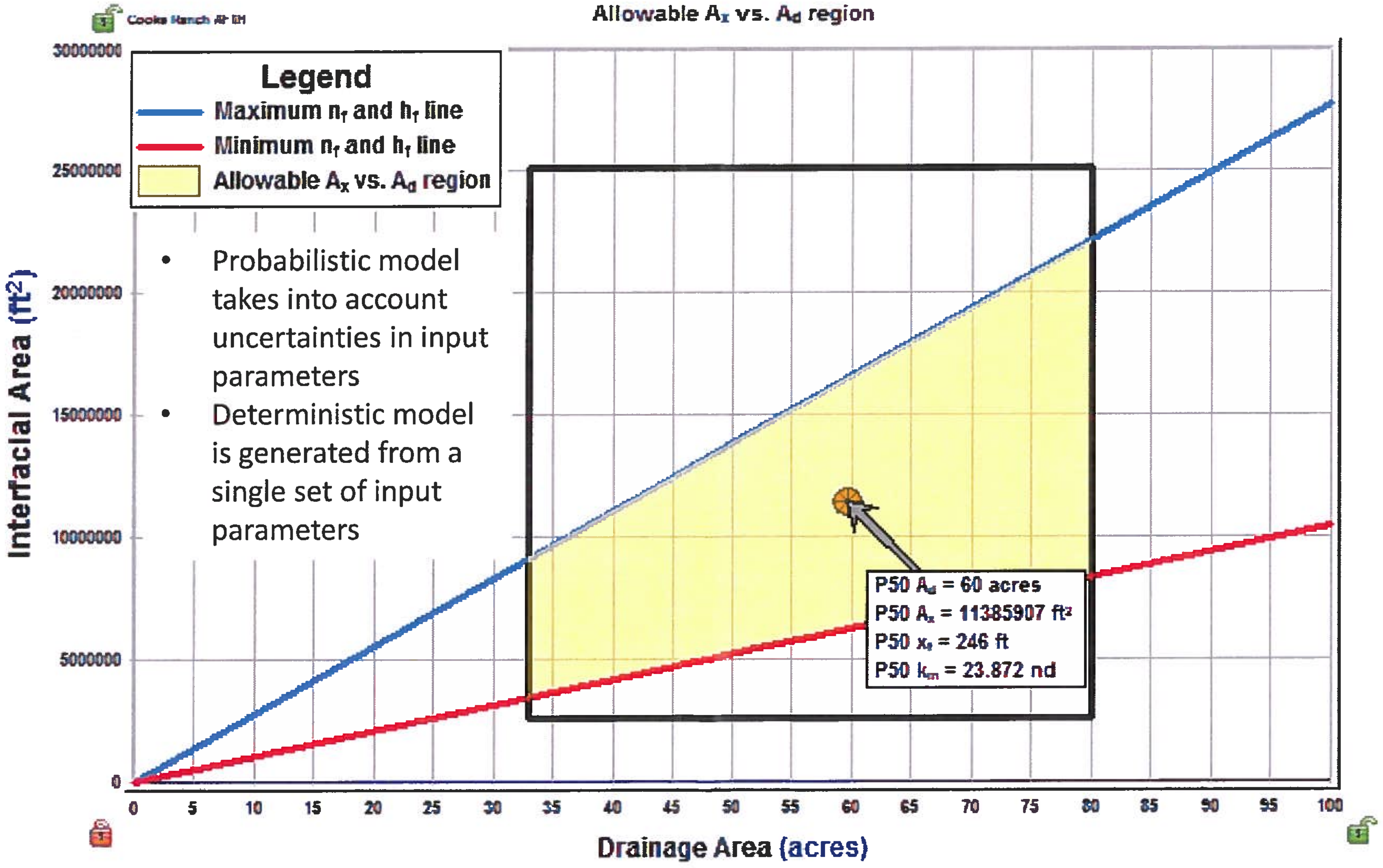

P50 A_d = 60 acres
P50 A_x = 11385907 ft^2
P50 x_f = 246 ft
P50 k_m = 23.872 nd

- Probabilistic model takes into account uncertainties in input parameters
- Deterministic model is generated from a single set of input parameters

Cooke Ranch F1H RTA

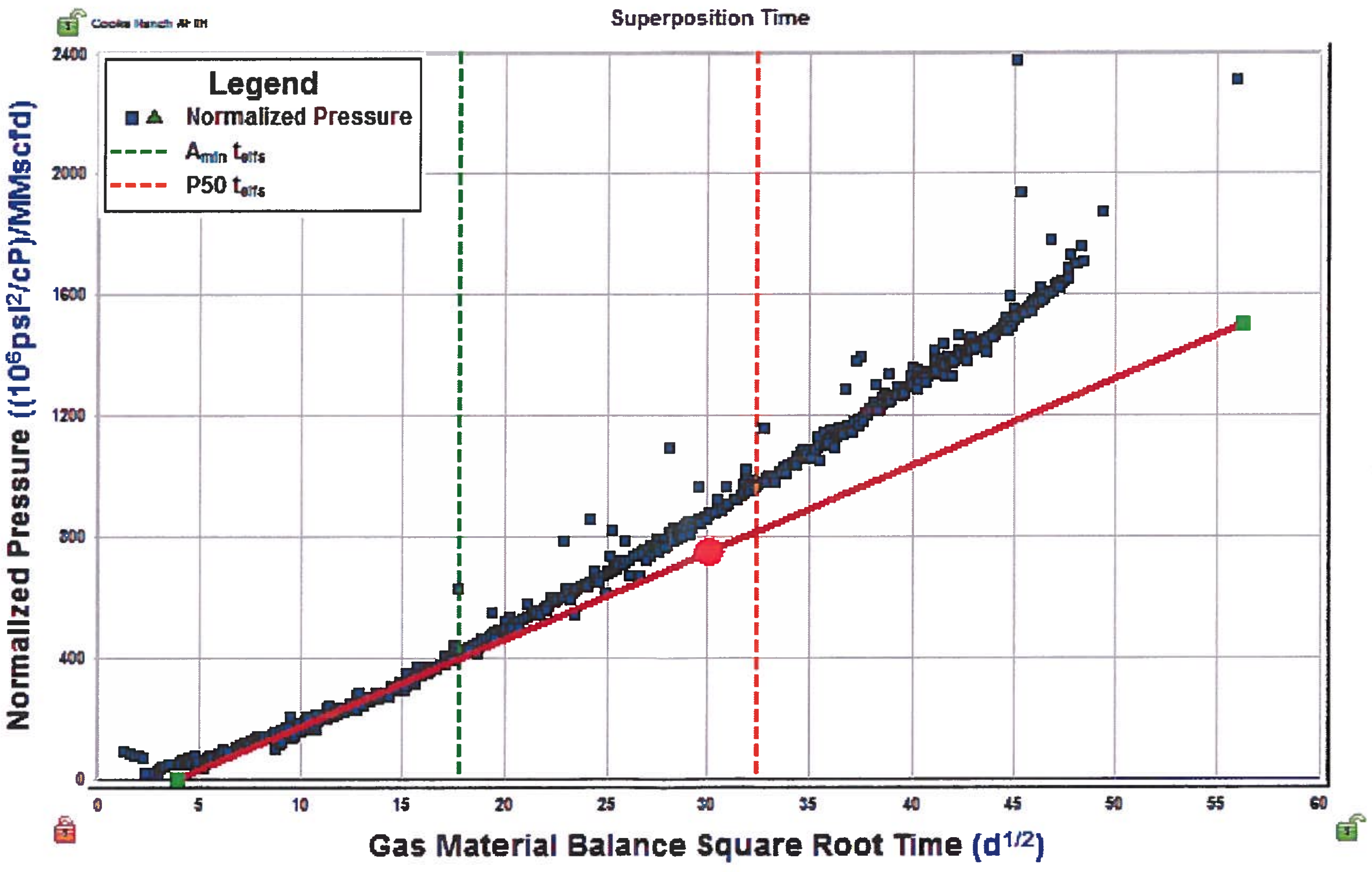

Cooke Ranch F1H RTA

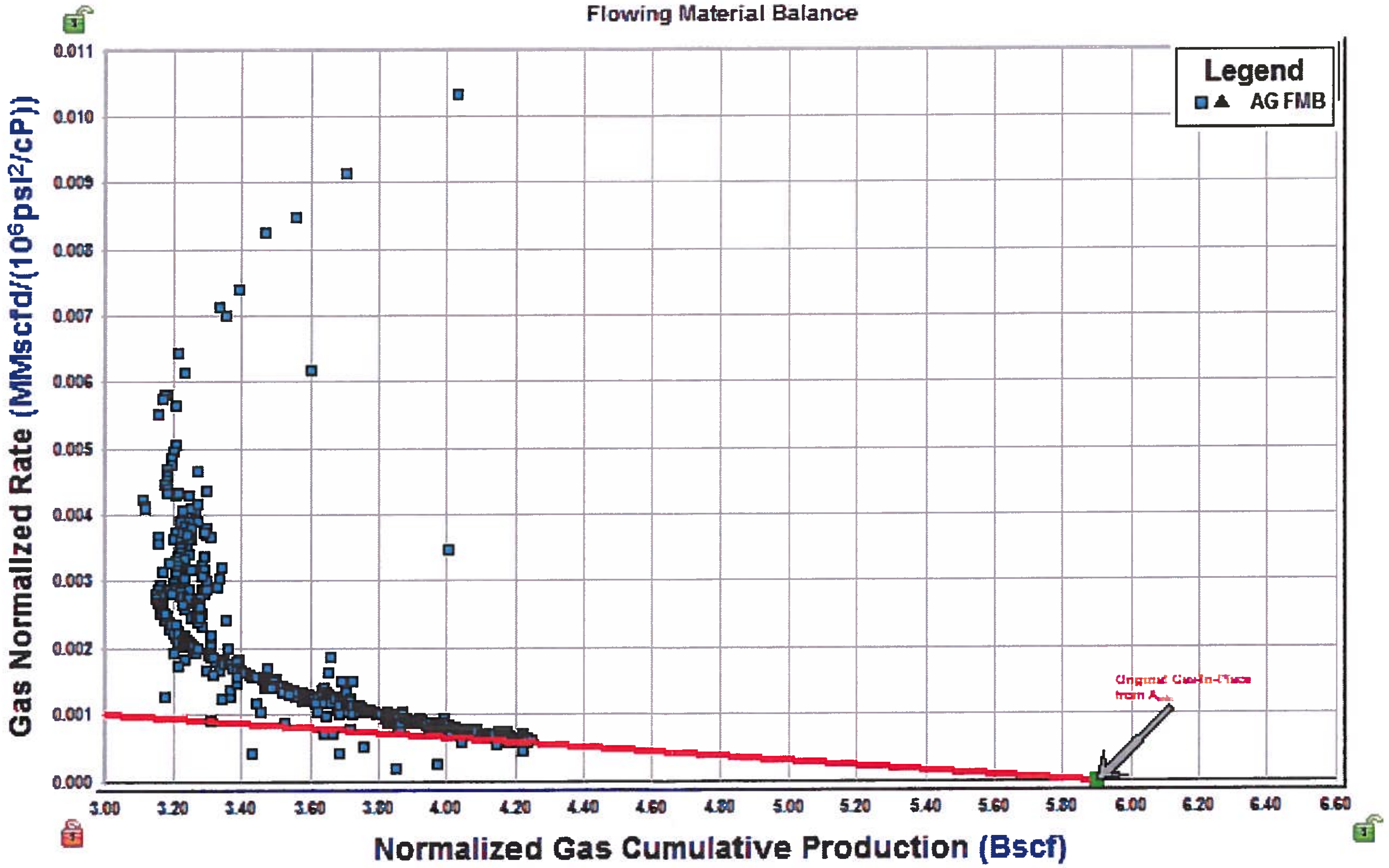

The Discovery, Reservoir Attributes, and Significance of the Hawkville Field and Eagle Ford Shale Trend, Texas

Charles Cusack[1], Jana Beeson[1], Dick Stoneburner[1], and Gregg Robertson[2]

[1]Petrohawk Energy Corporation, 1000 Louisiana St., Ste. 5600, Houston, Texas 77002
[2]First Rock, Inc., 600 Leopard St., Corpus Christi, Texas 78473

ABSTRACT

The Hawkville (Eagle Ford Shale) Field encompasses a 124 mile long by 25 mile wide oblong shaped portion of the Cretaceous platform, reaching from Webb County, Texas, on the southwest into Live Oak County, Texas, on the northeast. Thickness of the Eagle Ford across the field varies from 125 to 320 feet, with the entire section classified as net pay with good reservoir quality. Wireline log analysis and whole core data indicate 8-10% effective gas filled porosity, permeability in the range of 1.0-1.5 x 10^{-3} md (millidarcies), and gas saturation exceeding 80%, with the range of free gas in place from 140-212 BCF (billion cubic feet) per section.

The Eagle Ford Shale had less than 15 well penetrations in this particular area prior to the discovery; however, this well control, along with 2D seismic data, allowed for the recognition of specific geologic boundaries that defined the distinct accumulation. Production from the Eagle Ford ranges from dry gas to gas/condensate with a range of 10-120 BC/MMCF (barrels of condensate per million cubic feet of gas).

Since the discovery of Hawkville Field in October 2008, over thirty wells had been completed in the field by January 2010, with activity spreading across a large halo around the field to include five additional counties. The future activity will yield a much more complete understanding of the structure and stratigraphy of the entire Eagle Ford Formation and its relationship to commercial production.

INTRODUCTION

This paper describes the discovery, geology, and reserves of the Hawkville Field and gives a general overview of the entire Eagle Ford Shale trend. The Hawkville Field, in LaSalle and McMullen counties, Texas, was the initial commercial discovery for the Eagle Ford Shale with a high rate completion in the First Rock STS ("South Texas Syndicate") #1 in October of 2008. The Eagle Ford Shale has subsequently expanded to include thirteen counties covering a 180 mile expanse from Mexico on the southwest to DeWitt and Gonzales counties on the northeast. The Eagle Ford Shale has a unique hydrocarbon combination having oil updip, gas with retrograde condensate in the mid-depth range, and dry gas downdip. The total estimated recoverable hydrocarbons rank it in the top 10 oil and gas fields in the world, and top three in the United States (Fig. 1). The large aerial extent, abnormal reservoir pressures, and excellent rock properties combine to make this a world class reservoir. The unique combination of events which led to the new field discovery, the confirmation of the predicted reservoir quality, and the resulting impact of the enormous developing trend will be discussed.

Cusack, C., J. Beeson, D. Stoneburner, and G. Robertson, 2010, The discovery, reservoir attributes, and significance of the Hawkville Field and Eagle Ford Shale trend, Texas: Gulf Coast Association of Geological Societies Transactions, v. 60, p. 165-179.

Exhibit No. 78
DOCKET NO. 01-0297078, et al.
Talisman Energy USA, Inc.
January 7, 2016

Attachment 8

0, The Gulf Coast Association of Geological Societies. All Rights Reserved.

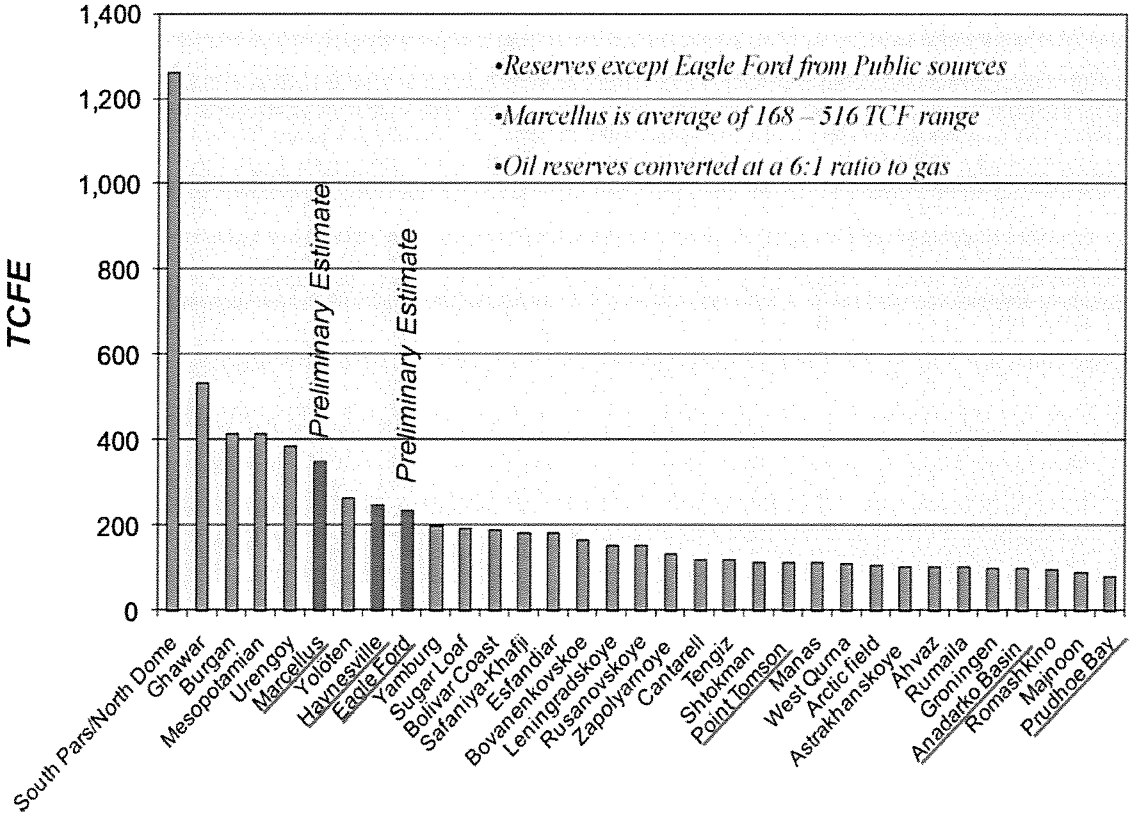

Figure 1. Largest oil and gas fields in the world with the largest in the United States highlighted in red. TCFE, trillion cubic feet equivalent.

THE DISCOVERY OF HAWKVILLE FIELD

In early 2008, Petrohawk Energy was rapidly developing their Fayetteville Shale acreage in central Arkansas and building onto their acreage position in the emerging Haynesville Shale in northern Louisiana. Success in these new unconventional resource plays and a rapidly developing understanding of what attributes were critical to an economic organic shale system fed a thirst for discovering a new frontier shale play that would provide Petrohawk a significant economic windfall as well as cementing its prominence among comparable shale players.

In January of 2008, Petrohawk partnered with First Rock, Inc. and began mapping the Eagle Ford along the Upper Cretaceous platform (Fig. 2). The Cretaceous-aged Eagle Ford lies below the base of the Austin Chalk formation and above the Buda Limestone (Fig. 3). Reservoir quality was determined from available porosity logs, but mostly surmised from anomalously higher resistivities in the shale section that is unique to an organic rich reservoir section (Fig. 4). The isopachs derived from old well logs and 2D seismic data quickly led us to focus on the area downdip to the paleo high formed by the Edwards Reef (also called the Stuart City Reef trend in southwest Texas). The Eagle Ford Shale doubles in thickness across the Edwards Reef, but the majority of it exists at depths that preclude economic horizontal development. The exception to this is on the west side of Pawnee Field in Live Oak County where the Edwards Reef is displaced to the north and updip by a large strike slip feature that causes the downdip Eagle Ford to be present at much shallower depths and to be much more attractive to the economics of drilling horizontal wells (Fig. 5). South of the Edwards Reef, another unique paleo feature is formed by the older Sligo shelf margin. This salt cored feature formed a southern baffle resulting in a restricted basin in which anoxic bottom conditions allowed for a very high retention of organic material.

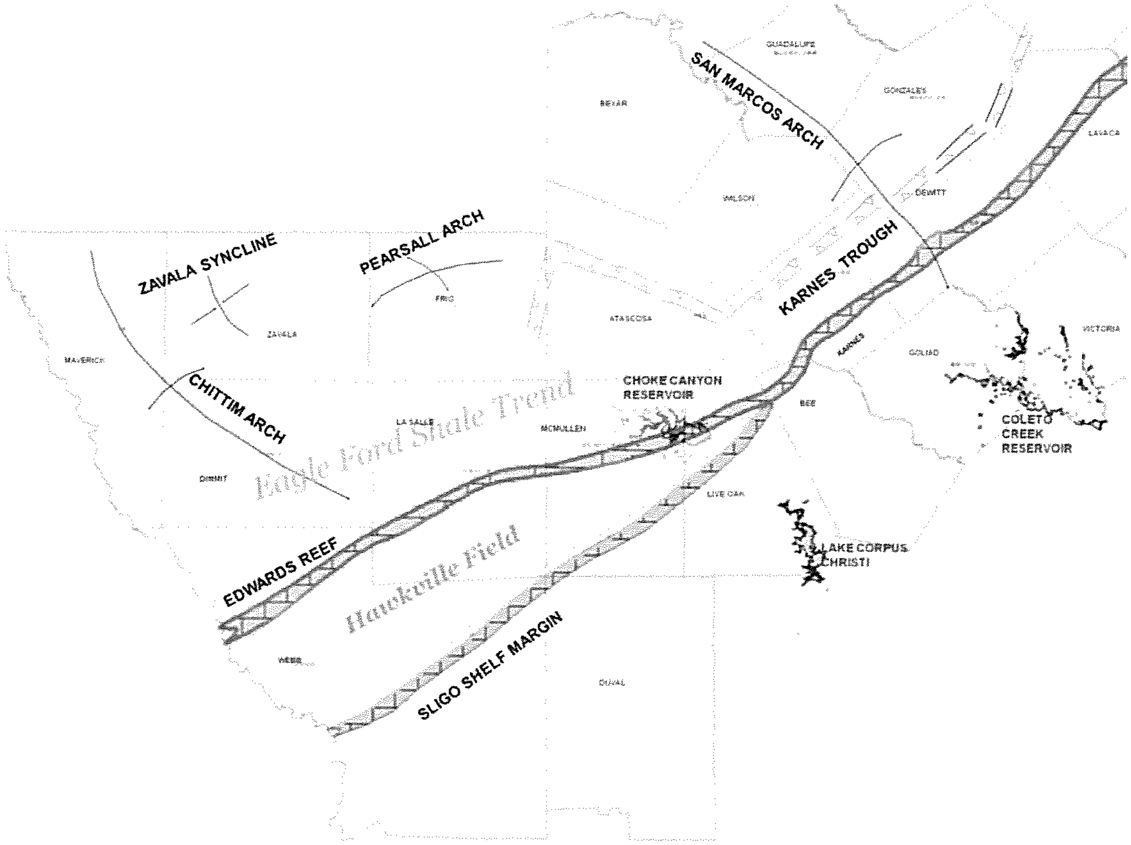
GUADALUPE
SAN MARCOS ARCH
GONZALES
BEXAR
LAVACA
WILSON
DEWITT
PEARSALL ARCH
ZAVALA SYNCLINE
KARNES TROUGH
FRIO
ATASCOSA
ZAVALA
VICTORIA
MAVERICK
KARNES
GOLIAD
CHOKE CANYON RESERVOIR
CHITTIM ARCH
Eagle Ford Shale Trend
LA SALLE
MCMULLEN
BEE
COLETO CREEK RESERVOIR
DIMMIT
LIVE OAK
LAKE CORPUS CHRISTI
EDWARDS REEF
Hawkville Field
SLIGO SHELF MARGIN
WEBB
DUVAL

Figure 2. Location of the Eagle Ford Shale trend on the Cretaceous platform with salient structural elements shown.

There were two key, pre-existing well logs in LaSalle County that showed a thickened Eagle Ford Shale section and reservoir parameters that solidified the confidence to proceed with leasing and drilling. The first was the 1998 Swift Energy Pielop #1 well (shown on Figure 5), which had a mud log with shows and the necessary openhole log suite we desired that was used to generate a shale evaluation log and demonstrated the rock parameters for a productive shale (Fig. 6). These calculated reservoir properties provided a very accurate prediction of the actual values derived from the logs and cores of the initial pilot holes. The second was the 1952 Phillips Petroleum LaSalle #1 well (shown on Figure 5) from which we were surprisingly able to obtain drill cuttings that had been stored at the Core Repository at the Texas Bureau of Economic Geology and confirmed that the shale had sufficient TOC (total organic content) and maturity to be productive (Fig. 7). Further confidence that there was sufficient reservoir quality to flow hydrocarbons was provided by reconnaissance information of Eagle Ford completions made by Burlington Resources, Pioneer Natural Resources, Lewis Energy, and Apache Corporation along the trend even though none of these had been verified to have produced commercial quantities.

The 2D seismic data were also invaluable as it was quickly determined that this anomalously thickened section downdip to the Edwards reef could be seen on the 2D data (Fig. 8). When the organic section reaches a thickness of about 150 feet, the normal trough event develops into a doublet with an extra peak which is very diagnostic of gross reservoir thickness. An extensive grid of 2D data was licensed from Seismic Exchange Incorporated and a purchase outline was drawn and given to the brokers who amazingly assembled 175,000 net acres before our first well was tested and encountered no competition. A key element in this unopposed success was leasing and drilling the first two wells under our partner's name, First Rock, Inc. The pilot hole in the First Rock

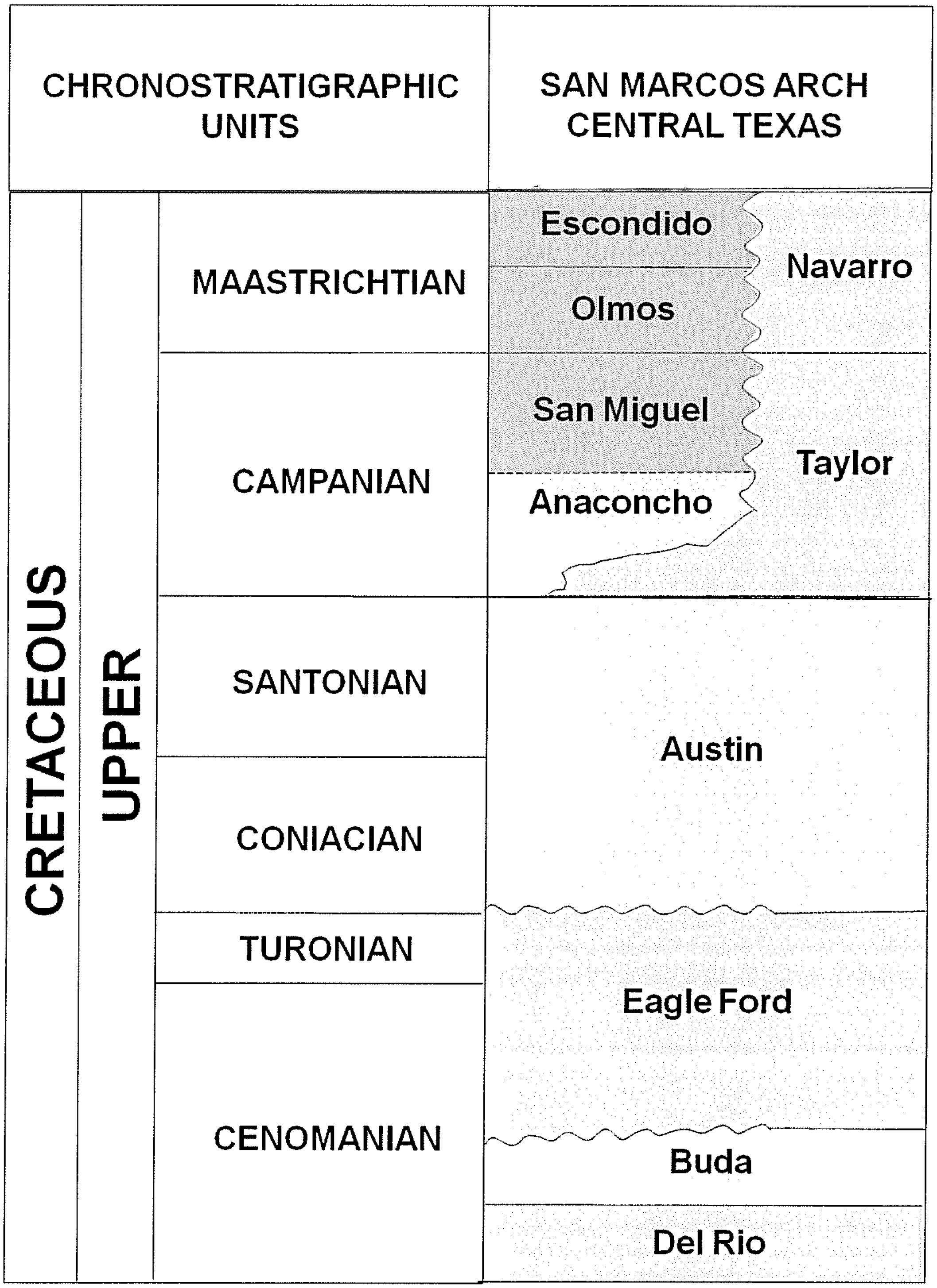
CHRONOSTRATIGRAPHIC UNITS
SAN MARCOS ARCH CENTRAL TEXAS
CRETACEOUS
UPPER
MAASTRICHTIAN
CAMPANIAN
SANTONIAN
CONIACIAN
TURONIAN
CENOMANIAN
Escondido
Olmos
Navarro
San Miguel
Anaconcho
Taylor
Austin
Eagle Ford
Buda
Del Rio

Figure 3. Upper Cretaceous stratigraphic column.

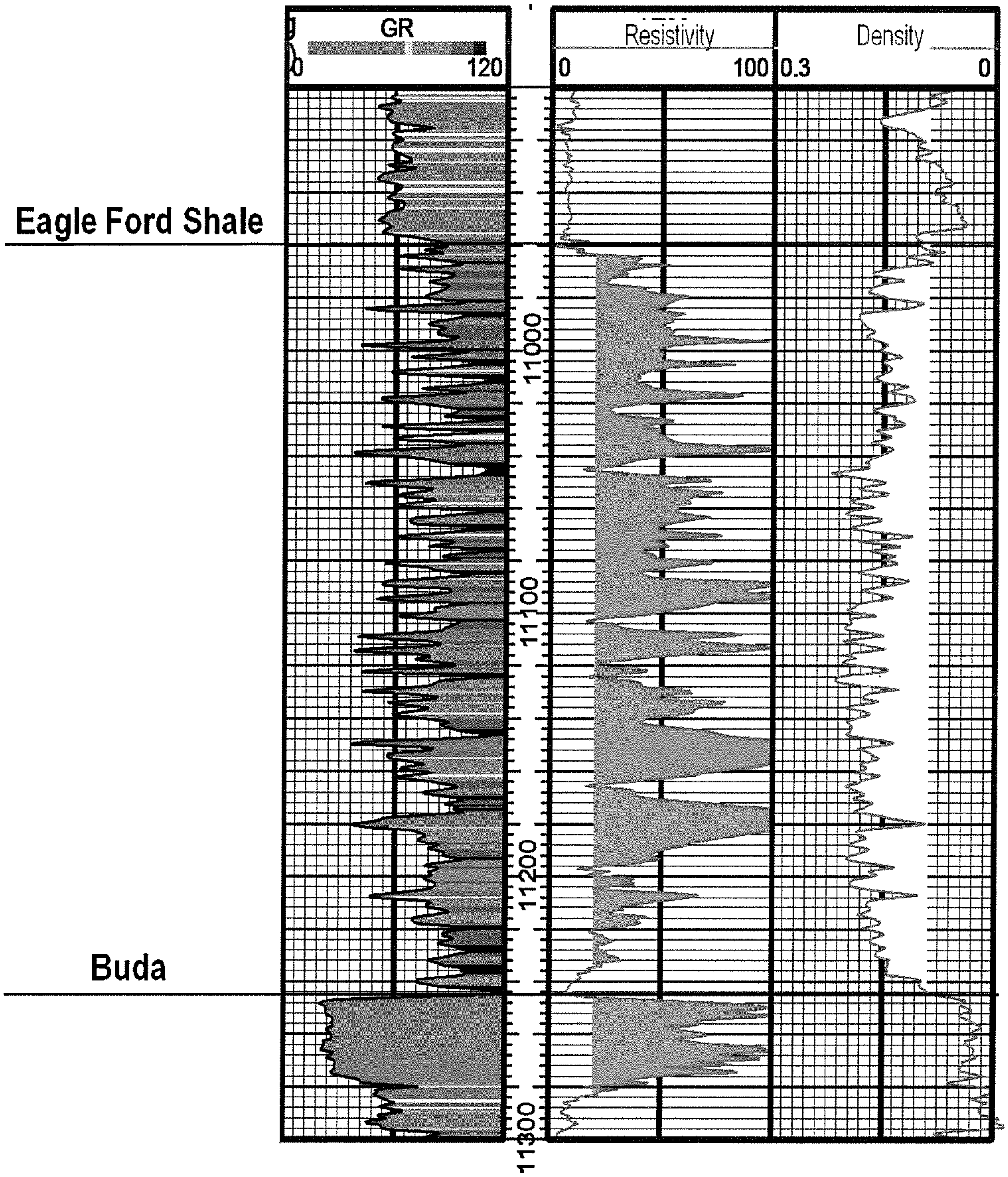

Swift Pielop #1

Figure 4. Type log (Swift Pielop #1) showing evaluation parameters for prospect development.

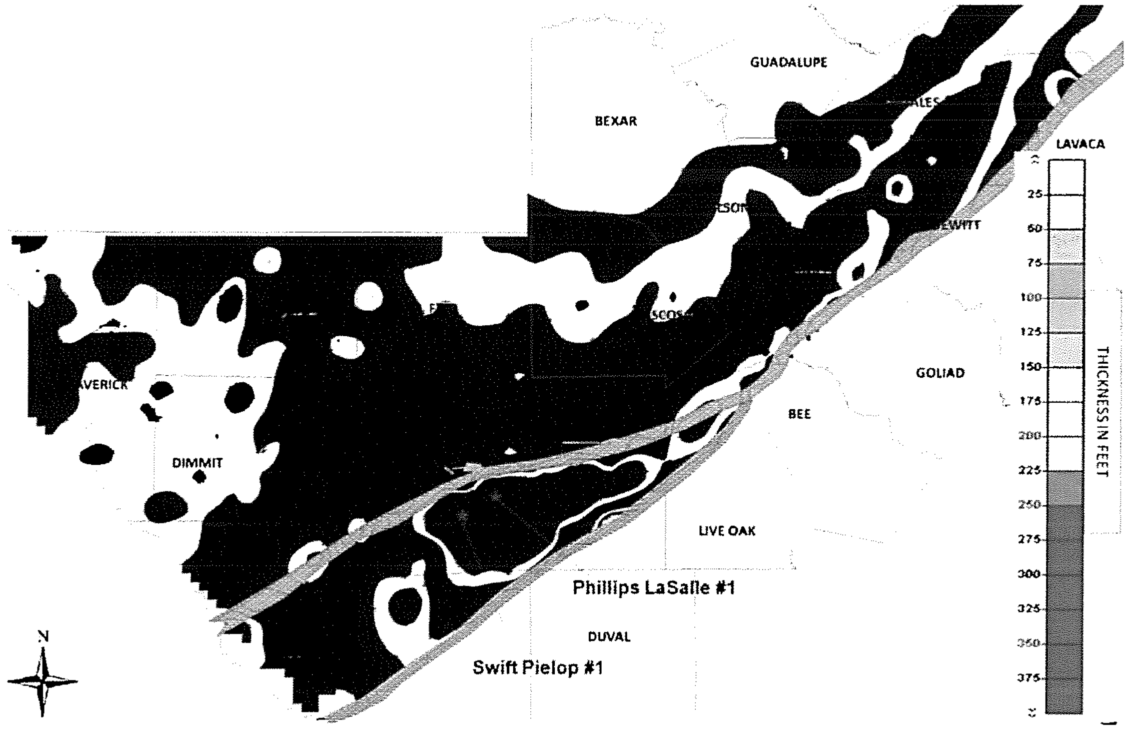

Figure 5. Regional Eagle Ford isopach showing the influence of the Edwards and Sligo shelf margins on deposition.

STS #1 was cored and logged in August 2008, and then sidetracked as a horizontal well reaching a total depth of 14,465 feet. It was completed with a 12 stage frac in October, 10 months after initiation of the mapping efforts. Initial production from the well was 7.6 MMCFGPD (million cubic feet of gas per day) and 251 BCPD (barrels of condensate per day) and the Hawkville Field was officially discovered. The next two delineation wells were drilled 15 miles on each side of the STS #1 well. They both also had pilot holes with cores and full logging suites, and discovered very similar reservoir properties confirming the continuity of the great reservoir properties across 30 miles of the field.

HAWKVILLE RESERVOIR PROPERTIES AND RESERVES

In the first year and a half since discovery, the Hawkville Field has been penetrated by 40 new delineation wells combined with 20 older wells, and integrated with 2D and 3D seismic data. These data provide very diagnostic support for the remarkable continuity of the reservoir properties that exist within a well defined area. The area now extends to the southwest limits tend across Webb County into Mexico, and extends along strike to the northeast for 120 miles across LaSalle and McMullen counties until reaching the intersection of the Edwards and Sligo reefs in Live Oak County. The dip dimension ranges from 5 to 30 miles from the updip edge on the Edwards Reef to a point of thinning towards the Sligo Reef (Fig. 9). The continuity of the reservoir is demonstrated in the cross sections in Figures 10 and 11. This total area covers 1,600 square miles. The new pilot holes drilled through the formation typically have full suites of induction, density, neutron, sonic scanner, formation imager, and elemental capture spectroscopy logs run, and are usually cored with either conventional or rotary cores. The wells that are drilled as laterals without pilot holes still have diagnostic gamma ray logs that show excellent correlations to the pilot holes confirming structure tops and gross reservoir thickness. The great reservoir quality is clearly defined by porosity on the density and sonic logs and typically, but not always defined by high resistivity on the induction logs. The density logs are the most diagnostic of reservoir quality and show a range across the

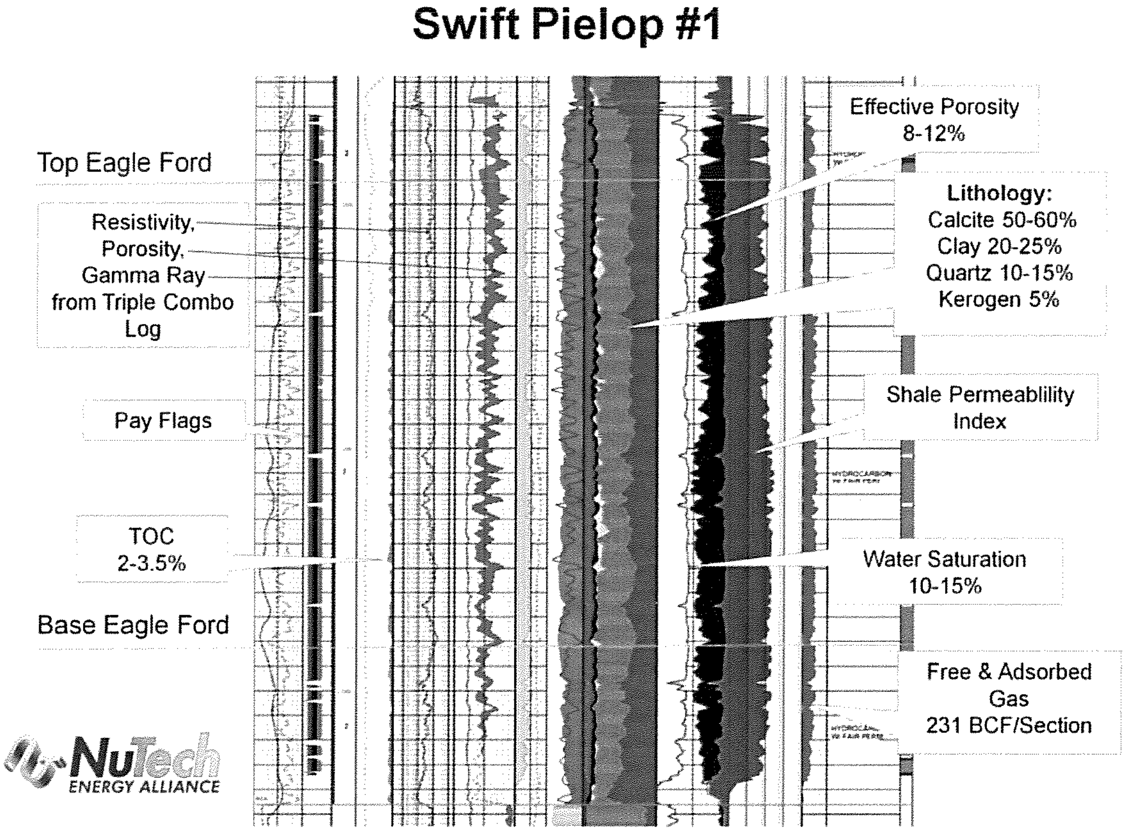

Figure 6. NuTech Shale Vision^{TM} analysis of the Eagle Ford Shale in the Swift Energy Pielop #1 well (reproduced with permission).

core of the field from 150 feet to 320 feet (using a density porosity cutoff of 9%) while averaging around 18% density porosity (Fig. 12). The detailed core analysis has been combined with the petrophysical interpretation to develop algorithms that calculate the critical reservoir properties.

The wireline log analysis is confirmed by the whole core data, which indicates 8-10% effective gas-filled porosity, permeability in the range of 1.0-1.5 x 10^{-3} md (millidarcies), and gas saturation exceeding 80% (Fig. 13). Remarkably, the core measured clay volumes from x-ray diffraction are only 10-20% and supports the high resistivities and low water saturations. Figure 14 shows a core photograph and core analysis that are integral to understanding the reservoir rock. The shale has as much as 70% calcite, being composed of mostly dispersed *Globotruncana* and *Globulina* foraminifers (Fig. 15). These foraminifers do not add much to the reservoir quality, but might contribute to the brittleness the rock exhibits as it is very receptive to fracing. These reservoir properties are about as good as any of the known organic shales and combined with a pressure gradient of 0.78 psi per foot yield original gas in place numbers of 160 to 200 BCF (billion cubic feet) per section, and free gas of 140 to 180 BCF per section. The downdip areas are dry gas and grade into a retrograde condensate area updip with the increasing to a maximum of 200 BCPMMCFG (barrels of condensate per million cubic of gas) at the Edwards Reef. In a geologic oddity, the dry gas to condensate line does not exactly follow the current structural grain, but follows the paleo structure as the western portion of the field has apparently been uplifted some since maturation (Fig. 16).

Using the original gas in place values coupled with the isopach thicknesses shown in Figure 5, the total Hawkville original gas in place calculates to be 227 TCF (trillion cubic feet). By using an estimated recovery efficiency of 30%, recoverable reserves are calculated to be 68 TCFE (trillion cubic feet equivalent). The type curve for the Petrohawk portion of the field shows 5.5 BCFE (billion cubic feet equivalent) per well which supports 80 acre drainage (Fig. 17). These recoveries and drainage areas are similar to other well documented shales. Simple math calculates that over 12,000 wells will be required to produce these reserves. About a third of the Hawkville Field is updip to the dry gas/condensate line and grades updip to about 200 BCPMMCFG.

TOTAL EAGLE FORD EXTENT AND RESERVES

Since the discovery of Hawkville, the Eagle Ford activity has exploded across a 13 county area from Webb and Maverick counties on the southwest to Gonzales and DeWitt counties on the northeast. As of the submission of this paper, there are about 60 rigs drilling in the trend (Fig. 18). The full economic extents are still being delineated and will take years to fully understand as the reservoir exists across the entire Gulf Coast, but varies considerably in thickness moving east and north and becomes depth challenged downdip of the majority of the Edwards reef. There is a wide band of a high yield condensate area from about the Edwards reef that grades into an oil window updip. A preliminary estimate of the total productive area from the Mexico border on the southwest to DeWitt and Gonzales counties on the northeast is 6,000 square miles. The estimated recoverable reserves for this total trend could be as high as 226 TCFE of oil, gas, and condensate equivalent. This will require about 50,000 wells to recover these reserves and ranks this discovery in the top 10 oil and gas fields in the world and top three in the United States of all time.

CONCLUSIONS

The discovery of the world class Hawkville Field and Eagle Ford Shale trend is a remarkable story that developed very rapidly due to a combination of five key elements. The first was partnering our experienced South Texas Cretaceous geologist with First Rock's experienced South Texas Cretaceous geologist. The second was applying Petrohawk's experience learned in other shale trends to map the key reservoir attributes. The third was quickly assembling all of the data needed to perform a quality technical evaluation and being fortunate enough to find two old wells, one with a pretty full logging suite and one with cuttings that could be analyzed. The fourth, and most important element, was an upper management team that made a quick decision to commit the capital and resources needed to lease the core of the field before the first well was drilled. The final key element is having a top notch operations staff that can efficiently drill and complete these wells ensuring high rate completions at a reasonable cost.

The Eagle Ford Shale exhibits remarkable reservoir quality and continuity and has quickly developed into a world class oil and gas field. While the full extent is still being delineated, it already has enough gas, condensate, and oil reserves to rank it in the top 10 fields in the world. The benefits of most of it containing high yield condensate or oil combined with an existing network of pipelines, and fairly easy surface access makes it highly attractive for rapid and highly economic development.

ACKNOWLEDGMENTS

I'd like to mention the key people that made this discovery possible. While Dick Stoneburner, who was our COO, and is now also President, and I made some technical contributions, we mostly provided guidance and support, as our geologist, Jana Beeson, and First Rock's geologist (and President), Gregg Robertson, did most of the detailed technical work. They worked thousands of hours on this project from inception through discovery, and continue to do so. Floyd Wilson, our CEO, Chairman of the Board, and President at the date of discovery, fully supported this effort, believed in the technical work, and approved the large amount of capital that was needed to capture the leases and drill the discovery and appraisal wells. The other key set of contributors was an aggressive land effort by Gregg, his landman, Robert Graham, and Petrohawk's land staff ensuring capture of the leases, as well as an outstanding effort by our operations group led by our Sr. VP of the Western Division, Charles Latch, and his VP of Operations, Chris Morro. Also thanks to Field Superintendent, Gary Gilbert, and Drilling Engineer, Keith Alverson. Finally, I'd also like to thank current team members who contributed to this article and ongoing effort such as Marie Henry, Tom Smith, and Scotty Tuttle.

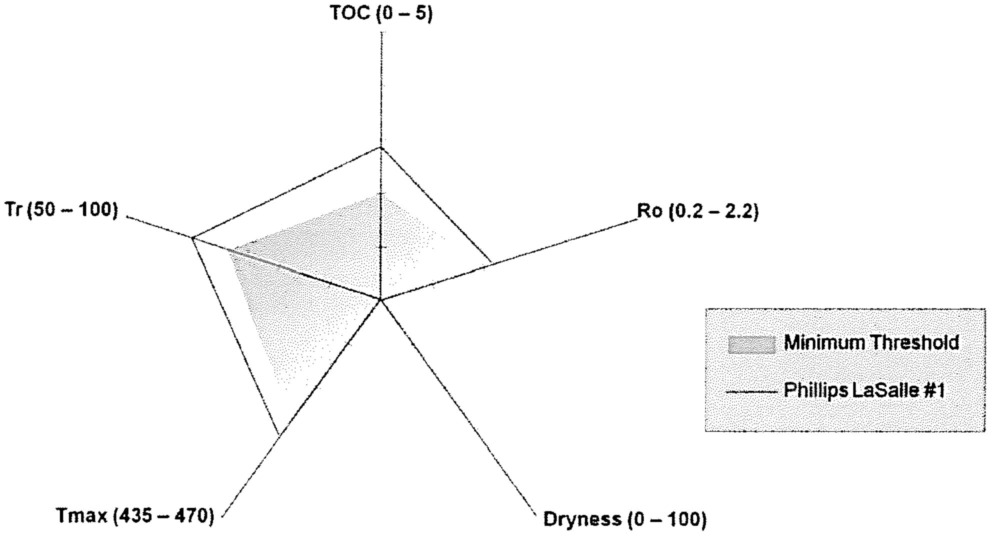

Figure 7. Eagle Ford Shale gas risk assessment diagram. "TOC" – total organic content, "Ro" – vitrinite reflectance, "Tmax" – measure of the amount of hydrogen-rich kerogen, and "Tr" – transformation ratio (fractional conversion). Data from Humble Geochemical Services (reproduced with permission).

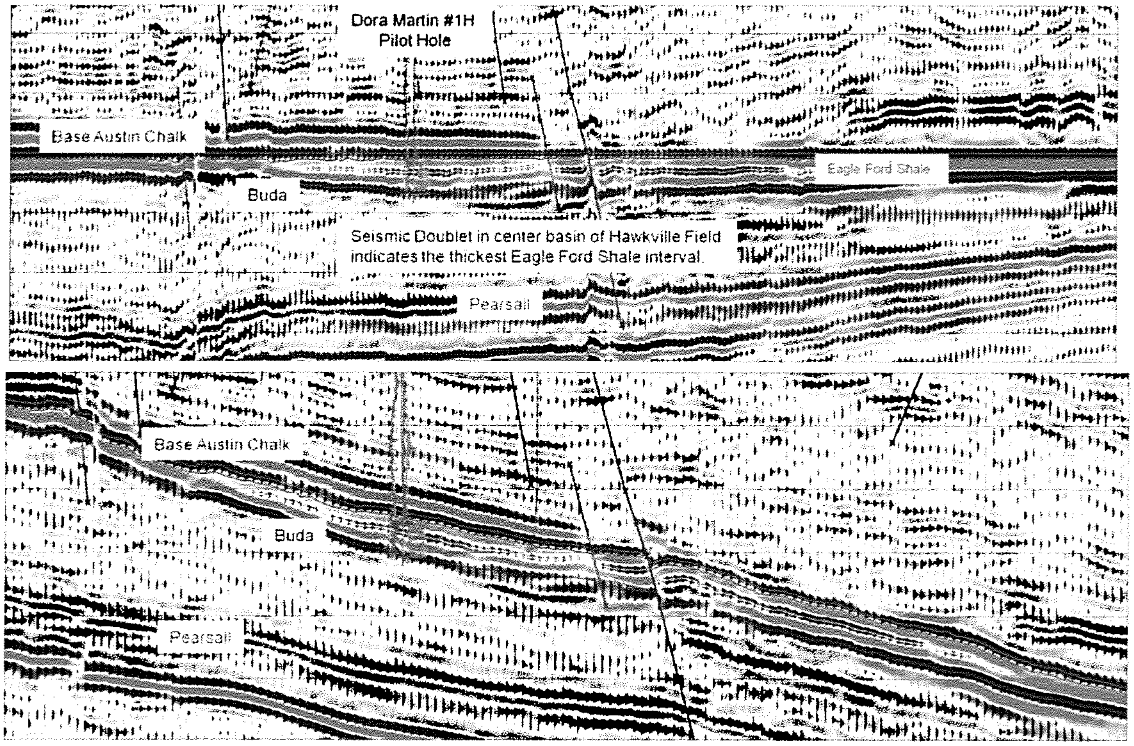
Dora Martin #1H
Pilot Hole
Base Austin Chalk
Eagle Ford Shale
Buda
Seismic Doublet in center basin of Hawkville Field
indicates the thickest Eagle Ford Shale interval.
Pearsall
Base Austin Chalk
Buda
Pearsall

Figure 8. Seismic line flattened on Base Austin Chalk (above) and in regular time presentation (below). Data owned by Seismic Exchange, Inc. (reproduced with permission). Interpretation by Petrohawk.

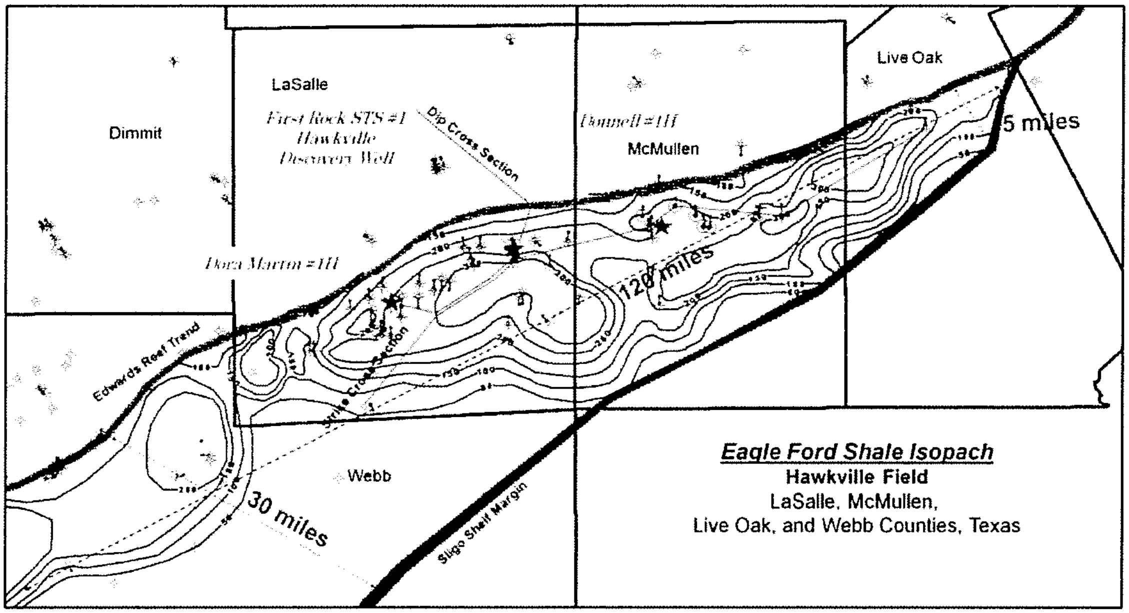
Dimmit
LaSalle
First Rock STS #1
Hawkville
Discovery Well
Dip Cross Section
Donnell #1H
McMullen
Live Oak
5 miles
Dora Martin #1H
120 miles
Edwards Reef Trend
Strike Cross Section
Webb
30 miles
Sligo Shelf Margin
Eagle Ford Shale Isopach
Hawkville Field
LaSalle, McMullen,
Live Oak, and Webb Counties, Texas

Figure 9. Aerial extent of Hawkville Field with Eagle Ford Shale isopach showing the variable thickness. The discovery well and the two delineation wells were spaced 15 miles apart.

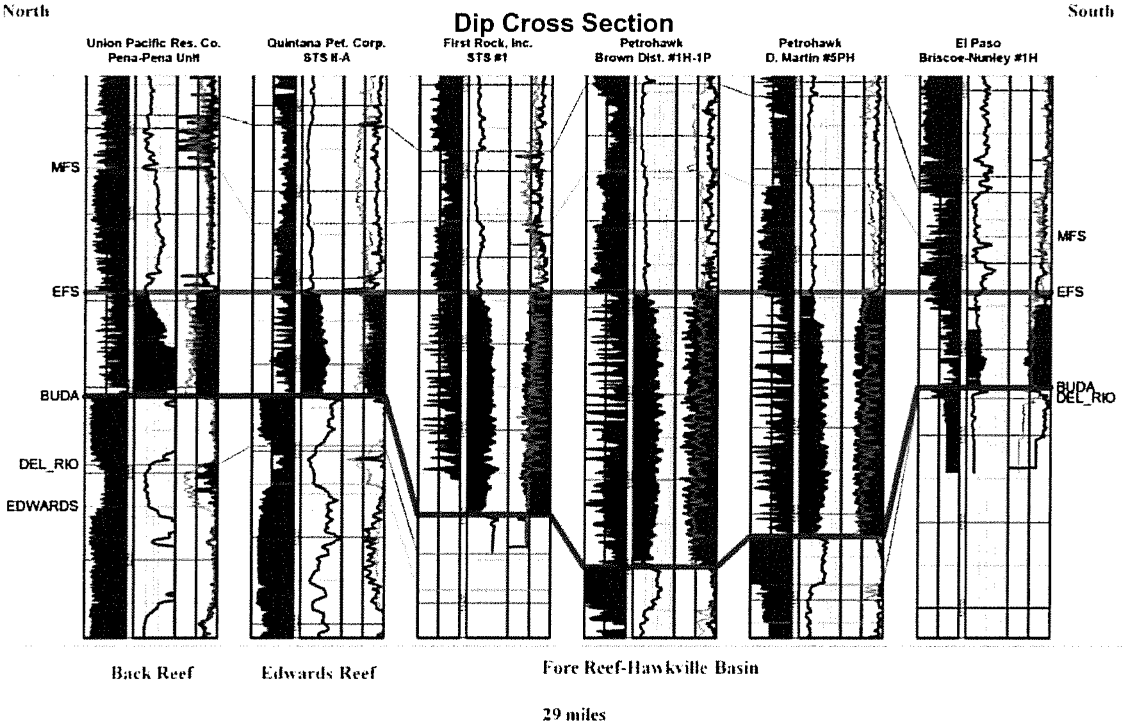

Figure 10. Dip cross section showing the expansion of the Eagle Ford in the fore reef depositional province.

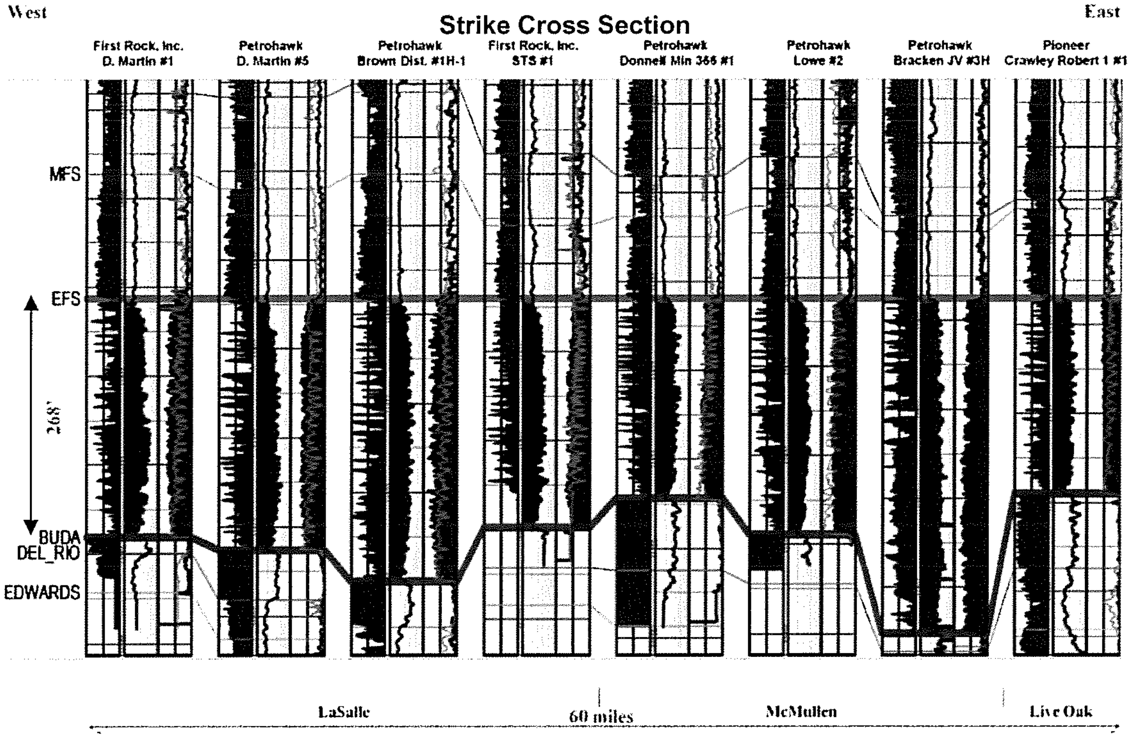

Figure 11. Strike cross section down the axis of the Eagle Ford "thick" showing the lateral continuity of the fore reef depositional province.

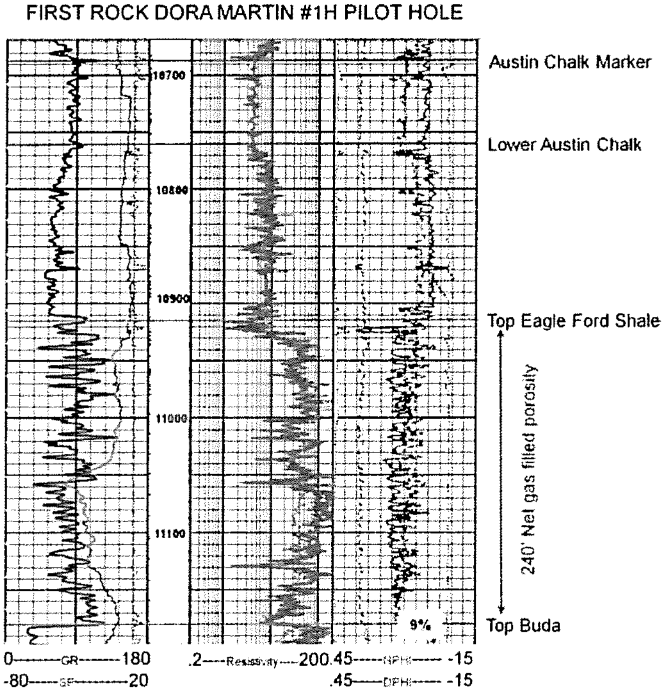

Figure 12. Type log (First Rock Dora Martin #1H pilot hole) from the Hawkville Field, showing the entire Eagle Ford is "net pay" with porosity substantially exceeding the minimum cutoff value of 9%.

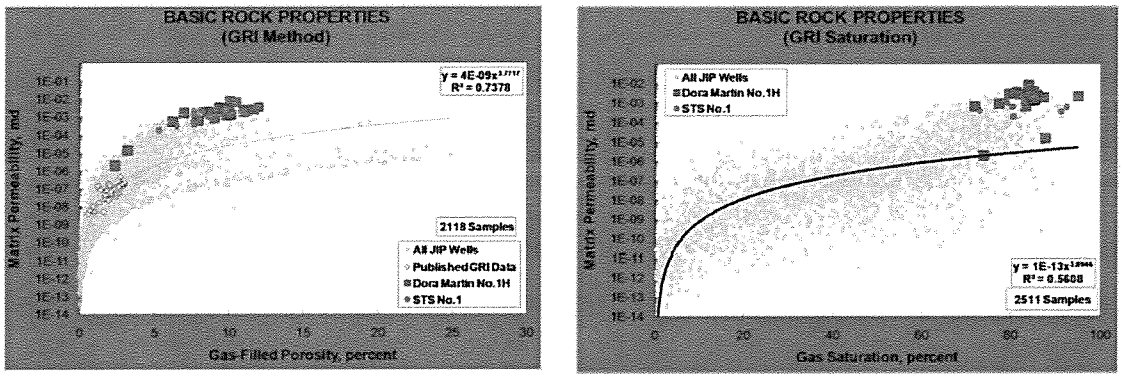

	GAS IN PLACE ANALYSIS - DORA MARTIN #1H				
		Bulk Density (g/cc)	Gas Content (scf/ton)	GIP (scf/acre-ft)	GIP (BCF/section)
Eagle Ford	Free Gas	2.40	368.1	1,203,327	197.9
	Sorbed Gas		27.5	90,050	14.8
	Total Gas in Place		395.7	1,293,376	212.7

Figure 13. Key reservoir properties from Dora Martin #1H core which show the Hawkville wells rank at the top of the entire universe of shale reservoirs. Data from Core Lab Gas Shale Formation Evaluation (reproduced with permission). scf, standard cubic feet.

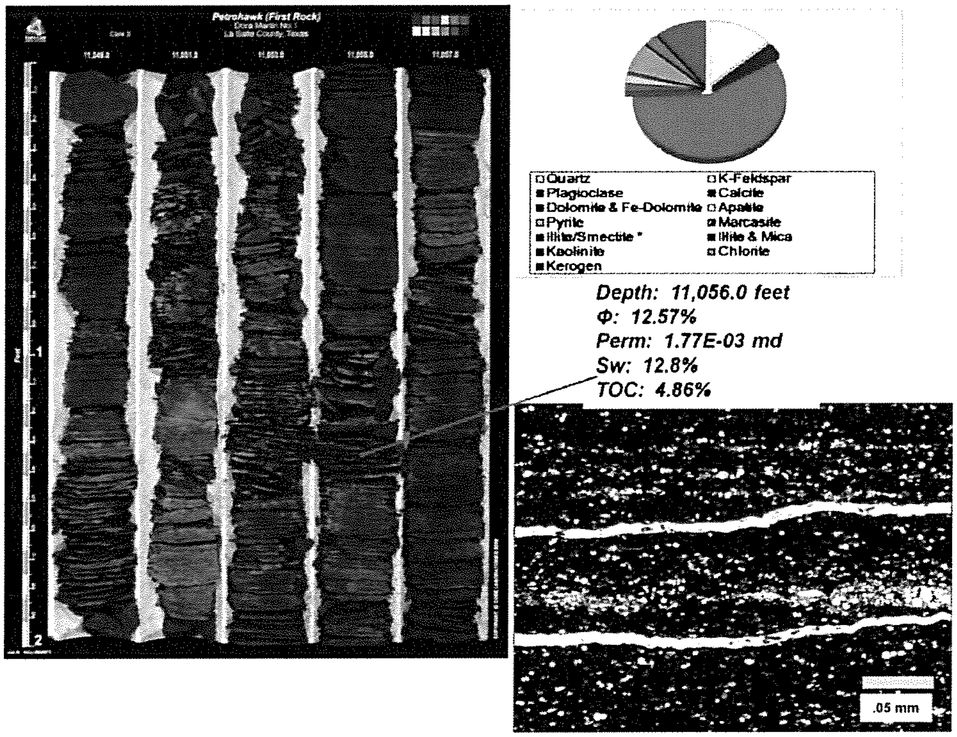
Petrohawk (First Rock)
Dora Martin No 1
La Salle County, Texas
Feet
1
2
☐ Quartz
☐ K-Feldspar
■ Plagioclase
■ Calcite
■ Dolomite & Fe-Dolomite
☐ Apatite
☐ Pyrite
▨ Marcasite
■ Illite/Smectite *
■ Illite & Mica
■ Kaolinite
▨ Chlorite
■ Kerogen
Depth: 11,056.0 feet
Φ: 12.57%
Perm: 1.77E-03 md
Sw: 12.8%
TOC: 4.86%
.05 mm

Figure 14. Photo of Dora Martin #1H core on left. Note alternating blocky and platy beds. Thin-section on lower right showing coring induced axial fractures as light colored horizontal streaks. Mineralogy in upper right derived from x-ray diffraction. Data from Core Lab (reproduced with permission).

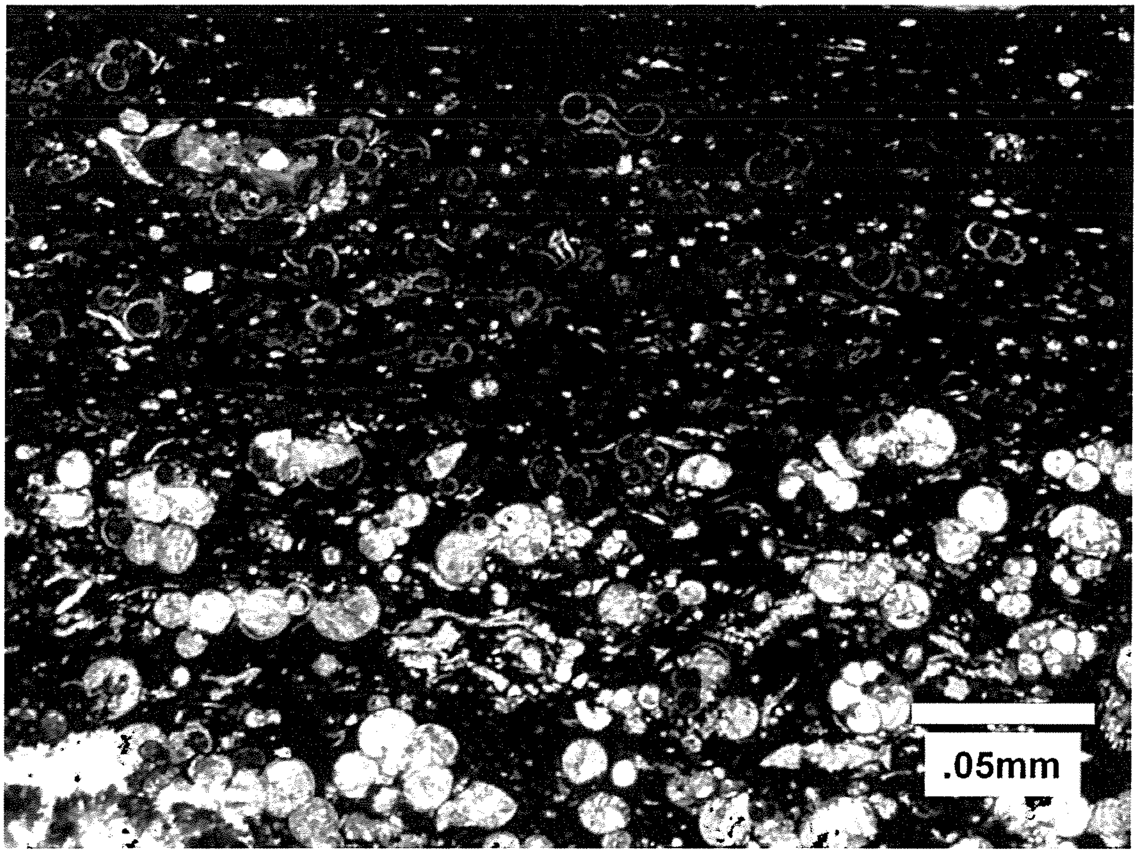

Figure 15. Thin-section photomicrograph from Dora Martin #1H core showing abundant *Globotruncana* planktonic foraminifers and *Globulina* calcareous foraminifers.

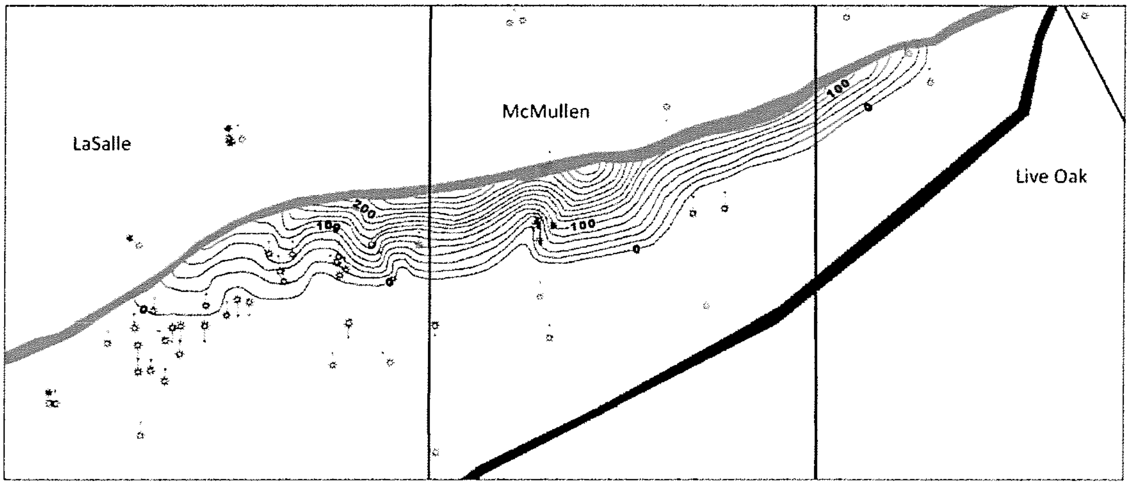
LaSalle
McMullen
Live Oak
200
100
100
100
0
0
0

Figure 16. Map of Hawkville Field with contours of the yield of BCPMMCFG. Values go from zero on the south to in excess of 200 BCPMMCFG at the northern edge.

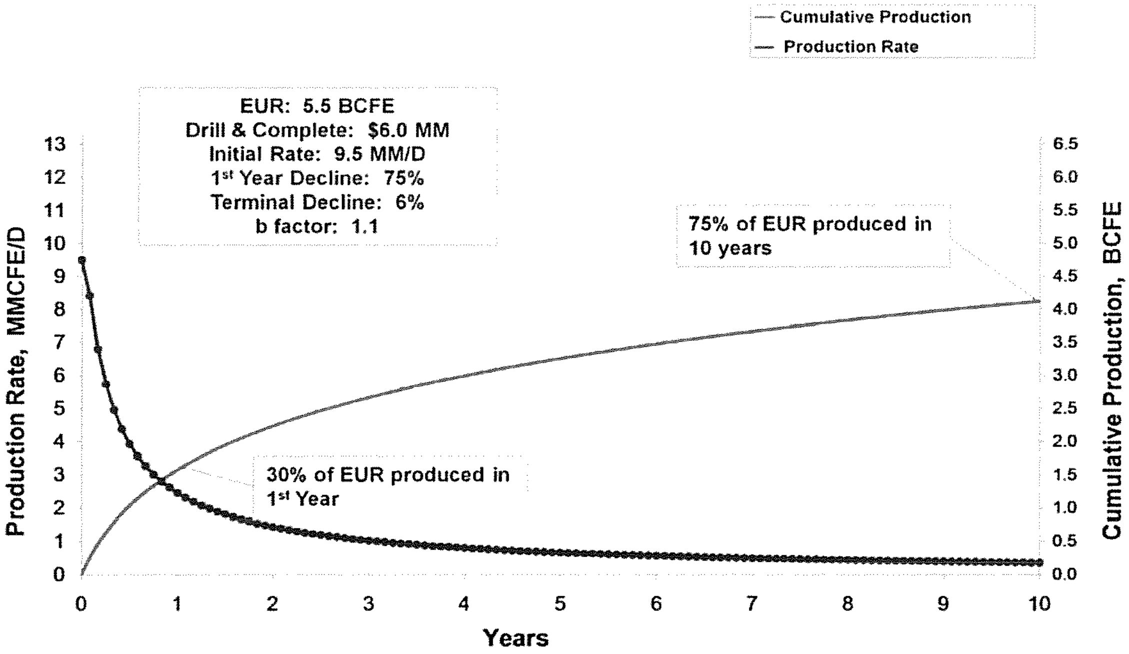

Figure 17. Type production decline curve of a Hawkville Field well showing that 75% of the 5.5 BCF EUR (estimated ultimate recovery) (projected over a 30 year life) is recovered in the first 10 years.

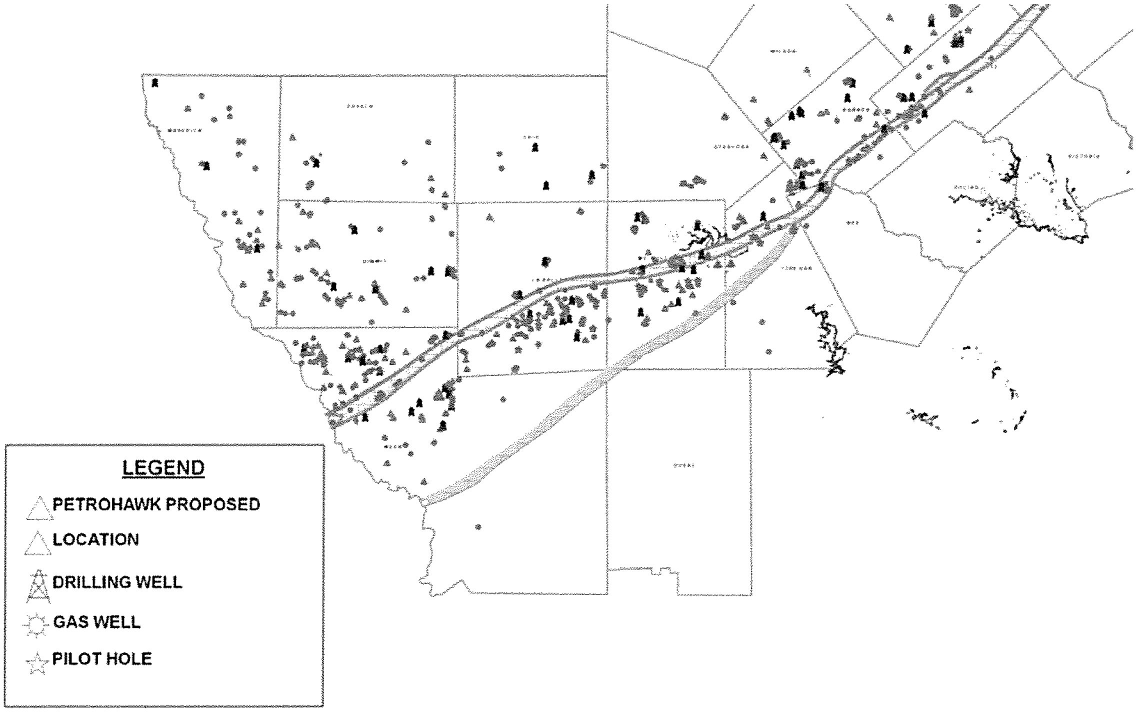
LEGEND
PETROHAWK PROPOSED
LOCATION
DRILLING WELL
GAS WELL
PILOT HOLE

Figure 18. Eagle Ford Trend activity map as of May 2010, showing the concentration and aerial extent of the play that began less than two years earlier.

LIST OF SOURCES

(1) The Core Photos and Analysis were provided by Core Laboratories as part of their Eagle Ford Shale Core Consortium of which Petrohawk is a charter member.

(2) The recoverable reserve estimate of up to 226 TCFE is from an internal Petrohawk volumetric calculation.

Cooke Ranch C1H PLT

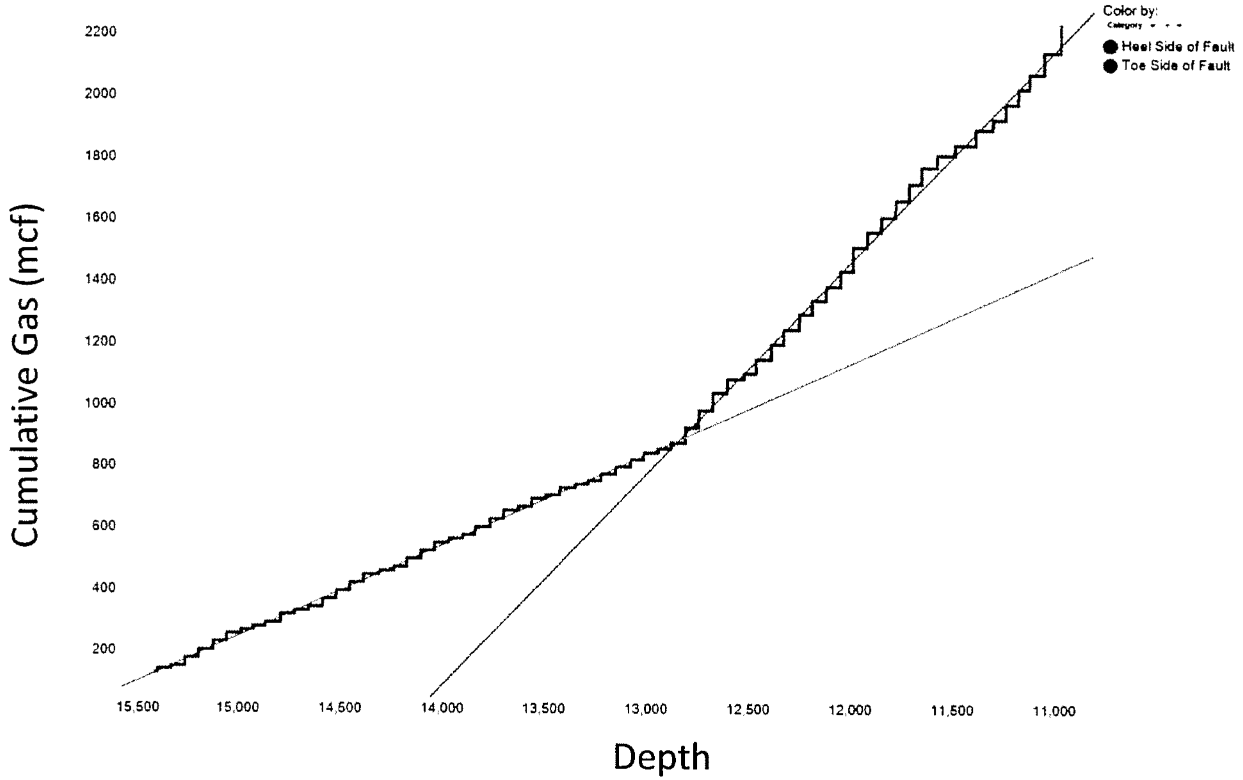

Well	Top Perf (MD)	Bottom Perf (MD)	Fault Depth (MD)	% of SLL On the Heel Side of the Fault	% Cum Production on the Heel Side of the Fault
C1H	11,000	15,722	12,875	40%	60%
C2H	10,900	15,145	12,500	38%	*57%
C3H	11,229	15,042	12,500	37%	*56%

* Calculated the ratio using the results of the C1H production log.

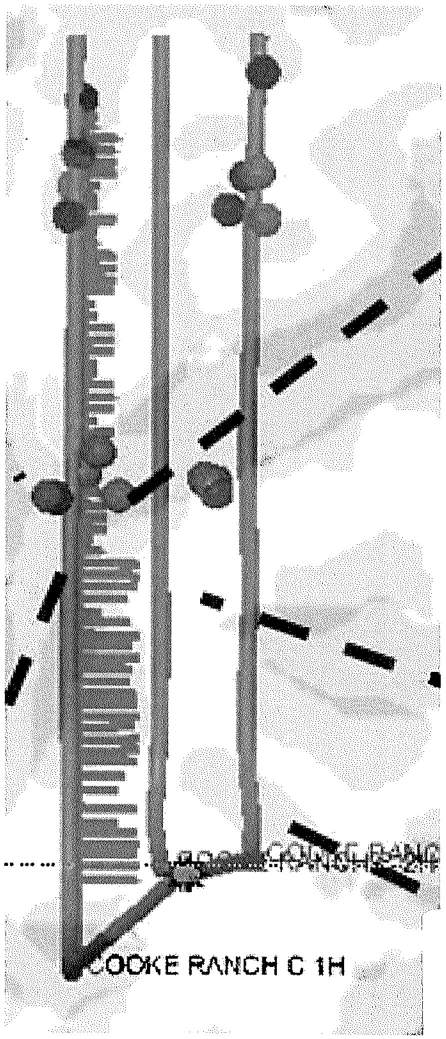

Excerpt from
Talisman Exh. 49

Exhibit No. 88
DOCKET NO. 01-0297078, e
Talisman Energy USA, Inc.
January 7, 2016

Attachment 9